INTRINSIC OPTICAL SIGNALS CHARACTERIZING ACUTE EXCITOTOXICITY IN THE HIPPOCAMPAL SLICE EVOKED BY THE MARINE TOXIN DOMOIC ACID

Trevor M. Polischuk

A thesis submitted to the Department of Anatomy
and Cell Biology in conformity with the requirements
for the degree of Doctor of Philosophy

Queen's University
Kingston, Ontario, Canada
April 1997

copyright © Trevor M. Polischuk, 1997

National Library of Canada
Acquisitions and Bibliographic Services
395 Wellington Street
Ottawa ON K1A 0N4
Canada

Bibliothèque nationale du Canada
Acquisitions et services bibliographiques
395, rue Wellington
Ottawa ON K1A 0N4
Canada

Your file Votre référence

Our file Notre référence

The author has granted a non-exclusive licence allowing the National Library of Canada to reproduce, loan, distribute or sell copies of his/her thesis by any means and in any form or format, making this thesis available to interested persons.

The author retains ownership of the copyright in his/her thesis. Neither the thesis nor substantial extracts from it may be printed or otherwise reproduced with the author's permission.

L'auteur a accordé une licence non exclusive permettant à la Bibliothèque nationale du Canada de reproduire, prêter, distribuer ou vendre des copies de sa thèse de quelque manière et sous quelque forme que ce soit pour mettre des exemplaires de cette thèse à la disposition des personnes intéressées.

L'auteur conserve la propriété du droit d'auteur qui protège sa thèse. Ni la thèse ni des extraits substantiels de celle-ci ne doivent être imprimés ou autrement reproduits sans son autorisation.

0-612-20581-9

Canada

QUEEN'S UNIVERSITY AT KINGSTON

SCHOOL OF GRADUATE STUDIES AND RESEARCH

PERMISSION OF CO-AUTHOR(S)

I/we, the undersigned, hereby grant permission to microfilm any material designated as being co-authored by me/us in the thesis copyrighted to the person named below:

TREVOR M. POLISCHUK	
Name of Copyrighted Author	Signature of copyrighted author
Name(s) of co-author(s)	Signature(s) of co-author(s)
R. David Andrews	

DATE: MAY. 8 '97.

To my entire family:

Albert, Ann, Gerald, and Loretta;

Kevin, Connie, Glenda, Alex, Derwyn, Vanessa, Darci, Jim, Steven, and Kim;

Stephen, Tiffany, Tangie, and Kaitlin;

and my bride, Carol Ann.

ABSTRACT

Excitotoxicity is defined by a group of compounds that can both excite and kill neurons at low doses. Excitotoxic processes include excessive stimulation of neurons by glutamate, the most common neurotransmitter in the mammalian brain, or by glutamate analogs, resulting in membrane derangements leading to neuronal cell death. These perturbations have been implicated in many pathological brain states, from acute disorders (stroke, epilepsy, food poisoning, traumatic head injury) to chronic neurodegenerative disease (senile dementia of the Alzheimer's type, Parkinson's disease, Huntington's chorea).

Intrinsic optical signals (IOSs) describe how an object either reflects, absorbs, or transmits light. One of the earliest events in the excitotoxic cascade involves cell swelling. Monitoring changes in light transmittance (LT) through the brain slice reveals real time changes in cell volume during excitotoxic insults over a large area of tissue.

Domoic acid (DOM) is a cyclic amino acid produced by marine algae and seaweed. DOM was responsible for a outbreak of severe food poisoning in Canada in 1987 from contaminated shellfish. Neurological symptoms ranged from migraine and memory loss to seizure and death. Since that time, it has been established that domoate is a potent glutamate agonist of non-NMDA (non-N-methyl-D-aspartate) glutamate receptors and can kill neurons in the human hippocampal formation.

The present study examined the effects of domoate on LT changes in the rat hippocampal slice preparation to characterize (1) if cell swelling played a role in the response; (2) which hippocampal regions were affected; (3) which receptors subtypes were involved; (4) if IOSs could be used to gauge DOM-induced toxicity; and (5) if specific antagonists of DOM were protective.

A brief, 1 min exposure to 10 μM DOM at 22°C or 37°C resulted in reversible LT changes of up to 60% in the dendritic regions of CA1 and dentate gyrus (DG) in a dose dependent manner. Cell body regions and area CA3 were minimally affected. The sodium channel blocker tetrodotoxin eliminated the evoked CA1 population spike but not the LT increase, indicating that the LT signal is not associated with action potential discharge. The AMPA/kainate receptor antagonists CNQX or DNQX or the broad-spectrum antagonist kynurenate reversibly blocked DOM-induced LT increases at 22°C. The NMDA receptor antagonist, AP-5, or the kainate receptor antagonist, GAMS, failed to block the response. Relative tissue resistance (R_{REL}) is an independent means of measuring cell swelling. Changes in R_{REL} evoked by DOM measured across CA1 dendritic regions paralleled changes in LT and were blocked by kynurenate. Spectral analysis of LT changes revealed a non-specific transmittance increase across 400-800 nm indicating generalized swelling as a source of the signal. The evoked field potential recorded in the CA1 cell body region (PYR) completely recovered upon LT reversal. In contrast, increasing DOM exposure to 10 min at 37°C elicited a distinct intrinsic optical sequence where the initial LT increase in dendritic regions evolved into an irreversible *decrease* in LT. At the same time, LT irreversibly *increased* in cell body regions (CA1 PYR and DG GC) and the evoked field potential was irretrievably lost. Spectral analysis of CA1 PYR revealed a wide-band transmittance increase indicating cellular swelling as a source of the signal. Subsequent histological examination demonstrated severe CA1 and DG neuron damage in slices exposed to domoate for 10 min at 37°C. The optical changes generated by domoate required extracellular Cl^- but not Ca^{2+}. Lowering temperature protected the slice from the irreversible damage to the CA1 region. Similar changes in LT at 1 min/22°C or 10 min/37°C were evoked by 10 μM AMPA. A new glutamate receptor antagonist highly specific for AMPA receptors, GYKI 52466, significantly protected against DOM- or AMPA-induced toxicity while NS-102, a new antagonist highly specific for kainate receptors, did not.

Based on theses findings, we propose that domoate binding to AMPA receptors open channels mediating Na^+ influx followed passively by Cl^- entry. Water follows, producing prolonged post-synaptic swelling in the CA1 and dentate regions where AMPA receptors are most abundant. Subsequent IOS changes in the tissue represent neuronal volume changes, an early excitotoxic event, involving previously unsuspected dynamic and compartmentalized volume changes first in dendrites followed by cell bodies leading to rapid neuronal death that can be imaged in real time. Imaging intrinsic optical signals allows a real-time view of early excitotoxic events and so may prove useful in assessing potentially therapeutic agents that reduce damage induced by excitotoxic agents or ischemia.

ACKNOWLEDGMENTS

A work of this nature is a product of many labours. It is therefore necessary to recognize a number of people who, through their efforts, made this thesis possible. First, I must thank the person who initiated me to the world of research, Dr. Paul M Gross. His tutelage gave me the courage to embark on my graduate studies and the tenacity to complete them.

Most significantly, I would like to thank Dr. R. David Andrew for his support, supervision, smarts, and salvation. Your contribution to this project was immeasurable and I will be forever en*light*ened by your wisdom.

Thanks to my fellow scientists and lab mates of the past...Mr. John R. Adams, Mr. Taylor F. Dowsley, and Dr. E. Philip Osehobo; present...Dr. Cathryn R. Jarvis, Mr. Mark Labron, Mr. Michael E. Lobinowich, Dr. Akef S. Obeidat, and Ms. Nicole G. Rolfe; and future...Mr. Trent Anderson and Ms. Indu Joshi. Thanks for your help, assistance, and most importantly, your friendship. As well, a note of recognition for every graduate student who passed through the department during my five year stay; too many to list but not to remember.

Thank-you to the entire staff of the Department of Anatomy and Cell Biology for efforts that are far too often unappreciated. A thanks to Mr. Dan S. Wainman of the Neurosurgical Research Unit: a friend, peer, and co-author. A debt of gratitude goes to Dr. Edward A. MacKinnon for all your assistance. Finally, I would like to give special thanks to my entire family for your ever-lasting love and support: thank-you Ann Marie, Albert James, and my loving and dedicated bride, Carol Ann.

TABLE OF CONTENTS

LIST OF TABLES

LIST OF FIGURES

TABLE OF ABBREVIATIONS

aCSF	artificial cerebral spinal fluid
alv	alveus
AMPA	α-amino-3-hydroxy-5-methyl-isoxazole-4-propionate
AP-5	2-amino-5-phosphonovalerate
ASP	aspartate
BBB	blood brain barrier
CA	cornus ammonis
CNQX	6-cyano-7-nitroquinoxaline-2,3-dione
CNS	central nervous system
DAG	diacylgycerol
DG	dentate gyrus
DNQX	6,7-dinitroquinoxaline-2,3-dione
DOM	domoate
EAA	excitatory amino acid
Fim.	fimbria
GAMS	γ-D-glutamylaminomethyl sulfonate
GLU	glutamate
GluR	glutamate receptor
GTP	guanosine triphosphate
GYKI-52466	1-(4-aminophenyl)-4-methyl-7,8-methylenedioxy-5H-2,3-benzodiazepine HCl
ICV	intracerebroventricular
IP_3	inositol-1,4,5-triphosphate
KA	kainate
Kyn.	kynurenate
LM	stratum lacunosum moleculare
mf	mossy fibre pathway
mGluR	metabotropic glutamate receptor
NBQX	2,3-dihydroxy-6-nitro-7-sulphamoyl-benzoquinoxaline
NMDA	N-methyl-D-aspartate
NS-102	5-nitro-6,7,8,9-tetrhydrobenzol[g]indol-2,3-dione-3-oxime
OR	stratum oriens
pp	perforant pathway
PSP	paralytic shellfish poison
PYR	stratum pyramidale
RAD	stratum radiatum
Sch.	schaeffer collaterals
Sub.	subiculum
T	transmittance
TTX	tetrodotoxin

CHAPTER 1

GENERAL INTRODUCTION

I. EXCITOTOXICITY

The amino acid L-glutamate (GLU) is the most common neurotransmitter in the central nervous system (CNS). Lucas and Newhouse (1957) found that high doses of glutamate given systemically to mice induced degeneration of retinal neurons. Later, the notion of excitotoxicity was put forward by Curtis and Watkins (1960) using newly developed micro-electrophoretic techniques to examine the depolarizing and excitatory properties of GLU upon mammalian neurons. They recorded neuronal depolarizations and characterized the structural requirements for interaction with an apparent receptor. However, the nonspecific excitability evoked by GLU throughout the entire CNS and the general lack of any known process to terminate its excitatory action, initially led researchers to reject GLU as a transmitter candidate.

A. THE CONCEPT OF EXCITOTOXICITY

The concept of excitotoxicity, the ability of a group of compounds to both excite and kill neurons at low doses (Hampson *et al.* 1992), was developed in the 1970s by John W. Olney. His early studies showed that systemic administration of GLU caused acute neuronal degeneration in the mouse retina (Olney 1969a) and lesions in certain periventricular nuclei (Olney 1969b). Initial scepticism was reduced when Olney demonstrated that CNS damage also occurred in primates following either oral or subcutaneous administration of GLU

(Olney *et al.* 1972). Similar damage resulted when the GLU analogue, kainic acid (kainate, KA), was injected focally into the brain or given by intracerebroventricular (ICV) injection (Olney *et al.* 1974). Olney attributed these findings to a direct excitotoxic action by GLU or KA upon neurons (as reviewed by Meldrum 1993).

Olney initially suggested that the depolarizing effect of EAAs might be directly responsible for neuronal degeneration and cell death (Olney and Ho 1970). Subsequent authors have noted that entry of Na^+, Cl^-, H_20, and/or Ca^{2+} are the critical events determining or defining excitotoxic cell death (reviews by Rothman and Olney 1986; Olney 1990; Meldrum 1993). Ionic imbalance created by Na^+ and Cl^- flux can result in stimulation of voltage-sensitive Ca^{2+} channels and/or an influx of H_20 leading to cell swelling and putative osmotic lysis and Ca^{2+} itself may initiate a number of mechanisms which contribute to cell death as reviewed below.

More recently, Choi (1990, 1992, 1994) has characterized excitotoxicity into two main categories: rapidly triggered and slowly triggered cell death (Choi 1990; 1992). ***Rapidly triggered cell death*** involves glutamate receptor stimulation over minutes and may result in acute or delayed neuronal degeneration. The acute phenomenon is characterized by neuronal swelling dependent on Na^+ and Cl^- influx (followed by obligate water entry) with cell death occurring within minutes. Any or all ionotropic glutamate receptor subtypes (NMDA, AMPA, or kainate) may be involved. Conversely, delayed cell death occurs hours later and is dependent on fast $[Ca^{2+}]_i$ fluxes primarily through NMDA receptors. ***Slowly triggered cell death*** consists of prolonged or repeated glutamate receptor stimulation over

hours, days or perhaps years (Beal 1992). However in this scenario, neuronal degeneration is dependent on slow $[Ca^{2+}]_i$ fluxes probably primarily mediated by AMPA and/or kainate receptors or possibly via metabotropic glutamate receptors (Choi 1994, 1995). In addition, calcium may increase through voltage-sensitive calcium channels, reversal of the Na^+/Ca^{2+} exchanger, membrane-stretch activated conductances, or activation of intracellular calcium stores.

B. THREE STAGES OF GLUTAMATE EXCITOTOXICITY

The hypothesis that excitotoxicity is mediated by glutamate receptors, cell swelling, and cell $[Ca^{2+}]_i$ overload can be incorporated into a three-stage model, analogous to current models of long-term potentiation: induction, amplification, and expression (Choi 1990, 1992, 1994) (Fig. 1.1A). ***Induction*** refers to initial cellular changes and derangements immediately attributable to glutamate exposure and stimulation. The immediate result is cytoplasmic increases in Na^+, Ca^{2+}, Cl^-, H_20, IP_3 (inositol-1,4,5-triphosphate), and DAG (diacylglycerol) which serve as triggers for subsequent events. These perturbations are potentially lethal and may be sufficient alone to kill neurons, for example though acute cell swelling (Rothman 1985; Rothman and Olney 1986; Friedman and Haddad 1994). Mechanisms that regulate this stage include glutamate receptor overstimulation or decreased neuronal energy levels, the latter resulting in insufficient pre-synaptic uptake and excessive release of glutamate (Coyle and Puttfarcken 1993). The induction stage is most often associated with rapidly triggered excitotoxicity, the focus of the present study.

Following induction of glutamate toxicity, several events may amplify these initial derangements, especially local elevations in $[Ca^{2+}]_i$ (Choi 1990, 1992; Nicotera and Orrenius 1992). ***Amplification*** refers to modulatory events that heighten production of cytoplasmic constituents induced by initial glutamate exposure (Fig. 1.1A) thereby increasing injury and promoting injury of additional neurons. Further increases in intracellular calcium can be achieved by release of Ca^{2+} from intracellular stores (Choi 1992), activation of certain enzyme families (C kinases, calmodulin-regulated enzymes, calpains, and phospholipases) (Meldrum and Garthwaite 1990), stimulation of voltage sensitive calcium channels, reversal of Na^+/Ca^{2+}exchanger (Choi 1992), nitric oxide formation (Beal 1995), increased excitability to endogenous agents (e.g. quinolinic acid), decreased levels of circulating endogenous antagonists (e.g. kynurenic acid) (Jhamandas *et al.* 1994), or further release of glutamate itself (Fig. 1.1B).

The extent that amplification alone leads to neuronal death is dependent on the intensity of the initial insult. Following intense activation of NMDA receptors in cultured neurons, swelling and elevation of $[Ca^{2+}]_i$ may reach lethal levels (Choi 1987, 1990). Therefore amplification may be more important to slowly triggered excitotoxicity than to rapidly triggered excitotoxicity.

The third stage, ***expression,*** occurs when derangements set in motion a final cascade of events responsible for neuronal death (Fig. 1.1A). Sustained local elevations in $[Ca^{2+}]_i$ trigger several destructive cascades (Fig. 1.1B). Many calcium-mediated pathways have been linked to such actions. Proteases, such as the calcium-activated calpain I, have been

linked to glutamate receptor activation in the hippocampus (Siman *et al.* 1989) and can degrade major neuronal structural proteins contributing to the breakdown of the cytoskeleton. Phospholipases break down the cell membrane and liberate arachadonic acid (Choi 1992). Elevated cytosolic Ca^{2+} also liberates endonucleases resulting in degradation and fragmentation of genomic DNA (Meldrum and Garthwaite 1990). Recent evidence links DNA fragmentation with apoptosis, another Ca^{2+}-dependent process of cell death, suggesting an overlap between excitotoxically induced necrosis and programmed cell death (Gwag *et al.* 1994; Choi 1995). Another cascade involves free radicals, highly reactive molecules which extract an electron from neighboring molecules, resulting in oxidative damage. Free radicals, whose formation is dependent on calcium-triggered enzymes, can cause lipid peroxidation, protein denaturation, oxidized DNA, and inhibition of the TCA cycle resulting in membrane rigidity, damaged membrane proteins, decreased membrane integrity, DNA damage, and decreased mitochondrial respiration (Choi 1992; Coyle and Puttfarcken 1993). Enzyme candidates include phospholipase A_2 (Chan *et al.* 1985), xanthine oxidase (Dykens *et al.* 1987), and nitric oxide synthase (Garthwaite *et al.*1988; Meldrum and Garthwaite 1990; Dawson *et al.* 1991).

C. CELL SWELLING

Early researchers in the field of brain swelling in the first two decades of this century had distinguished two forms of brain swelling following injury, stroke or seizure. As described by Long (1982):

> "One was considered to be extracellular accumulation of water and was called edema. The diagnostic feature was that the cut brain wept fluid. Edema was differentiated from brain swelling, which was thought to be intracellular and characterized by the dryness of the cut brain. Brain edema was thought to be traumatic in origin while brain swelling was usually toxic or metabolic. Throughout of this period of time, the origins of brain edema and swelling were completely unknown".

Today, two forms of brain edema are recognized: vasogenic and cytotoxic. The former involves overall brain swelling due to fluid leakage from the vasculature because of openings in the blood brain barrier (BBB), whereas the latter refers to cell swelling without any loss of the normal impermeability of the BBB (as reviewed by Kimelberg 1995). Cytotoxic brain swelling is the focus of this thesis.

Recent literature reflects the critical importance that calcium plays in mediating excitotoxic neuronal death induced by glutamate (Fig. 1.1B), especially in reference to delayed or slowly triggered cell death. However, ionic fluxes and water movement mediating excitotoxic neuronal swelling may be more important in acute, rapidly triggered cell death. Rothman (1985) found in cultured hippocampal neurons, that swelling produced by GLU could be prevented by removing Cl^- from the extracellular bath. This suggested that the initial swelling was caused by Na^+ influx leading to neuronal depolarization, with secondary Cl^- and H_20 entry. These experiments suggested that the pathophysiology of EAA neurotoxicity was rather straight forward: Na^+ produces a steady depolarization which leads to an influx of chloride. Cations are then drawn into the neuron, which results in water entry and cell lysis (Rothman 1985, 1992; Rothman and Olney 1986; Choi 1987, 1990). Rothman concluded that the swelling directly led to neuronal death because cultured neurons always

swelled prior to dying and disintegrating. In the isolated chick retina, acute toxic reactions in response to GLU and GLU agonists can be abolished by the removal of Na^+ or Cl^- from the incubation medium (as reviewed by Olney 1990).

Subsequent experiments by Choi (1987) modified this hypothesis. He showed that cultured neocortical neurons could tolerate periods of swelling induced by exposure to GLU and then recover if Ca^{2+} was not present during the GLU incubation. If Ca^{2+} was added, neurons died slowly over the next 18-24 hours so for cultured neurons at least, swelling was not necessarily an antecedent of neuronal cell death. However, these experiments did not examine the *earliest* acute excitotoxic events involved in rapidly triggered cell death.

While it has been accepted that Ca^{2+} plays a crucial role in mediating excitotoxicity *in vitro*, direct evidence outside the culture dish is still lacking. Furthermore, the role of cell swelling in the excitotoxic process may not be fully appreciated in culture studies. For example, cell swelling of sufficient magnitude *in vivo* will elevate intracranial pressure and diminish brain perfusion (Rothman 1992; Kimelberg 1995). Cultured neurons may not have comparable receptor expression comparable to the *in vivo* situation. The intimate neuron-glia relationship is lost in culture monolayers so GLU uptake will be compromised. Also, such experiments did not explore the differential toxicities of various GLU agonists (NMDA vs. non-NMDA vs. metabotropic). Finally, a distinctive feature of EAA neurotoxicity is age related vulnerability (Garthwaite and Garthwaite 1990). For example, in 8 day old cerebellar slices, dividing, premigratory and migrating granule cells are insensitive to GLU agonists whereas differentiating granule cells in the internal layer are vulnerable to NMDA but not

to KA. Golgi cells are vulnerable to KA but not to NMDA. Neurons in the intracellebellar nuclei can be killed by both agonists whereas Purkinje cells at this age are not permanently damaged by either. Clear differences in the toxic profiles of various agonists are also seen in young hippocampal slices: NMDA kills all differentiating neuronal types, whereas quisqualate is more selective for CA3 pyramidal cells and KA is toxic to a scattered population (reviewed by Garthwaite and Garthwaite 1990).

More recent studies have shown that removal of Na^+ prevents anoxia-induced injury in dissociated rat CA1 hippocampal neurons and elimination of extracelluar Ca^{2+} did not prevent cell death (Friedman and Haddad 1994). Swelling of neuronal cell bodies is also observed in hypoxic hippocampal slices as measured with infrared microscopy (Dodt *et al.* 1993). Swelling in response to glutamate agonist exposure has been observed but poorly characterized. Most studies focus on cell body swelling (Ikeda *et al.* 1995; Riepe and Carpenter 1995) but dendritic volume changes may be more dynamic (Andrew and MacVicar 1994; Park *et al.* 1996). Confocal microscopy has revealed pyramidal cell body swelling in response to kainate application (Riepe and Carpenter 1995). Observations under Normarski optics have shown cell body swelling of rat cortical neurons in response to GLU itself (Ikeda *et al.* 1995). Morphological alterations and volume changes have been observed in cultured mouse neocortical dendrites in response to hypoxia or NMDA application (Park *et al.* 1996). Additionally, glial swelling in response to glutamate and GLU agonists may also play a role in excitotoxic cell death (Staub *et al.* 1993; Kimelberg 1995).

The exact mechanism by which water enters cells remains unknown and our

understanding of neuronal volume regulation is limited (Basavappa and Ellory 1996; Andrew *et al.* 1997). The discovery of aquaporin water channel proteins has provided some insight into the mechanism of membrane water permeability. Although two forms of aquaporins are found in the brain (AQ1 and AQ4), they are both primarily associated with ventricular linings and glia (King and Agre 1996). Neuronal volume regulation is largely driven by ionic conductances (e.g. ion channels, co-transporters, and exchangers) with subsequent water movement through specific water conducting channels (Somjen 1993; Basavappa and Ellory 1996). Aquaporins have been critically study in many organ systems (e.g. kidney, lung, salivary gland) but remains poorly understood in the brain and thus remains as a candidate water channel in central nervous system neurons (King and Agre 1996).

In conclusion, there is a basis for believing that excitotoxins can destroy neurons by either a rapid, acute fulminating phase which is Na^+ or Cl^- (but not Ca^{2+}) dependent, or by a prolonged process which is Ca^{2+} dependent. However, the time course and cellular compartments involved in neuronal swelling are still poorly described and remain to be resolved.

D. GLUTAMATE RECEPTOR PHARMACOLOGY

Two main types of glutamate receptors exist: metabotropic and ionotropic (Hollmann and Heinemann 1994). ***Metabotropic*** glutamate receptors activate second messenger systems through G-protein coupling. Cloning studies have revealed seven genes for metabotropic receptors based on molecular classifications, entitled mGluR1-7 (Watson and

Griddlestone 1995). mGluR1 and mGlur5 are pro-excitant, are linked to GTP and activate PLC, liberating the dual second messengers IP_3 and DAG (Choi 1990, 1992; Hollmann and Heinemann 1994; Watson and Griddlestone 1995). mGluR2-4 and 6-7 are pro-inhibitory, negatively linked to adenyl cyclase production that decreases cAMP levels. Receptor activation may decrease glutamate release, promote long term depression and decrease Ca^{2+} influxes (Choi 1992; Burt 1993).

Ionotropic glutamate receptors open cationic channels when bound. This second category is subsequently broken down into three broad subtypes based on the differential sensitivity to excitement by: (1) N-methyl-D-aspartic acid (NMDA), (2) alpha-amino-3-hydroxy-5-methyl-4-isoxazolepropionic acid (AMPA), and (3) kainic acid (KA). As revealed by molecular biology, the ionotropic receptors consist of specific subunits which determine their binding properties, cationic selectivity and degree of sensitization (Seeburg 1993). Glutamate receptor subunits can form channels in a number of combinations. Twenty-eight recombinant glutamate receptor (GluR) cDNAs have been cloned since 1989, when the first functional glutamate receptor, GluR1, was isolated (as reviewed by Hollmann and Heinemann 1994). These 28 GluR genes include 22 members of the ionotropic receptor class which are categorized into 11 subfamilies.

Molecular studies have identified two main subtypes of ***NMDA receptors*** (NMDARs). Moriyoshi *et al.* (1991) identified the cDNA for NMDAR1 by functional expression cloning. The cDNAs for the NMDAR isoforms 2A-D were cloned shortly thereafter (Maguro *et al.* 1992; Katsuwanda *et al.* 1992; Monyer *et al.* 1992). Formation of

functional NMDARs depends on the co-expression of NMDAR1 and R2, which leads to the formation of ion channels for Na^+, K^+, and fast Ca^{2+} fluxes (Michaelis 1996). NMDAR1 is the key subunit in the formation of the receptor complex. In its absence, no NMDA-activated ion channels are formed. Six separate binding sites are recognized on NMDA receptors. Three sites are associated with the extracellular domain: (1) a ligand (glutamate) site, (2) a glycine co-agonist site, and (3) a polyamine facilitatory site. Three others are associated with the receptor channel and are considered inhibitory: (1) a voltage dependent Mg^{2+} site, (2) a dissociative anesthetic site, and (3) a Zn^{2+} site (reviews by Choi 1990; Michaelis 1996).

Of interest in this study are ***non-NMDA receptors*** because of their reported affinities for domoic acid. Evidence for separate kainate and AMPA receptors came from differential sensitivity of spinal cord C-fiber afferents to kainate and quisqualate. It was later found that quisqualate also activates metabotropic receptors and it became necessary to rename the 'quisqualate receptors' to 'AMPA receptors', after the more selective agonist (Davies *et al.* 1979; review by Bettler and Mulle 1995). Ligand-binding experiments and biophysical studies using recombinant receptors indicate that four genes encode AMPA receptor subunits and five encode kainate receptor subunits.

Receptors incorporating the GluR1-4 subunits, in homomeric or heteromeric combinations, exhibit properties like those of native ***AMPA receptors*** (Keinänen *et al.* 1990; Bettler and Mulle 1995). AMPA receptor channels can be reconstituted *in vitro* by expressing any one or two of the four subunits. These subunits are approximately 900 amino

acids in length and occur in two forms with respect to an alternatively spliced exonic sequence of 38 residues (as reviewed by Seeburg 1993). The two forms, named "flip" and "flop", display different expression profiles in the mature and developing brain. The significance of this finding is demonstrated in the GluR2 subunit. Recombinant expression studies show that this subunit confers to heteromeric receptors the Ca^{2+} impermeability characteristic of some native AMPA receptors (Jonas and Sakmann 1992). This is in contrast to receptor combinations assembled from GluR1, 3, 4 subunits that are significantly permeable to Ca^{2+}, in addition to Na^{+} and K^{+}. Thus, recombinant AMPA receptors *lacking* the edited GluR2 subunit are permeable to Ca^{2+} (although 5-10 times less permeable than that of the NMDA receptor [Dingledine *et al.* 1992]).

This unique property of the GluR2 subunit has been mapped to a single residue in MD2, the second of four putative membrane domains (Hume *et al.* 1991). The critical amino acid is the product of an RNA editing mechanism that converts the CAG (glutamine/Q; Ca^{2+} permeable) codon present in the GluR1, 2, 3 transcripts into the CGG (arginine/R; Ca^{2+} impermeable) codon found in mature GluR2 mRNAs (Bettler and Mulle 1995; Brusa *et al.* 1995).

Kainate receptors consist of five known genomic subunits (GluR5-7, KA1-2) of just under 900 amino acid residues each (Watson and Griddlestone 1995). Subunits GluR5-7 represent low affinity KA receptors while KA1-2 represent the high affinity KA receptors (Hollmann and Heinemann 1994) Additionally, the GluR5-6 subunits can also assemble as heteromeric receptors in pairwise combination with the KA1-2 subunits (Bettler and Mulle

1995). Like AMPA receptors, kainate receptors mediate Na^+ and K^+ fluxes but may also, in the appropriate subunit combinations, mediate Ca^{2+} fluxes as well. RNA editing has been observed for the kainate receptor subunits GluR5-6 but not for GluR7. However unlike AMPA receptors, GluR6(R) ans GluR6(Q) are both permeable to Ca^{2+} with GluR6 having a higher Ca^{2+} permeability (Egebjerg and Heinemann 1993; Köhler *et al.* 1993).

The order of efficacy for the classical agonists, glutamate, kainate, AMPA, and domoate can be used to distinguish kainate from AMPA receptors (Fig. 1.2). In addition, the desensitization properties of AMPA and kainate receptors to these agonists further distingiush between these two receptor classes (Bettler and Mulle 1995).

In many experimental paradigms, it has been difficult to distinguish pharmacologically responses mediated by non-NMDA agonists and thus to assign categorically a receptor involved in excitation to one type or the other. AMPA receptors can mediate stimulation and most of the reported actions of kainate are mediated by AMPA receptors (Bettler and Mulle 1995). Conversely, kainate receptors have been shown to both inhibit (Chittajulla *et al.* 1996) or enhance (Terrain *et al.* 1991; Malva *et al.* 1996) glutamate release. Since the non-NMDA receptors continue to be defined by the selective agonists kainate and AMPA and despite recent advances in understanding the structure of non-NMDA receptor sub-unit proteins, the functional distinction between KA and AMPA receptors is still unclear (Zhou *et al.* 1993).

II. DOMOIC ACID

Domoic acid (DOM) is a cyclic amino acid and potent neurotoxin that is structurally related to GLU and other glutamate analogues (Fig. 1.3). It belongs to the group of amino acid analogues called excitotoxins, a term which relates to the ability of these compounds both to excite and to kill neurons at low doses (Hampson *et al.* 1992). DOM was first classified as an excitatory amino acid when it was established that it had excitatory effects on frog spinal motor neurons and rat spinal interneurons (Biscoe *et al.* 1975). Since then, the endogenous EAAs GLU and aspartate (ASP) have been characterized as the major neurotransmitters at excitatory synapses (Fleck *et al.* 1993) and the roles of EAAs in the pathophysiology of neurodegenerative disease is currently being elucidated. Specifically, EAA neurotoxicity could be a key feature of the approximately 30 neurodegenerative disorders, including chronic states such as amyotrophic lateral sclerosis, Parkinson's disease, Huntington's disease, senile dementia of the Alzheimer type and acute states such as epilepsy, stroke, traumatic head injury, food poisoning, carbon monoxide poisoning and hypoglycaemia (Shaw 1992; Spencer *et al.* 1992; Coyle and Puttfracken 1993; Meldrum 1993; Jhamandas *et al.* 1994; Cendes *et al.* 1995; Blandini *et al.* 1996).

A. HISTORY

In Moncton, New Brunswick, on November 22, 1987, two patients were admitted,

suffering from gastroenteritis and mental confusion (Todd 1990). Two additional cases were reported to the Quebec Region of the Health Protection Branch just days later (Perl *et al.* 1990; Todd 1990). These were two elderly men who had vomited and become confused with memory loss (Todd 1990). It was found that all four had eaten mussels purchased from different retail stores. However, all of the mussels, *Mytilus edulis* (Strain and Tasker 1991), originated from Prince Edward Island (Perl *et al.* 1990; Todd 1990). Samples from all cases were sent to the Research Laboratories in Ottawa for paralytic shellfish poison (PSP) testing by the mouse bioassay (Perl *et al.* 1990; Todd 1990). Although the symptoms did not include paralysis, it was decided to inject extracts into mice to either eliminate or confirm the possibility of PSP and to ascertain if any other toxic substance might be present (Todd 1990). All the mice died between 15 and 25 minutes following induction of an excitable state characterized by hind leg scratching of their shoulders, a novel reaction atypical of PSP (Perl *et al.* 1990; Todd 1990). After additional samples from P.E.I. caused the same reaction, the distribution of mussels was suspended on November 29, 1987 (Perl *et al.* 1990). As more cases were identified, Health and Welfare Canada issued a warning on December 1, 1987, advising the public to avoid eating mussels from P.E.I. (Perl *et al.* 1990, Todd 1990). However, by mid-December, over 250 cases of poisoning had occurred, including five deaths (Todd 1990).

Collaborating government and university laboratories analyzed mussels obtained from relevant homes, stores, and restaurants as well as from wild and cultivated mussel beds in P.E.I. for potential toxic agents. Acid extracts of mussel tissue were injected

intraperitoneally into CF1 white mice according to the PSP mouse bioassay (Perl *et al.* 1990). The assay was considered positive for the toxin if the mice demonstrated scratching within hours of injection (Perl *et al.* 1990). Chemists quickly isolated a compound and in December of 1987 identified the EAA domoic acid as the toxin responsible for the outbreak (Wright *et al.* 1989; Perl *et al.* 1990; Todd 1990). Since that time, study into the structure, neuronal effects, and mechanism of action of DOM has accelerated.

DOM was originally isolated from the seaweed *Chondria armata*. This belongs to the same family of algae as *Digenea simplex* from which kainic acid (KA) is derived, another GLU analogue that is structurally related to DOM (Fig. 1.3) (Stewart *et al.* 1990). However in the toxic mussel incident, the source of DOM was eventually traced to the pennate diatom *Nitzshia pungens* (Hampson *et al.* 1992; Adams and Swanson 1994). This microalga formed a dense bloom in the area of the mussel beds and was consumed by the shellfish, whereupon the DOM was retained in the digestive gland of the mussel with apparently no deleterious effect upon the host shellfish (Hamspon *et al.* 1992). Subsequent investigation uncovered the presence of three geometrical isomers and one diastereomer of the DOM molecule in the digestive glands (Wright *et al.* 1990). Several synthetic DOM derivatives were subsequently published (Hampson *et al.* 1992).

B. BEHAVIORAL EFFECTS

Some of the most convincing observations of the neuroexcitant and pro-convulsant effects of DOM stem from extensive clinical examinations of patients who suffered

deleterious effects from the contaminated mussels in 1987. Common symptoms in over 250 reported cases included both gastrointestinal and neurological problems, specifically headache, migraine, loss of short-term memory, seizure, coma, and even death (Perl *et al.* 1990; Teitelbaum *et al.* 1990; Cendes *et al.* 1995).

Teitelbaum *et al.* (1990) studied the neurological manifestations in 14 severely affected patients and assessed the neuropathological findings in four others who died within four months of ingesting the mussels. In the acute phase of the mussel-induced intoxication, the patients had headache, seizures, hemiparesis, opthalmoplegia, and abnormalities ranging from agitation to coma. On neuropsychological testing several months later, 12 of the 14 patients had severe anterograde-memory deficits. Positron-emission tomography showed decreased glucose metabolism in the medial temporal lobes, including the cerebral cortex, hippocampus, and amygdala. Another patient suffered generalized convulsions and partial progressive status epilepticus in the three weeks following ingestion. One year after the acute episode, complex partial seizures developed (Cendes *et al.* 1995).

Many behavioral studies have been carried out using animal models as well (Stewart *et al.* 1990; Sutherland *et al.* 1990; Chiamulera *et al.* 1991; Dakshinamurti *et al.* 1991; Petrie *et al.* 1991; Strain and Tasker 1991; Tasker *et al.* 1991). Subcutaneous injections of DOM (2.5 mg/kg) into adult rats resulted in repetitive head scratching, wet dog shakes, and clonic seizure activity (Stewart *et al.* 1990). Microinjections of DOM (25 ng/0.5 uL saline) into the hippocampal formation of rats exhibited long-lasting anterograde amnesia for spatial information in the Morris water task, indicating hippocampal impairment (Sutherland *et al.*

1990). Single intraperitoneal injection of DOM (2 mg/kg) into mice also resulted in significant impairment on the acquisition of the place task in the Morris water maze (Petrie *et al.* 1991). Intraperitoneal injections of DOM (4 mg/kg) also produced a series of behavioral changes including sedation, rigidity, stereotypy, balance loss, and discrete or generalized seizures (Tasker *et al.* 1991; Strain and Tasker 1991). A DOM-induced behavioral profile in rats was characterized at low doses (0.03 nmol/rat) after ICV administration by "preconvulsive" behaviours as wet dog shakes, hypermotility, increased salivation, and mild facial clonus (Chiamulera *et al.* 1991). At higher doses (0.3 nmol/rat), DOM caused clonic convulsions followed by the status epilepticus syndrome. Similar behaviourial changes were observed after ICV administration of KA or AMPA, although less potent. Subcutaneous injection of DOM (3.0 mg/kg) into Sprague-Dawley rats resulted in head scratching, wet dog shakes and clonic seizure activity (Stewart *et al.* 1990). Tasker *et al.* (1991) utilized serial systemic injections of DOM (3.4 - 430 μg/mL) in mice and established a very characteristic, dose-dependent, sequence of behavioral changes: normal, hypoactivity, sedation-akinesia, rigidity, stereotypy, loss of postural control, tremors-convulsions, and death, the order of which was very reproducible. Further evidence of DOM's role in seizure activity was shown by acute experiments using rats in which intrahippocampal administration of 100 pmol amounts of DOM led to generalized bilateral seizure discharge activity as measured by electroencephalography (Dakshinamurti *et al.* 1991).

C. HISTOPATHOLOGY

One way to measure the excitotoxic effects of DOM is through histological examination. The hippocampus has been a common research target in DOM excitotoxicity due to the original clinical observations following the 1987 outbreak (Todd 1990; Perl *et al.* 1991), previous behavioral studies (Sutherland *et al.* 1990; Chiamulera *et al.* 1991; Dakshinamurti *et al.* 1991; Petri *et al.* 1991; Strain and Tasker 1991; Tasker *et al.* 1991) and the convincing post-mortem studies of patients who died after eating contaminated mussels (Perl *et al.* 1990; Teitelbaum *et al.* 1990; Cendes *et al.*1995). Consequently, histological examination of the hippocampus has revealed many of the excitotoxic effects of DOM.

Post-mortem assessment of patients who died seven days to three months after eating contaminated mussels was reported by Teitelbaum *et al.* (1990). Neuropathological studies in the four patients who died after mussel induced intoxication demonstrated neuronal necrosis and loss predominantly in the hippocampus and amygdala. The pattern of hippocampal damage was similar to that seen in animals with neurotoxic reactions due to KA. Hippocampal necrosis was observed in H1 and H3 regions (homologues of areas CA1 and CA3 in rats) with minimal damage in H2. In two patients, there was even some cavitation and tissue collapse in area H1. Necrosis of dentate granule cells was also observed in three of four patients. Abnormalities also included astrocytosis. Another patient showed obvious atrophy of the hippocampi and dilatation of the ventricular system and microscopically, the hippocampi showed complete neuronal loss in H1 and H3, almost total loss in H4, and moderate loss in H2. Neurons in the dentate gyrus were focally diminished

in numbers (Cendes *et al.* 1995).

Strain and Tasker (1991) demonstrated the effect of systemic administration of DOM (4 mg/kg) on the mouse hippocampus using light and electron microscopic techniques. Extensive damage was observed in the CA3 region (82.1%) with lesser degrees of damage observed in other hippocampal regions (CA1>CA2>dentate granule cells). Electron microscopy of the CA3 region following DOM revealed two subpopulations of damaged neurons: i) swollen cells that exhibited vacuolization of their cytoplasm and ii) shrunken irregularly shaped electron-dense cells. Similar observations of systemically administrated DOM have also been shown in the rat (Stewart *et al.* 1990; Tryphonas *et al.* 1990). Stewart *et al.* (1990) demonstrated little change of dentate granule neurons 60-150 min post-DOM administration, but many neurons within the hilus showed advanced degenerative changes, and pyramidal neurons in layers CA1 and CA3 typically assumed a shrunken, condensed appearance.

Rats receiving microinjections of DOM (25 ng/0.5 μL saline) into the hippocampal formation that produced long-lasting anterograde amnesia (significant impairment of the place task in the Morris water maze) subsequently revealed degeneration of CA3 (95%) and CA1 (40%) pyramidal cells and dentate gyrus granule cells (65%) upon histological examination (Sutherland *et al.* 1990). Dakshinamurti *et al.* (1991) reported significant neuronal loss in the hippocampal CA3 region in response to microinjection of DOM (100 pmol) while the pyramidal cells from the CA1 and CA2 region were spared. DOM-induced lesions of the hippocampus have also been reported (Stewart *et al.* 1990; Stone 1993).

D. ELECTROPHYSIOLOGICAL EFFECTS

Microinjection of DOM (100 pmol/μL saline) into the hippocampal CA3 cell region resulted in generalized bilateral electrical seizure discharge activity, the seizure latency varying inversely with the dose (Dakshinamurti *et al.* 1991). Unitary extracellular recording in the rat hippocampus showed increased firing of both CA1 and CA3 pyramidal neurons in response to micro-iontophoresis of DOM (Debonnel *et al.* 1989a,b).

In the isolated rat spinal cord (dorsal root fibre), extracellular recordings of depolarization were recorded in response to DOM. Neuropharmacological actions of KA and several KA derivatives were also examined for electrophysiological effects in the isolated dorsal root fibre of the newborn rat. All consistently caused depolarization of the neurons with DOM causing the most significant depolarizations (Ishida and Shinozaki 1991).

E. KAINIC ACID VS DOMOIC ACID

On the basis of structural similarities (Fig. 1.3) and common origins of DOM and KA, it has been suggested that DOM has a similar profile and mechanism of action to that of KA. Much work has been done to compare and contrast these two neuroexcitants.

Previous attempts to classify DOM-receptor specificity have been ambiguous and contradictory. It is clear that DOM binds non-NMDA ionotropic receptors. Some studies suggest DOM binds KA receptors (Watkins *et al.* 1990; Krogsgaard-Larsen and Hansen 1992; Lomeli *et al.* 1992; Lanius and Shaw 1993). Other studies suggest that DOM binds AMPA receptors (Hampson *et al.* 1992). It is probable that DOM acts through both

receptors as does KA (Chiamulera *et al.* 1991; Corsi *et al.* 1993; Bettler and Mulle 1995).

Early studies by Biscoe *et al.* (1975) showed DOM to be more potent than both GLU and KA in exciting rat and frog spinal neurons. Tasker *et al.* (1991) compared behavioral toxicity produced by DOM injections with that produced by KA in mice, finding that the dose-response curves for both compounds were statistically similar and that both toxins were equally efficacious at inducing behavioral responses. However, the TD_{50} values (dosage at which 50% of experimental animals reach threshold) were 3.9 and 31.9 mg/kg for DOM and KA, respectively. They concluded that DOM was 8-11 times more potent than KA following systemic administration. Strain and Tasker (1991) demonstrated that, in general, neuronal damage was more widespread following intraperitoneal administration of KA (32 mg/kg) than DOM (4 mg/kg) in the mouse. Overall damage in the CA1 region was greater in the mice injected with KA (37.1%) than in mice injected with DOM (23.5%). In the CA3 region, however, the percentage of cells exhibiting damage was greater following DOM (82.1%) than KA (58.8%). These observations suggest somewhat different binding characteristics between DOM and KA and that the effects of these two EAAs are not identical at equitoxic doses.

Unitary cellular recordings were obtained from pyramidal neurons in response to equal concentrations of micro-ionotophoresed DOM or KA into either CA1 or CA3 regions of rat hippocampus (Debonnel *et al.* 1989a, 1989b). In both areas, the activation induced by DOM was threefold greater than that induced by KA. Rats treated with DOM at 3 nmol/rat ICV displayed clonic convulsions and status epilpeticus, while rats treated with KA showed

an almost identical behavioral profile but not until 10 nmol/rat ICV (Chiamulera *et al.* 1991).

Neuropharmacological actions of DOM, KA, and several kainate derivatives were examined for electrophysiological effects in the isolated spinal cord and the dorsal root fibre of the newborn rat. DOM consistently caused the most significant depolarization of the neurons in all cases (Ishida and Shinozaki 1991). Olney (1990) found that DOM was several times more potent than KA in destroying neurons in the chick embryo retina and in causing persistent limbic seizures and seizure-related brain damage in the adult rat. He concluded that DOM displayed a KA-like neurotoxic profile but was 3 to 5 times more potent than KA. Stewart *et al.* (1990) utilized subcutaneous administration of DOM at 2.5 mg/kg to adult rats which resulted in acute-seizure brain-damage syndrome almost identical to that induced in rats by KA but at 12.0 mg/kg.

F. ANTAGONISM OF DOMOIC ACID

Unfortunately, there are no specific DOM antagonists yet available. The endogenous, broad-spectrum EAA antagonist ***kynurenic acid*** (Schwarcz *et al.* 1990) protects mice against behavioral signs of neurotoxicity and from lethality following systemic administration of DOM-contaminated extracts of mussels (Pinsky *et al.* 1989). It also protects mice for more than 4 h against DOM-induced seizure activity (Pinsky *et al.* 1990). Protection against KA-induced toxicity by kynurenate has also been demonstrated (Gramsbergen and Smulders 1990).

Another non-NMDA antagonist, γ-D-glutamylaminomethyl sulfonic acid (***GAMS***)

displays selective antagonism of KA-receptor mediated responses in some preparations (as reviewed by Zhou *et al.* 1993). GAMS blocks myoclonic seizures induced by KA ICV injections in mice (Turski *et al.* 1985). Davies and Watkins (1985), in a study of iontophoretically applied EAA agonists and antagonists to neurons in the intact cat spinal cord, found that GAMS was a potent antagonist of KA. Another study utilized [^{3}H]-AMPA binding displacement studies to examine binding affinities for various compounds. KA was ~300x less effective in displacing AMPA while GAMS was ~3000x less effective (Giberti *et al.* 1991). These findings suggest that GAMS binds a distinct subtype of non-NMDA receptor which is specific for KA and therefore may antagonize DOM-induced responses.

The EAA antagonist 6-cyano-7-nitroquinoxaline-2,3-dione (***CNQX***) blocks the action of DOM at non-NMDA receptor sites (as reviewed by Olney 1990; Stewart *et al.* 1990; Watkins *et al.* 1990; Terrain *et al.* 1991; Malva *et al.* 1996; Tasker *et al.* 1996; Xi and Ramsdell 1996) and in conjunction with GAMS, can be used as a useful tool to distinguish the effects of KA- and AMPA-receptor mediated responses (Zhou *et al.* 1993). CNQX effectively blocked the presynaptic action of DOM-induced increases in $[Ca^{2+}]_i$ (Mavla *et al.* 1996) and neurotransmitter release (Terrain *et al.* 1991) from hippocampal mossy fibre synaptosomes and on DOM currents induced in hippocampal neurons *in vitro* (Terrain *et al.* 1991). In the chick embryo retina, DOM-induced lesions were also blocked by CNQX (Stewart *et al.* 1990). A similar antagonist, 2,3-dihydroxy-6-nitro-7-sulphamoyl-benzoquinoxaline (***NBQX***) also reduces DOM-induced depolarization, as well as the effects of KA and AMPA (Corsi *et al.* 1993; Zhou *et al.* 1993) and blocks AMPA-receptor mediated

responses (Zhou *et al.* 1993). Yet another quinoxalone, 6,7-dinitroquinoxaline-2,3-dione (***DNQX***) has similar actions (Zhou *et al.* 1993). Behavioral toxicity (speed and severity of convulsion) in mice evoked by systemic injection of DOM is reduced by both DNQX and NBQX (Tasker *et al.* 1996). Although the quinoxaline family of antagonists antagonizes DOM-mediated activity, it does not totally discriminate between AMPA and KA receptors (Honoré *et al.*1998) and thus is limited as a pharmacological tool.

New antagonists are better able to discriminate between AMPA and KA receptors. ***LY215490*** (Watson and Griddlestone 1995) and the non-competitive antagonist ***GYKI 52466*** [1-(4-aminophenyl)-4-methyl-7,8-methylenedioxy-5H-2,3-benzodiazepine HCl] (Ouardouz and Durand 1991; Donevan and Rogawski 1993; Renard *et al.* 1995; Watson and Griddlestone 1995; Rammes *et al.*1996) act specifically at AMPA receptors while ***NS-102*** [5-nitro-6,7,8,9-tetrhydrobenzol[*g*]indol-2,3-dione-3-oxime] has a high degree of specificity at kainate receptors (Johansen *et al.* 1993; Verdoon *et al.* 1994; Watson and Griddlestone 1995). An investigation of these novel compounds in antagonizing the actions of DOM has not been performed previously and is a subject of this thesis.

Finally, Hampson *et al.* (1992) showed that several synthetic DOM derivatives inhibited DOM binding at KA receptor sites in rat forebrain membranes. This suggests the possibility of developing a specific DOM antagonist by manipulating discrete functional groups within the chemical framework of the DOM molecule itself. Compounds of this nature are not yet available.

G. CURRENT OPINION ON DOMOIC ACID

Investigation into the actions and properties of DOM peaked during the late 1980's and early 1990's, but studies persist today for three primary reasons. First, DOM has become a potent tool in the investigation of the pharmacological properties of glutamate receptors. Together with the three standard ionotropic glutamate receptor agonists (NMDA, AMPA, KA), DOM has become an important agonist due to its potency and high non-NMDA specificity. In addition, DOM can be isolated in relatively large quantities and high purity levels, which is rare for a naturally produced toxin (Iverson and Truelove 1994).

Second, the toxic mussel outbreak of 1987 in Canada is not an isolated incident. Rather, DOM-contaminated seafood and algal blooms are still a threat. The coastal waters of northern California, Washington State, Oregon, Vancouver Island, Australia, and New Zealand plus other bodies of water including the Northern Adriatic Sea, Gulf of St. Lawrence, and Bay of Fundy have all tested positive for DOM contamination since 1991 (Horner *et al.* 1993; Walz *et al.* 1994; Wekell *et al.* 1994; Viviani *et al.* 1995; JS Ramsdell *personal communication*).

Finally, the issue of specificity of DOM on non-NMDA glutamate receptor subtypes remains unresolved. That is, the physiological significance of domoate interaction with AMPA-preferring receptors (GluR1-4) and high (KA1-2) and low (GluR5-7) affinity kainate receptors is still unknown. For example, the claim that DOM is a 'classical kainate agonist' is now uncertain (Tasker *et al.*1996). Certainly there is compelling evidence that both DOM and KA produce toxicity by similar mechanisms as detailed above. But although DOM and

KA share many properties, recent evidence suggests they are not biologically identical. Differences in behavioral properties of the two excitotoxins provide indirect evidence that their mechanisms of action are different (Tasker *et al.* 1991). Variability in hippocampal damage (Strain and Tasker 1991), specific binding (Kunig *et al.* 1995), and pharmacological profiles (Tasker *et al.* 1996) of DOM and KA have also been reported, implying that DOM may mediate toxicity via a slightly different pool of receptors than does KA. As such, continued investigation into DOM seems prudent.

In summary, domoic acid is a potent exogenous marine neurotoxin which is a structural analogue of the excitatory amino acids GLU and KA, belonging to a functional group termed excitotoxins. DOM is the contaminant responsible for the toxic mussel outbreak in eastern Canada in 1987 which caused a wide range of neurological disorders, including memory loss, seizures, neuronal necrosis, and death. DOM binds to non-NMDA receptors with high affinity and is a potent KA and AMPA receptor agonist. By binding to GLU receptors in the hippocampus, DOM depolarizes pyramidal neurons and leads to excitotoxicity, especially in the CA1 and CA3 regions. The potency of DOM is several times that of KA and patterns of toxicity can be different. The action of DOM is blocked by CNQX, DNQX, NBQX, or kynurenic acid and is potentially blocked by GAMS while newer antagonists such as GYKI 52466 and NS-102 may be used as tools to determine specific receptor binding.

III. THE HIPPOCAMPUS

The hippocampal formation represents a cortical structure with well defined dendritic/somatic layers and axonal pathways. One of the main advantages of using the hippocampal slice is that cell body and dendritic zones are laminar and therefore visually distinct using light microscopy. The advantages of *in vitro* brain slices over cell culture are numerous. First, intimate neuron/glia interactions remain intact. Second, a large spatial resolution is possible, allowing for immediate side-by-side comparisons between different hippocampal sub-regions (CA1 vs CA3 vs DG). Third, the heterogeneity of glutamate receptors in the hippocampus is maintained and fourth, local electrical neuronal circuitry is also maintained (Fig. 1.4). Finally, extrinsic factors (temperature, pH, osmolality, bath applied agonists) can be precisely and rapidly altered and controlled. Additionally, a real-time view of volume changes can be observed, unlike *in vivo* preparations (as reviewed by Kimelberg 1995). Disadvantages include a lack of extrinsic hippocampal circuitry and an inability to study long term activities (i.e. over eight hours). As well, high affinity uptake mechanisms very effectively limit the diffusion of glutamate and thus application of other EAA agonists are preferred. Figure 1.4 provides a schematic representation of the anatomy of the transverse hippocampal slice.

A. THE LIMBIC SYSTEM

The limbic system can be defined as a series of medioparasagittal C-shaped structures including the cingulate gyrus, parahippocampal gyurs, hippocampal formation, fornix, and amygdala (Burt 1993). These structures, the connections between them, and in conjunction with neocortical association areas, play key roles in behavioral expression of emotion, learning, memory, conditioned responses, feeding and thirst, and olfaction (Martin 1989; Burt 1993). Most of the components of the limbic system are located close to the midline forming a complex three dimensional configuration (Martin 1989).

B. HIPPOCAMPAL ANATOMY

The hippocampal formation in the rat consists of three major portions: Ammon's horn (hippocampus proper), the subiculum (*Sub.*), and the dentate gyrus (*DG*) (Fig. 1.4). The hippocampus proper is further subdivided into three cell body areas: CA1, CA2 and CA3. Each area of the hippocampus proper, in transverse section, contains the histological layers: alveus (*alv*), stratum oriens (*OR*), stratum pyramidale (*PYR*), stratum radiatum (*RAD*) and stratum lacunosum moleculare (*LM*).

The cells are linked in a trisynaptic circuit via four excitatory pathways (Lopes de Silva *et al.* 1990) (Fig. 1.4). The perforant pathway (*pp*) provides the entorhinal cortical projection to the hippocampus and makes synaptic connections with granule cell dendrites of the dentate gyrus. The mossy fibre pathway (*mf*) consists of axons from dentate granule cells which form synaptic connections with the apical dendrites of CA3 pyramidal cells.

Axons which extend from the CA3 pyramidal cell bodies bifurcate, the main branch running in the fimbria (*Fim.*) and the collaterals forming the Schaeffer collateral/commissural pathway (*Sch.*) which curves back through CA3 and synapse with the apical dendrites of the CA1 pyramidal cells. CA1 axons also bifurcate, one branch which travels to the subiculum and the other to the fimbria, joining axons from area CA3 to travel to the septum, hypothalamus, bed nucleus of the stria terminalis, nucleus accumbens, and contralateral hippocampus.

C. GLUTAMATE RECEPTOR DISTRIBUTION

GLU immunoreactivity is high in target zones of these excitatory afferents (as reviewed by Schröder 1993). ***NMDA receptors***, revealed by autoradiography of displaced [^{3}H]L-glutamate, are found predominantly in the RAD and OR of area CA1 and inner portions of the DG molecular layer (Monaghan *et al.* 1983; Cotman *et al.* 1987; Insel *et al.* 1990; Schröder 1993). Only moderate levels are found in RAD and OR of CA3. Labeled binding of NMDA receptors peaks at postnatal day 21 with intensity levels CA1>DG>CA3 (Insel *et al.* 1990). mRNA for NMDAR1 is found in both DG granule cells and pyramidal cells of CA1-CA3 (Moriyoshi *et al.* 1991). Although mRNA expression is equally abundant between CA1 and CA3, ligand binding is less pronounced in CA3 than in CA1 (as reviewed by Schröder 1993). Post-synaptic localization of NMDA receptors has been shown on dendrites in cultured hippocampal neurons (Mattson *et al.* 1991) and in areas CA3 and CA1 of the hippocampal slice (Spruston *et al.* 1995).

In general, ***AMPA receptor*** subtypes co-localize with NMDA receptors in the hippocampus, with the highest levels found in CA1 RAD and OR (Cotman *et al.* 1987). In adulthood, intensity of [^{3}H]AMPA binding is CA1>DG>>CA3 (Insel *et al.* 1990). Immuno-labelling for the GluR1 receptor protein (the AMPA receptor subtype most sensitive to DOM) reveals densely stained dendrites in the CA1 RAD with "spotted" labeling in the CA1 OR and CA1 LM (as reviewed by Schröder 1993). In-situ hybridization localized GluR1 mRNA in CA1 and partially in CA3. In CA3, the labeling was often lacking (Blackstone *et al* 1992). Using separate antibodies to GluR1, GluR2/3 and GluR4, a dense labeling for GluR1 and GluR2/3 with lighter staining for GluR4 is observed in all hippocampal regions. However, within the stratum radiatum of CA1-CA3, immunoreactive profiles for GluR1-4 are positive only in CA1. Ultrastructurally, there is dense postsynaptic labelling but no presynaptic labelling (Petralia and Wenthold 1992; as reviewed by Schröder 1993). All AMPA GluR subunits are confined to spines, dendritic membrane, and cytoplasm surrounding the nucleus but absent from axons and presynaptic terminals (Leranth *et al.* 1996). In rat hippocampal cultures, a GluR1 antibody stained all neurons within the somata and dendrites but not the axons. Variable degrees of staining occurred in different individual neurons between the dendritic spines and the dendritic shafts. Essentially identical distributions were obtained with a GluR2/3 antibody (Craig *et al* 1993).

Hippocampal binding sites for ***kainate receptors***, in general, exhibit a distribution complimentary to that of NMDA and AMPA receptors (Cotman *et al.* 1987). Kainate receptors bound by [^{3}H]kainate are primarily concentrated in the stratum lucidum of CA3

and secondarily in the molecular layer of the DG with significantly lower levels (4-10x lower) in CA1 RAD and OR (Ulas *et al.*1990). Labeled binding of kainate receptors in CA3 and DG peaks at postnatal day 21 with intensity levels CA3>DG>CA1 (Miller *et al.* 1990). KA1 mRNA distribution (high affinity KA receptor mRNA) was studied in the rat (as reviewed by Schröder 1993). Highest levels were expressed in CA3 pyramidal neurons with the CA1 region largely devoid of label. This distribution is similar to the high levels of high-affinity [^{3}H]kainate binding observed in the rat CA3 and DG regions but not in CA1. The distribution for combinations of the high and low affinity kainate receptor subunits (GluR5-7 and KA1-2) is particularly characteristic of the CA3 region of the hippocampus (as reviewed by Seeburg 1993). Additionally, post-synaptic kainate receptors have not been identified in adult hippocampal neurons. Rather, kainate receptors are localized presynaptically in the CA3 subregion (Represa *et al.* 1987; Miller *et al.* 1990; reviewed by Henley 1995) and may promote (Terrain *et al.* 1991; Malva *et al.* 1996) or inhibit (Chittajulla *et al.* 1996) toxicity in the CA3 in the presence of an intact mossy fibre projection.

IV. INTRINSIC OPTICAL SIGNALS

Intrinsic optical signals can be defined as the light that is reflected, absorbed, or transmitted by an object (Fig. 2.1). Changes in light scattering that develop over a period of seconds and were thought to represent swelling during neuronal activity, were first demonstrated in crab nerve (Hill and Keynes 1949; Hill 1950; Cohen and Keynes 1971; Cohen 1973) and in cerebral cortical slices (Lipton 1973). More recently, changes in the intrinsic optical properties of nerve tissue have been reported to be correlated with neuronal activity (Grinvald *et al.* 1986; Lieke *et al.* 1989; MacVicar and Hochman 1991; Frederico *et al.* 1994) and evidence has accumulated that the predominant source of the signal in the brain slice is cellular swelling (Andrew and MacVicar 1994; Kriesman *et al.*1995; Turner *et al.* 1995; Holthoff and Witte 1996). However alterations to the way that light passes through brain tissue may arise in several ways.

What are we imaging? Imaging the brain *surface* involves gathering scattered (reflected) light; imaging the brain *slice* involves collecting minimally scattered (transmitted) light. When stimulated, brain tissue *in situ* undergoes cytochrome reduction, increased blood flow, hemoglobin oxidation and cell swelling, each decreasing reflectance because of absorbency at certain wavelengths. However, cell swelling decreases reflectance by reducing light scattering across the spectrum (Federico *et al.* 1994). In submerged brain slices, reduced scattering means increased transmittance (particularly at the longer wavelengths)

whereas absorbency appears to be a minor factor (MacVicar and Hochman 1991)

Imaging analysis techniques have been used to observe changes in intrinsic optical signals in brain tissue. Grinvald and colleagues (1986) recorded changes in reflectance in activated areas of cat and rat brain cortex. These techniques have been used to image functional organization of primate (Ts'o *et al.* 1990) and cat (Bonhoffer 1995) visual cortex. This technology has been modified to measure changes in light transmittance (LT) in brain slices (MacVicar and Hochman 1991).

Increases in LT through hippocampal slices during synaptic stimulation are post-synaptic in origin (MacVicar and Hochman 1991). Additionally, transmittance increases in response to hypo-osmotic aCSF have also been imaged in the submerged hippocampal slice (Andrew and MacVicar 1994; Kreisman *et al.* 1995; Andrew *et al.* 1997). More recently, large changes in transmittance have been measured in area CA1 of the hippocampal slice, an area susceptible to damage by stroke, in response to lowered oxygen and glucose levels (Obeidat and Andrew 1994; Turner *et al.* 1995). Neo-cortical brain slices have also been used in IOS studies. Holthoff and Witte (1996) used juvenile rat slices to monitor synaptically evoked changes while Rolfe and Andrew (1996) examined glutamate agonist-induced transmittance induced by exogenously applied NMDA and KA.

Cell swelling decreases light scattering (McGann *et al.* 1988; McMannus *et al.*1993). In other words, as LT increases through brain tissue, reflectance decreases (Lipton 1973; MacVicar and Hochman 1991) and reflectance will be reduced across a wide light spectrum: a non-specific wavelength response. Using a series of filters (MacVicar and Hochman 1991)

or a wide band spectrometer (Kriesman *et al.* 1995; Andrew *et al.* 1997) to analyze LT through hippocampal slices shows a continuous spectrum of change across the light spectrum, a characteristic implicating cell swelling as the source of the transmitted signal. Others have shown *in vivo* that there are also wavelength specific changes not associated with cell swelling, such as cytochrome oxidation or hemoglobin reduction (Grinvald *et al.* 1986). However, cell swelling appears to be a major source of intrinsic signals in the slice preparation (MacVicar and Hochman 1991; Andrew and MacVicar 1994). Spectral analysis of the transmitted light can therefore be used to implicate cell swelling as a source of the intrinsic optical signal.

Cell swelling is also indicated by extracellular resistance measurements (Traynelis and Dingledine 1989; Andrew *et al.* 1997). This approach involves producing a transient electrical field across a hippocampal slice and measuring voltage deflections in response to changes in cell volume (Fig. 2.1). An increased voltage change indicates cell swelling, based on the assumption that the system obeys Ohm's Law (V=IR). In other words, under a constant current, *increased* resistance due to shrinkage of extracellular space and cellular swelling results in increased voltage deflection across the tissue. Measurement of extracellular electrical resistance in hippocampal slices during spreading depression revealed an associated increase in tissue resistance, suggesting that the extracellular space is decreased and cell volume has increased during the time that neurons strongly depolarize (Traynelis and Dingledine 1989). Changes in cell volume in response to osmotic stress in the hippocampal slice correlate well with both changes in LT and extracellular tissue resistance

(Andrew *et al.* 1997). Measurement of extracellular tissue resistance can therefore be used as an independent indicator of cell volume change.

The use of intrinsic optical signal imaging is proving to be a valuable tool in neuroscience research but the underlying physiological events are only now being established. The biophysical processes underlying changes in the intrinsic optical properties of neurons remain unknown. Changes in light scattering by biological cells may include a combination of many possibilities, such as (1) decreased "wrinkling" of the plasma membrane; (2) diffraction of light at the edges of cells; (3) refraction due to differences in the refractive index of medium, cytoplasm, and extracelluar space; (4) reflection from subcellular organelles; and (5) opacity of cytoplasm. Understanding the spatio-temporal features of physiological and pathological neuronal activity requires monitoring of populations of neurons that classical intracellular and extracellular electrophysiological techniques cannot provide. Consequently, complimentary techniques which permit the monitoring of large brain areas over time are of continued interest.

V. HYPOTHESIS

This literature review has examined and discussed both historical and current opinions about glutamate excitotoxicity, the marine toxin domoic acid, the hippocampal formation of the mammalian brain, and the use of intrinsic optical signals in brain research. As such, it has been clearly established that:

1. Early excitotoxic events involve cell swelling mediated by ionic fluxes.
2. Domoic acid is an excitotoxic glutamate agonist.
3. The rodent hippocampus contains ionotropic glutamate receptors.
4. Cell swelling increases light transmittance through brain tissue.

Therefore, the following hypothesis was tested: Domoic acid exposure evokes events involving acute neuronal swelling and cell death which can be imaged as a dynamic spatio-temporal process in the hippocampal slice to reveal new aspects of excitotoxicity.

VI. FIGURES

Figure 1.1: Theoretical schemes of excitotoxicity. **A)** Choi's three stages of glutamate toxicity. (Adapted from Choi 1992; 1994) **B)** Summary of potential routes of excitotoxic glutamate pathways emphasizing the central role of calcium in mediating neuronal death (©Trevor M. Polischuk 1997).

A)

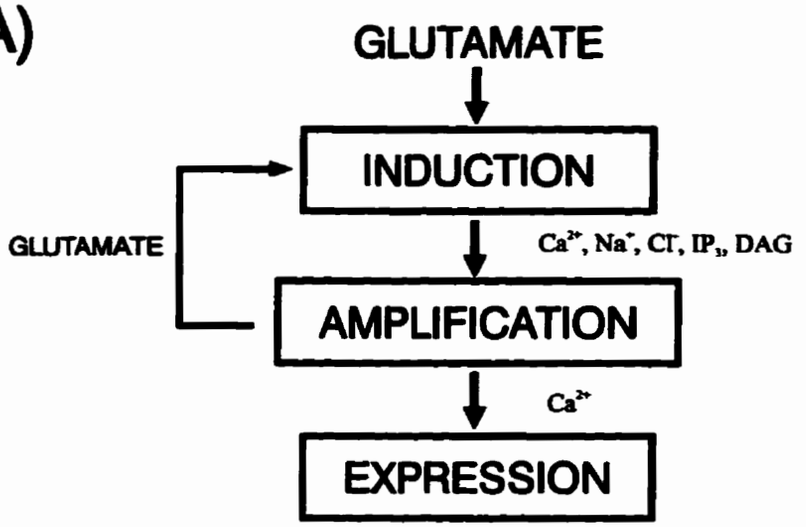
GLUTAMATE
INDUCTION
GLUTAMATE
Ca^{2+}, Na^{+}, Cl^{-}, IP_3, DAG
AMPLIFICATION
Ca^{2+}
EXPRESSION

B)

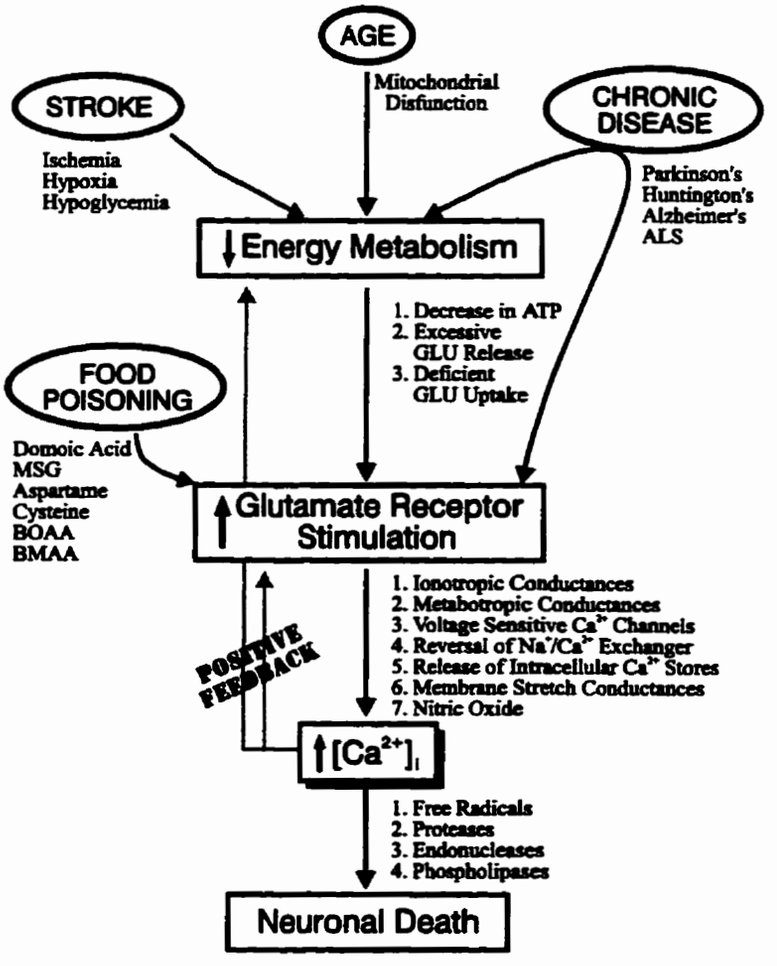
AGE
Mitochondrial Disfunction
STROKE
Ischemia
Hypoxia
Hypoglycemia
CHRONIC DISEASE
Parkinson's
Huntington's
Alzheimer's
ALS
↓Energy Metabolism
1. Decrease in ATP
2. Excessive GLU Release
3. Deficient GLU Uptake
FOOD POISONING
Domoic Acid
MSG
Aspartame
Cysteine
BOAA
BMAA
↑Glutamate Receptor Stimulation
1. Ionotropic Conductances
2. Metabotropic Conductances
3. Voltage Sensitive Ca^{2+} Channels
4. Reversal of Na^{+}/Ca^{2+} Exchanger
5. Release of Intracellular Ca^{2+} Stores
6. Membrane Stretch Conductances
7. Nitric Oxide
POSITIVE FEEDBACK
↑$[Ca^{2+}]_i$
1. Free Radicals
2. Proteases
3. Endonucleases
4. Phospholipases
Neuronal Death

Figure 1.2: Phylogenetic relationship among cloned AMPA and kainate receptor subunits. The order agonist efficacy and binding affinity is indicated. *DOM*, domoate; *KA*, kainate; *GLU*, glutamate. (Adapted from Bettler and Mulle 1995)

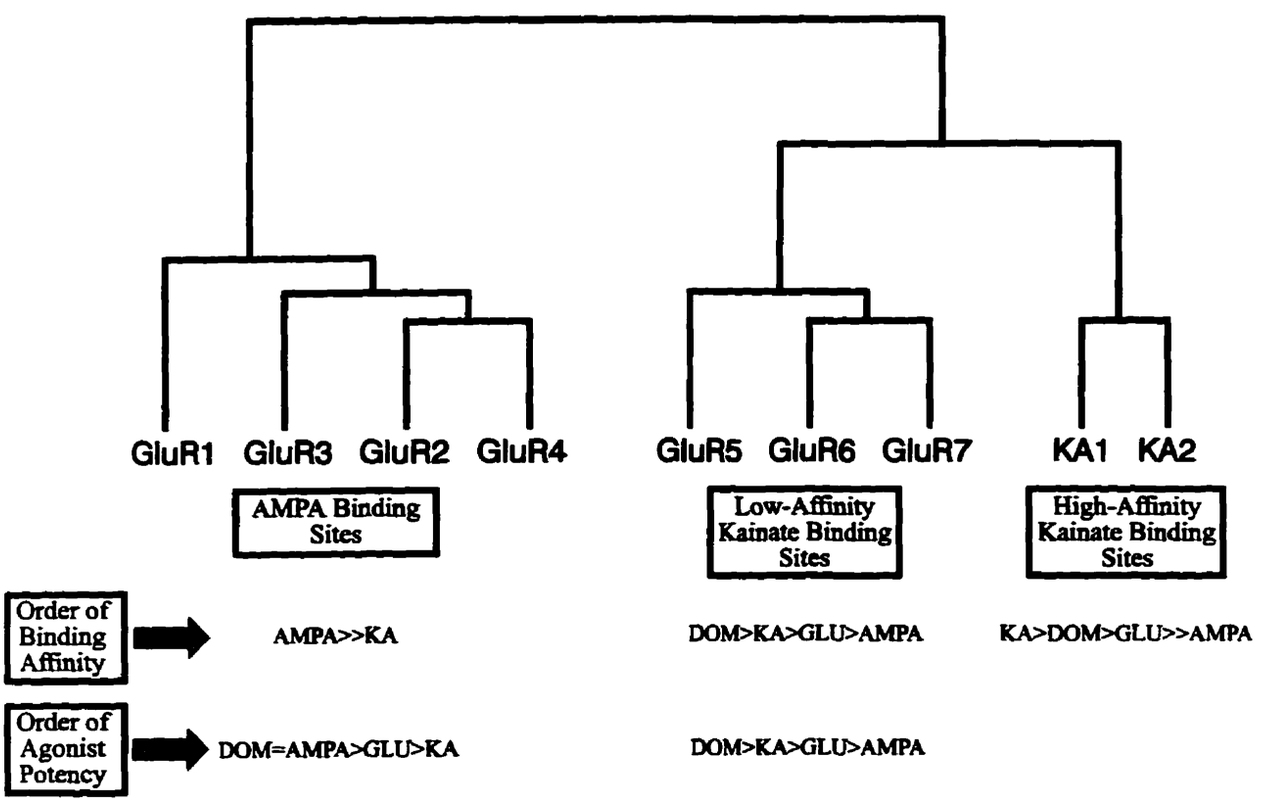
GluR1
GluR3
GluR2
GluR4
GluR5
GluR6
GluR7
KA1
KA2
AMPA Binding Sites
Low-Affinity Kainate Binding Sites
High-Affinity Kainate Binding Sites
Order of Binding Affinity
AMPA>>KA
DOM>KA>GLU>AMPA
KA>DOM>GLU>>AMPA
Order of Agonist Potency
DOM=AMPA>GLU>KA
DOM>KA>GLU>AMPA

Figure 1.3: The chemical structure of domoic acid, glutamic acid and kainic acid. (Adapted from Teitelbaum *et al.* 1990)

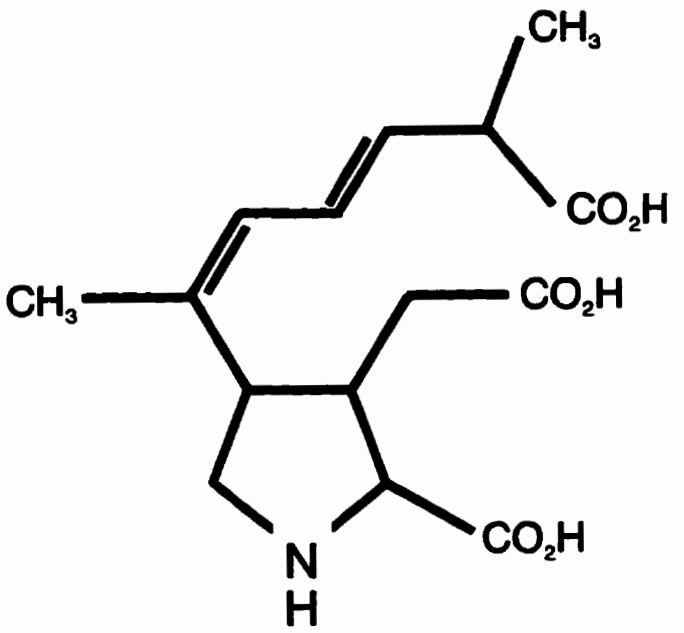

Domoic acid

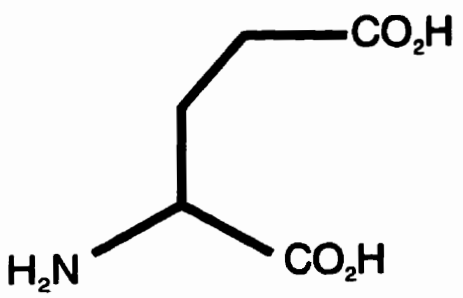

Glutamic acid

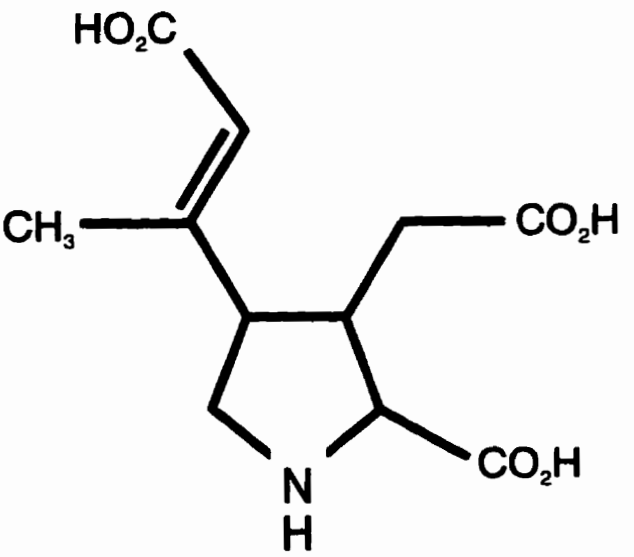

Kainic acid

Figure 1.4: Anatomy of the transverse hippocampal slice. Extracellular field recordings were made in the stratum pyramidale (*PYR*) of CA1. Axons of the Schaeffer collateral pathway (*Sch*) in the stratum radiatum (*RAD*) were stimulated which orthodromically activated CA1 dendrites. *alv* alveus; *Fim.* Fimbria; *GC* granule cells of the dentate gyrus; *LM* stratum lacunosum moleculare; *mf* mossy fibre pathway; *pp* perforant pathway; *OR* stratum oriens; *Sub.* subiculum. (Diagram by R.D. Andrew)

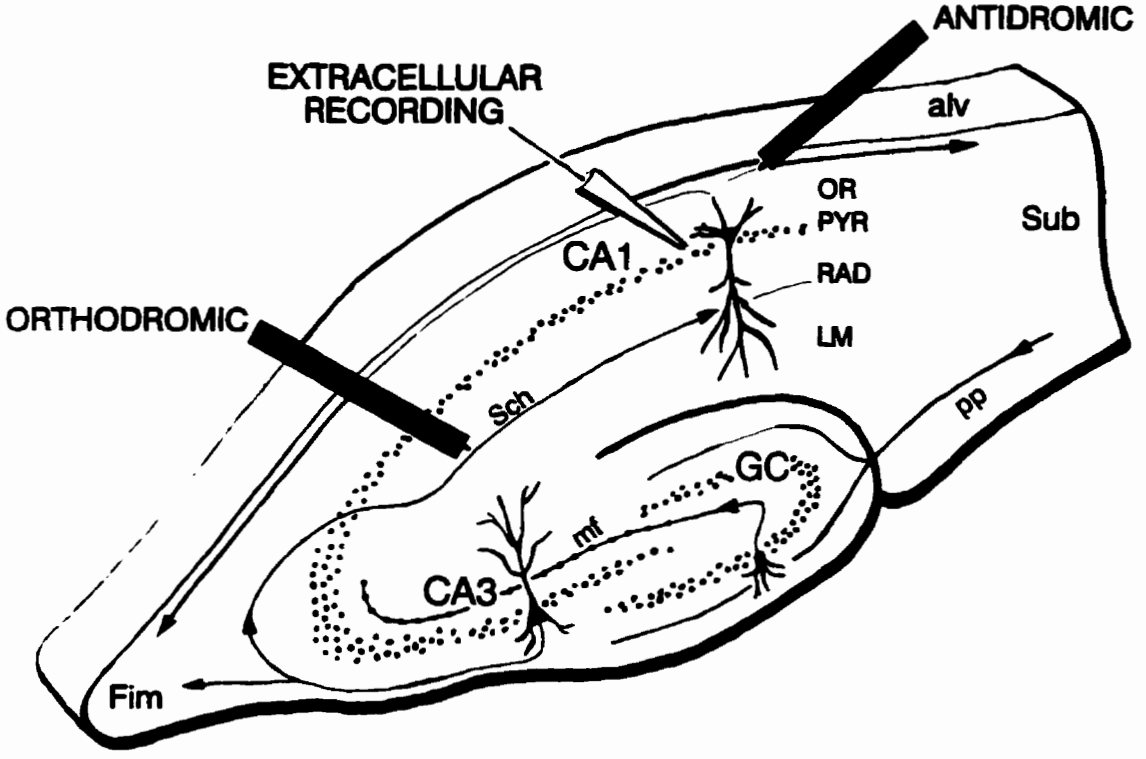
ANTIDROMIC
EXTRACELLULAR
RECORDING
alv
OR
PYR
Sub
CA1
RAD
ORTHODROMIC
LM
Sch
pp
GC
mf
CA3
Fim

CHAPTER 2

REAL-TIME IMAGING OF INTRINSIC OPTICAL SIGNALS DURING EARLY EXCITOTOXICITY EVOKED BY DOMOIC ACID IN THE RAT HIPPOCAMPAL SLICE

Canadian Journal of Physiology and Pharmacology **74**:712-722 (1996)

ABSTRACT

Excitotoxicity involves neuronal depolarization and eventual cell death primarily through excess activation of glutamate receptors. Neuronal cell swelling is considered an early excitotoxic event mediated by ionic influx (mainly Na^+ and Cl^-) followed by water. Changes in the intrinsic optical signals of nerve tissue correlate with neuronal activity such that light transmittance (LT) increases across the brain slice as cells swell. The present study examined the effects of domoic acid, a potent excitotoxic food contaminant and glutamate analogue, on intrinsic optical signals in the rat hippocampal slice. A brief 1 min exposure to 10 μM domoate at 22°C elevated LT by 58% in the apical dendritic region of CA1 and, to a lesser extent, in the molecular layer of the upper dentate gyrus. The responses peaked by 5 min and slowly reversed during a 30 min wash. The same responses were evoked by a 1 min application of 10 μM AMPA (α-amino-3-hydroxy-5-methyl-isoxazole-4-propionate) at 22°C. Minor changes were observed in the CA3 region and the lower blade of the dentate gyrus. At 37°C, exposure to 10 μM domoate for 10 min resulted in apparent irreversible neuronal damage in the CA1 and upper dentate regions.

The Na^+ channel blocker tetrodotoxin (1 μM) eliminated the evoked CA1 population spike but not the LT increase, indicating that the domoate signal is not associated with action potential discharge pre- or postsynaptically. However, the response to domoate at 22°C was reversibly blocked by the non-specific glutamate receptor antagonist kynurenate and the non-

NMDA (non-N-methyl-D-aspartate) receptor antagonists CNQX (6-cyano-7-nitroquinoxaline-2,3-dione) and DNQX (6,7-dinitroquinoxaline-2,3-dione). The response was *not* blocked by the NMDA receptor antagonist AP-5 (2-amino-5-phosphonovaleate) nor the kainate receptor blocker GAMS (γ-D-glutamylaminomethyl sulfonate). Relative tissue resistance (R_{REL}) measured across the CA1 dendritic region increased rapidly in response to domoate and fell slowly over 30 min, which parallelled the LT response described above. The increase in R_{REL} was blocked by kynurenate.

We propose that domoate binding to AMPA receptors open channels mediating ionic influx, presumably Na^+ followed passively by Cl^-. Water follows, producing prolonged post-synaptic swelling in the CA1 and dentate regions where AMPA receptors are most abundant. At higher temperature this swelling can progress to permanent neuronal injury. Imaging intrinsic optical signals allows a real-time view of early excitotoxic events and so may prove useful in assessing potentially therapeutic agents that reduce damage induced by excitotoxic agents or ischemia.

[*Key Words*: excitotoxicity, CA1, cell swelling, light transmittance, AMPA, glutamate, imaging]

INTRODUCTION

Excessive activation of glutamate receptors causes neuronal damage, a phenomenon termed excitotoxicity (Olney 1990; Beal 1992). Domoic acid is a naturally occurring cyclic amino acid produced by marine algae and seaweed (Takemoto 1978; Adams and Swanson 1994) with structural similarities to that of glutamate (Wright *et al.* 1989). Domoate was first classified as an excitatory amino acid when it was shown that it evoked discharge in frog spinal motor neurons and rat interneurons (Biscoe *et al.* 1975). In 1987, an outbreak of food poisoning in eastern Canada resulted from human consumption of mussels contaminated with domoate (Wright *et al.* 1989). Symptoms ranged from headache and nausea to memory loss, seizure, coma and in some cases, death (Perl *et al.* 1990; Teitalbaum *et al.* 1990). This firmly established domoate as a potent excitotoxin. It acts as a glutamate receptor agonist of the non-N-methyl-D-aspartate (non-NMDA) subtype (Stewart *et al.* 1990; Hampson *et al.* 1992; Corsi *et al.* 1993). NMDA receptors may directly mediate abnormal rises in intracellular Ca^{2+} that may trigger degenerative processes (Choi 1987). However, there is recent evidence for an involvement of non-NMDA receptors in pathological processes (Choi 1990; Sheardown *et al.* 1990; Teitalbaum *et al.* 1990; Kaku *et al.* 1991; Mosinger *et al* 1991; Beal 1992; Peillet *et al.* 1992; Smith and Meldrum 1992; Buchan *et al.* 1993; Li and Buchan 1993; Chen *et al.* 1995; Lees 1996).

In cultured neurons, the early excitotoxic state is characterized by an acute

fulminating phase of ionic fluxes and associated inward water movement that causes neuronal swelling and possibly osmolysis (Rothman 1985; Rothman and Olney 1986; Choi 1987; Choi 1990; Rothman 1992). However in the intact brain, the study of early excitotoxic events at the cellular level is difficult. Histological evidence shows that swelling of neuronal cell bodies is an early excitotoxic event in the ischemic brain, a process also observed in brain slices using infrared microscopy (Dodt *et al.* 1993). However one might expect swelling first in dendritic regions, the predominant site of glutamate binding (Cotman *et al.* 1987).

Changes in the intrinsic optical properties of brain tissue are correlated with neuronal activity (Grinvald *et al.* 1986; Lieke *et al.* 1989; MacVicar and Hochman 1991; Federico and MacVicar 1993) and cellular swelling (Andrew and MacVicar 1994; Kreisman *et al.* 1995; Turner *et al.* 1995; Holthoff and Witte 1996). Changes in light scattering, thought to represent swelling during neuronal activity, has been demonstrated in crab nerve (Hill and Keynes 1949; Hill 1950; Cohen and Keynes 1971; Cohen 1973) and in cerebral cortical slices (Lipton 1973). Alterations, then, to the way that light passes through brain tissue can provide information about regional activation.

The present study utilizes a recently developed method for examining intrinsic optical signals associated with cell volume changes, producing a real time view of early excitotoxic events in the rat hippocampal slice evoked by the potent glutamate agonist, domoic acid.

METHODS

Hippocampal Slice Preparation

The animals used in this experiment were cared for in accordance with the priciples and guidelines of the Canadian Council on Animal Care. Male Sprague-Dawley rats, 21-28 days old (Charles River, St. Constant, Quebec, Canada) were housed in a controlled environment (25°C, 12 hour light/dark cycle) with food and water available *ad libitum*. A rat was placed in a rodent restrainer and guillotined. The excised brain was hemisected and each hippocampus exposed under cold artificial cerbrospinal fluid (aCSF). Transverse slices were cut (400 μm) using a manual tissue slicer and stored at 22°C in aCSF oxygenated with 95% O_2/5% CO_2. Slices were incubated in aCSF for a minimum of 1 hour before being transferred to the imaging chamber.

The aCSF contained (in mM): NaCl 120.0, KCl 3.3, $NaHCO_3$ 26.0, $MgSO_4$ 1.3, NaH_2PO_4 1.2, D-glucose 11.0, and $CaCl_2$ 1.8 dissolved in distilled water at pH 7.3-7.4. The aCSF was used for the dissection of the hippocampus, for the incubation and superfusion of slices, and as a vehicle for drug administration. The osmolality of the aCSF and its variants was 295 ± 2 mOsm as measured with a freezing point depression osmometer (Precision Systems Inc.). High K^+ aCSF was produced by elevating KCl to 40 mM and re-adjusting the osmolality with distilled water. This reduced the concentration of all aCSF constituents other than KCl by approximately 25%.

Domoate (DOM), kynurenate (KYN), α-amino-3-hydroxy-5-methyl-isoxazole-4-

propionate (AMPA), γ-D-glutamyl-aminomethyl-sulfonate (GAMS), and tetrodotoxin (TTX) were obtained from the Sigma Chemical Co. (St. Louis, MO). 2-amino-5-phosphonovaleate (AP-5), 6-cyano-7-nitroquinoxaline-2,3-dione (CNQX), and 6,7-dinitroquinoxaline-2,3-dione (DNQX) were obtained from RBI (Natick, MA).

Imaging Intrinsic Optical Signals

Intrinsic optical signals were monitored using techniques previously described (MacVicar and Hochman 1991; Andrew and MacVicar 1994). A slice was transferred to an imaging chamber where it was weighted at the edges with silver wire and submerged in flowing, oxygenated aCSF (2.0 mL/min) at 22°C or 37°C. The slice was viewed with an inverted microscope with only a coverslip between the slice and the 1.6x objective (Fig. 2.1A). Slices were transilluminated from above by a halogen lamp with a voltage regulated power supply (Leica). Video frames were obtained at 30 Hz using a charge-coupled device (CCD camera) which was set for maximum gain and a medium black level. Frames were averaged and digitized using an image processor board (DT3867, Data Translation) in a 486 computer controlled by Axon Imaging Workbench software (Axon Instruments) as diagrammed in Figure 2.1A. Each averaged image was stored on a removable hard drive (Bernoulli).

Experiments entailed acquiring an averaged image every 8 seconds (256 frames @ 30 Hz). The first averaged image in a series served as a control (T_{cont}) which was subtracted from each subsequent experimental image (T_{exp}) of that series. A series of subtracted images

revealed areas in the slice where light transmittance (LT) changed over time. LT was expressed as the digital intensity of the subtracted image (T_{exp}-T_{cont}) divided by the gain of the intrinsic signal which was set using the software program. This value was then expressed as a percentage of the digital intensity of the control image of that series. That is,

$$LT = \frac{(T_{exp}-T_{cont}) / gain}{T_{cont}} \times 100\% = \frac{\Delta T}{T}\%$$

The control image was displayed in bright field using a gray intensity scale. Each subtracted image was displayed using a pseudo-colour intensity scale. With gamma set to 1.0, the output of the CCD is linear with respect to change in light intensity. To quantify and graphically display data, regions of interest (ROI) were boxed using the Axon Imaging Workbench software. The average digital intensity of each ROI was sampled, stored as text files, and graphed using SigmaPlot for Windows software (Jandel Scientific). A graphics program (CorelDRAW 3.0) was used to import and label images. Statistical analysis was performed using a Student-t test.

Measurement of Relative Tissue Resistance (R_{REL})

Slices (600 μm thick) were pinned at the edges with 0.1 mm stainless steel pins to a strip of lens paper overlying a Sylgaard matrix in the recording chamber. Oxygenated (95% O_2/5% CO_2) aCSF was delivered at 0.5-1.0 mL/min. Both the chamber and the aCSF were at 22°C. The slice was transilluminated from below with a fibre optic light source and

viewed through a dissecting microscope. The level of aCSF was kept just above the upper surface of the slice and the stimulating electrode tips were embedded approximately 100 μm in the slice to better confine the evoked current field within the tissue. The measurement of tissue resistance is "relative" because some current must flow above the slice if it is to remain submerged.

The electrical resistance of hippocampal tissue was evaluated using a modification of the method used by Traynelis and Dingledine (1989). A biphasic square current pulse (50 ms duration; 50-70 nA; 3 Hz) was passed between two sharpened stimulating electrodes (Rhodes Electronics) positioned 5 mm apart in the CA1 RAD (Fig. 2.1B). The amplitude of the 50 ms voltage deflection plateaued within 5 ms and was measued at its midpoint (i.e. at 25 ms) to rule out capacitive effects. Two glass micropipettes (5-20 MOhms) positioned 150-250 μm apart and placed between the stimulating electrodes differentially recorded the voltage change during stimulation (Fig. 2.1B). Voltage signals were taped, averaged and the amplitude measured with Pclamp software (Axon Instruments) to determine changes in relative voltage. The relative tissue resistance (R_{REL}) was calculated using Ohm's Law and values were plotted over time.

RESULTS

Regional response

A series of pseudo-coloured images showed a rapid progressive increase in light transmittance (LT) in CA1 stratum radiatum (RAD) in response to a 1 min exposure of 10

μM domoate (Fig. 2.2A) at 22°C. Smaller responses were observed in the CA1 stratum oriens (OR), CA1 stratum pyramidale (PYR), stratum lacunosum moleculare (LM), and the upper dendrtic blade of the dentate gyrus (upper DG). LT peaked rapidly after the domoate application and then slowly returned to original levels during a 30 min wash (Fig. 2.2A).

Neither separately increasing the domoate exposure time to 10 min nor increasing the temperature to 37°C affected the reversibility of the response (data not shown). However, when *both* parameters were increased together, a complex and irreversible sequence developed (Fig. 2.2B). Initial LT increases in both the CA1 RAD and OR spontaneously returned to baseline and continued into the negative range, suggesting cell shrinkage (Fig. 2.2B). Simultaneously, LT in the CA1 cell body layer (PYR) rapidly increased (Fig. 2.2B) and did not reverse (arrows, Fig. 2.2B). Accordingly, the pharmacological studies described below were carried out using a domoate exposure (1 min, 22°C) that was clearly reversible and caused minimum damage to the tissue.

The average pixel intensity sampled from four discrete hippocampal areas were plotted over time to demonstrate the time course of the response in one slice (Fig. 2.4A). The responses to a 1 min exposure peaked by 5 min and were completely reversible at 22°C; the changes returned to baseline levels by 25-30 min (Fig. 2.4A). As shown in Table 2.1, five out of the seven hippocampal areas analysed displayed significant increases in light transmittance to varying degrees in an order that was readily reproducible (CA1 RAD > CA1 OR > CA1 PYR = LM = upper DG) and consistent from slice to slice. The largest peak LT response was 58±3% (mean ● SE) in CA1 RAD as measured in 10 slices. Two monitored

areas, the lower blade of the DG and CA3 RAD, did not exhibit significant change (Table 2.1), nor did the alveus (not shown). A brief exposure (1 min) to 10 μM AMPA evoked an identical peak response to that of domoate in CA1 RAD (Fig. 2.2C). The peak responses of domoate (58±3%; n=10) and AMPA (53±6%; n=5) were not significantly different ($P<0.01$).

To further illustrate the region-specific response to domoate or AMPA, slices were exposed to aCSF containing 40 mM KCl (replacing equimolar NaCl) for 3 min. The elevated K^+ levels evoked a generalized transmittance increase over most areas of the slice (Fig. 2.3A). Table 2.1 summarizes the generalized response to high K^+ aCSF in 5 slices versus the region-specific increase in light transmittance in response to domoate.

We produced a dose response curve (Fig. 2.4B) by measuring peak LT in CA1 RAD following exposure to increasing concentrations of domoate applied for 1 min at 22°C ($n \geq 5$ for each dose). In each slice the peak response in CA1 RAD in response to 10 μM domoate was set at 100%. The peak response at other dosages were normalized with respect to this value. There were no increases in LT at concentrations at or below 1 μM while 10 μM yielded a near-maximum change. No significant increase from the 10 μM response was observed at 100 μM.

Are domoate responses receptor-mediated?

To determine if the increased LT observed in response to domoate involved action potential discharge (and therefore dependence on pre-synaptic events), slices were exposed to 10 μM domoate for 1 min following exposure to 1 μM TTX (5 min). The orthodromically

evoked field potential, consisting of an excitatory post-synaptic field potential with one or two overriding population spikes was with 5 min of TTX exposure (data not shown). In 5 of 5 slices tested, the intrinsic optical signal evoked by DOM was unaffected by TTX. That is, the LT increase developed in the same hippocampal regions (Fig. 2.3B) with a similar time course to the control response. These data are summarized in Figure 2.6C.

Another series of experiments examined which type of receptor mediated the transmittance increase. A slice was first exposed to 10 μM domoate (1 min, 22°C) to establish a control response (Fig. 2.5A-E). This was followed by incubation for 15 min with one of five different glutamate antagonists. Then the response to a second 1 min pulse of domoate was observed in the presence of the antagonist. Imaging demonstrated that kynurenate, a broad spectrum glutamate receptor antagonist, blocked the response (n=5 slices; Fig. 2.5A) as did the specific AMPA receptor antagonists CNQX (n=5 slices; Fig. 2.5B) or DNQX (n=7 slices; Fig. 2.5C). The average pixel intensity of area CA1 RAD in response to domoate alone (*control*) and to domoate following incubation with 50 μM CNQX was plotted over time in one representative slice (Fig. 2.6A).

Neither the specific NMDA receptor antagonist AP-5 (n=5 slices) nor the reported kainate receptor antagonist GAMS (n=5 slices) blocked the domoate-induced increase in LT as revealed by imaging of the peak change using a grey scale (Figs. 2.5E and 2.5D, respectively). The average pixel intensity of area CA1 RAD evoked by domoate in the presence of AP-5 was plotted over time (Fig. 2.6B), showing little effect of AP-5 on the domoate response.

Figure 2.6C summarizes the average peak response in CA1 RAD to 1 min of 10 μM domoate alone (control) and in the presence of various glutamate antagonists. Each effective antagonist (KYN, CNQX and DNQX) was washed out for at least 30 min before domoate was re-applied to determine if the responses were reversible. The post-wash response returned to near control levels in the KYN and CNQX experiments, demonstrating that a slice could respond and reverse consistently to at least three domoate exposures. The effects of DNQX were more difficult to wash out.

Tissue resistance

To confirm that the elevated light transmittance was a result of cell swelling, relative changes in tissue resistance (R_{REL}) were calculated by measuring the voltage change across CA1 RAD (Fig. 2.1B). A slice was first exposed to aCSF made hyperosmotic using mannitol (+60 mOsm; 3 min). A decrease in voltage indicated a decrease in R_{REL} (Fig. 2.7A), suggesting an increased extracellular volume fraction (cell shrinkage). In saline made hyperosmotic with membrane permeant glycerol (+60 mOsm) there was no obvious increase in R_{REL} (data not shown), suggesting that the mannitol increase was caused by elevated tissue resistance and not increased aCSF conductance. Conversely, a 3 min application of aCSF made hypo-osmotic by dilution with distilled water (-60 mOsm) increased R_{REL}, indicative of cellular swelling (Table 2.2). Exposure to aCSF containing 10 μM domoate (3 min) caused a large increase in R_{REL} (Fig. 2.7A). This large and reversible increase in R_{REL} across CA1 RAD in response to a similar domoate exposure parallelled the time course of the light

transmittance increase and subsequent reversal at 22°C (Fig. 2.4A). Note that there is not a perfect correspondence in time between changes in LT and R_{REL} because a different chamber and a longer (3 min) exposure were used for R_{REL} measurements.

The glutamate antagonist kynurenate, which effectively blocked the LT increase evoked by domoate (Figs. 2.5A, 2.6C), was tested to determine if the increase in R_{REL} was also reduced. A control response evoked by a 3 min exposure to 10 μM domoate was first measured (Fig. 2.7B). The slice was then incubated in aCSF with 1 mM kynurenate for 15 min and then again exposed to the domoate for another 3 min. Figure 2.7B illustrates that the R_{REL} increase induced by domoate was blocked by kynurenate. The experiment was repeated in 2 other slices. Peak R_{REL} responses are summarized in Table 2.2.

DISCUSSION

Domoate stimulates specific regions in the hippocampus

The present study shows that domoate caused a rapid and reversible increase in light transmittance (LT) particularly in the CA1 RAD and OR which are dendritic regions containing high concentrations of NMDA and AMPA receptors (see below). The CA1 pyramidal cell body layer was only minimally affects at 22°C, unless the temperature and exposure time were elevated together, in which case there evolved an irreversible swelling in the cell body region. LT increases in neighbouring CA3 region was comparatively small. Whereas these region-specific increases were reproducible and reversible at 22°C, high K^+ aCSF elicited a general and widespread increase in LT across most regions of the

hippocampus. The exceptions were all cell body regions and the alveus, areas with low numbers of astrocytes. High K^+ aCSF promotes glial swelling due to K^+ uptake followed by Cl^- and water influx into glial cells (Walz and Hinks 1985, 1986). The result is a generalized LT increase in all areas of the slice where astrocytes are numerous.

Increased transmittance evoked by domoate is mediated via the AMPA receptor subtype

The domoate-induced LT increase was unaffected by TTX and was therefore independent of action potential discharge, meaning it was a postsynaptic event. Domoate targeted dendritic regions, particularly the CA1 RAD and OR. The response to domoate was dose-dependent and reversible. These observations indicate that the domoate response is receptor mediated.

Domoate is an agonist of glutamate receptors of the ionotropic class. The specific receptor sub-types which bind domoate are kainate and AMPA receptors (Hampson *et al.* 1992; Corsi *et al.* 1993; Zhou *et al.* 1993; Hollmann and Heinemann 1994). We found that the broad-spectrum glutamate antagonist kynurenate (Schwarz *et al.* 1990), blocked 1) the elevated tissue transmittance and 2) the elevated tissue resistance, which provides two independent lines of evidence for mediation of cell swelling by glutamate receptors. Kynurenate is known to act as a cerebroprotectant following domoic acid poisoning (Pinsky *et al.* 1989, 1990). The NMDA receptor antagonist AP-5 did not block the domoate response, indicating that the response was not mediated by NMDA receptors. GAMS, which displays selective antagonism of kainate receptor-mediated responses (Davies and Watkins

1985; Turski *et al.* 1985; Zhou *et al.* 1993) also did not reduce the domoate response, suggesting that it was not mediated by the kainate receptor subclass. Both competitive AMPA receptor antagonists (CNQX, DNQX) reversibly blocked LT increases in response to domoate. The highly specific non-competitive AMPA receptor antagonist GYKI 52466 also blocked domoate evoked increases in LT (Polischuk and Andrew 1995). CNQX (but not AP-5) blocked similar increases in LT evoked by kainate (Andrew, Adams, Polischuk 1996). Thus, our examination of various glutamate receptor antagonists indicates that the domoate-induced LT was mediated through AMPA receptors, as further supported below.

Upon exposure to domoate, CA1 RAD consistently displayed the greatest increase in light transmittance, followed by CA1 OR and then CA1 LM. This order was consistently reproducible and corresponds to regions strongly immuno-labelled for the GluR1 receptor protein (Schröder 1993). Specifically, immuno-labelling for GluR1 which is the AMPA receptor subtype most sensitive to domoate (Bettler and Mulle 1995) revealed densely stained dendrites in the CA1 RAD with spotted labelling in the CA1 OR and CA1 LM but little staining in area CA3 (Schröder 1993). In addition, other studies have shown that the CA1 RAD and CA1 OR contain high levels of receptors which are now considered to represent the AMPA subtype (Rainbow *et al.* 1984; Cotman *et al.* 1987; Swanson *et al.* 1987; Hawkins *et al.* 1995).

Domoate (this study) or kainate (Andrew, Adams, Polischuk 1996) only minimally increases LT in the CA3 region, an area containing high concentrations of glutamate receptors of the kainate subtype (Cotman *et al.* 1987). Domoate does exhibit affinity for

kainate receptor subtypes GluR5-7, KA1 and KA2 (Lomeli *et al.* 1992) but these are localized mainly in the rat CA3 and DG regions and not CA1 (reviews by Schröder 1993; Seeburg 1993). As well, it has been demonstrated *in vivo* that domoate can target both CA1 and CA3 pyramidal neurons in addition to other brain areas (lateral septal nucleus, fimbria, caudate nucleus) in rats (Stewart *et al.* 1990; Strain and Tasker 1991; Gross *et al.* 1995) and in humans (Teitelbaum *et al.* 1990). Afferents from these extrahippocampal sites are absent in the slice preparation where domoate may directly activate only CA1 neurons. We suggest that the abundant kainate receptors on CA3 neurons, although bound by domoate, do not mediate sufficient ionic influx to cause cell swelling comparable to the CA1 and dentate regions where AMPA receptors are the highest in the brain (Hawkins *et al.* 1995).

Domoate activates post-synaptic cell swelling

Independent of elevated light transmittance (Andrew and MacVicar 1994; Holtoff and Witte 1996), increases in relative tissue resistance (R_{REL}) provides an indicator of cellular swelling in brain slices (Traynelis and Dingledine 1989). An increase in R_{REL} parallels the rise in LT in CA1 RAD (Henn and Turner 1993; Andrew, Adams, and Polischuk 1996). We measured a rapid increase in R_{REL} across CA1 RAD in response to a bath application of domoate followed by a slow return to baseline levels by 30 min. The ability of kynurenate to block domoate-evoked increases in both light transmittance and R_{REL} provides strong evidence that cell swelling evoked by domoate is mediated by glutamate receptors.

Exactly what are we imaging? A logical scenario is that binding of AMPA receptors

by domoate opens ligand-gated channels that permit Na^+ influx and K^+ efflux as the neurons depolarize. Chloride is drawn inward by the Na^+, followed by osmotically obligated water, but exactly which channels are involved is not known. This is an excitotoxic model suggested previously in studies of cultured neurons (Rothman 1985; Rothman and Olney 1986).

Domoate application for 1 min causes temporary loss of the field potential (Polischuk and Andrew 1996b), the result of strong deploarization of the CA1 population as also seen with kainate application (Rieppe and Carpenter 1996). It could be argued that the resulting K^+ efflux through domoate-activated channels on the CA1 dendrites is taken up by adjacent glia. This would be followed by Cl^- and water (Walz and Hinks 1985, 1986), leading to glial swelling. Thus the small imaging changes seen in CA1 PYR following high K^+ aCSF or domoate could simply reflect the paucity of glia in the region. However, other observations are difficult to attribute to glial swelling. First, the most likely mechanism for glial swelling would be through K^+ uptake from depolarized dendrites (Walz and Hinks 1985). However, we measured only minor swelling in the CA3 dendritic regions which, like CA1, depolarize in response to kainate (Robinson and Deadwyler, 1981). Since glia in CA3 and CA1 regions display similar swelling in high K^+ aCSF, it seems unlikely that glia in the CA1 region are somehow more prone to swelling evoked by domoate. Second, there is good evidence that neuronal cell bodies in CA1 stratum pyramidale can resist cell swelling possibly by shutting down channels that normally would facilitate influx of ions and water (Somjen *et al.* 1993). Moreover, the soma's small surface-to-volume ratio compared to dendrites means fewer

receptor-mediated channels per unit volume, so ionic fluxes and resultant volume change may be smaller at the cell body. It follows that the fine distal dendrites comprising CA1 LM should display the highest transmittance changes. They do not, perhaps because they have fewer AMPA receptors than their more proximal regions (Cotman *et al.* 1987; Schröder 1993).

In summary, a brief exposure to domoate induces a dramatic, reversible increase in light transmittance in specific regions of the hippocampal slice in a dose dependent manner. Domoate particularly targets the postsynaptic dendritic regions of area CA1, the order of which is readily reproducible (RAD > OR > LM). Increased LT evoked by domoate is mediated by the AMPA receptor, which probably leads to Na^+ influx followed by Cl^- and water. The resultant cell swelling in the locale of the receptor sites can be detected both by elevated LT and, more generally, by increased tissue resistance. Because the dendritic swelling can progress to irreversible cell damage particularly to the CA1 population, it represents an early event in the excitotoxic process. We propose that imaging of intrinsic optical signals offers a real-time view of early excitotoxic events and so may prove useful in assessing potentially therapeutic glutamate antagonists that inhibit excitotoxicity.

TABLES

Table 2.1: Peak changes in light transmittance evoked by domoate or high K^+ aCSF in hippocampal regions at 22°C.

	% maximum response	
Hippocampal Region	10 μM DOM (n=10)	40 mM KCl (n=5)
CA1 OR	55.6±3.5*	68.1±1.2
CA1 PYR	24.2±2.1*	14.3±2.3
CA1 RAD	100	100
CA1 LM	28.2±2.1*	69.5±2.2**
Upper DG	26.0±4.5*	69.6±1.5**
Lower DG	4.2±2.0	69.1±1.2**
CA3 RAD	6.2±2.3	54.4±1.5**

Data (mean±SE) are presented as a percentage of the maximal response (set at 100%) measured in CA1 RAD. The responses in CA1 OR, CA1 PYR, CA1 LM and upper DG (molecular layer) were significantly lower than the response measured in CA1 RAD but were significantly greater than those of the remaining regions (*; $p<0.01$). For the response to elevated K^+, there was no significant difference between CA1 RAD and other dendritic regions. The response was significantly greater than the DOM response (**; $p<0.01$) in the LM, molecular layer of the upper and lower DG, and CA3 RAD.

Table 2.2: Peak changes in relative tissue resistance (R_{REL}) measured in CA1 RAD at 22°C.

Treatment	R_{REL}	n
Hyperosmotic aCSF (+60 mOsm)	-0.59±0.06	3
Hypo-osmotic aCSF (-60 mOsm)	0.68±0.09	3
DOM (10 mM)	1.07±0.09	3
DOM (10 mM) + kynurenate (1 mM)	0.34±0.06*	3

Numbers are mean ± SE. The peak change in response to DOM + kynurenate was significantly lower than DOM alone (*; $p<0.01$).

FIGURES

Figure 2.1: Schematic representations of the imaging and tissue resistance equipment. **A)** Diagram of the imaging equipment. Hippocampal slices were superfused with artificial cerebrospinal fluid (*aCSF*). A voltage-regulated, broadband halogen light source supplied illumination to the inverted microscope (*objective*). Transmitted light was collected and digitized using a charge-coupled device (*CCD camera*) and data were transferred to an image board. Images were averaged and digitized for processing and display on a 486 PC. **B)** Measurement of relative tissue resistance in the hippocampal slice. Recording micropipettes were positioned within the CA1 stratum radiatum. Two bipolar stimulating electrodes supplied a biphasic current pulse across the slice.

A)

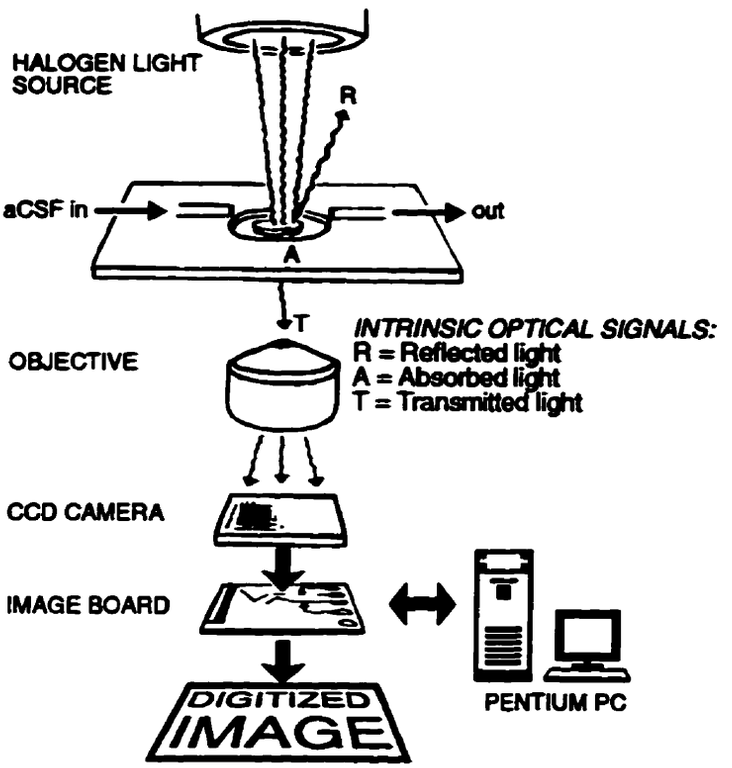
HALOGEN LIGHT SOURCE
R
aCSF in
out
A
T
OBJECTIVE
INTRINSIC OPTICAL SIGNALS:
R = Reflected light
A = Absorbed light
T = Transmitted light
CCD CAMERA
IMAGE BOARD
DIGITIZED IMAGE
PENTIUM PC

B)

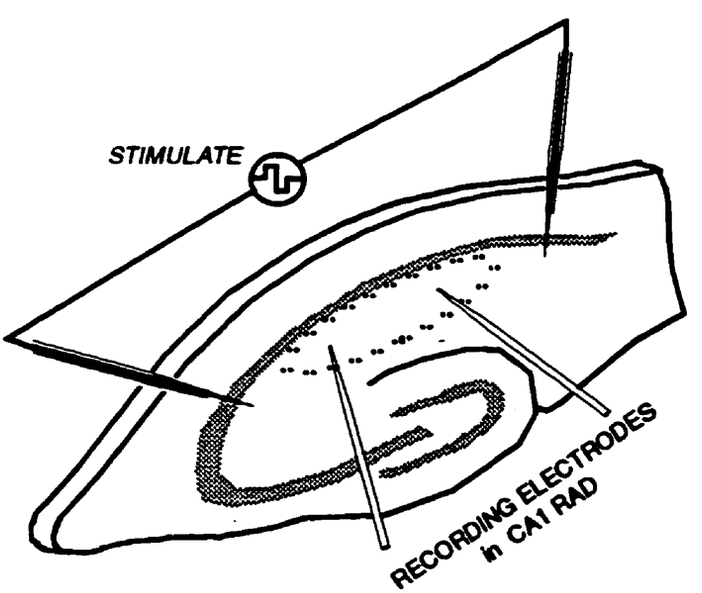
STIMULATE
RECORDING ELECTRODES in CA1 RAD

Figure 2.2: Digitized, pseudo-colored images demonstrating light transmittance changes (ΔT/T%) in the rat hippocampal slice over time. Bright field images are shown at left. **A)** A 1 min exposure to 10 μM domoate (*DOM*) at 22°C evoked the largest LT increase in CA1 stratum radiatum (*RAD*). CA1 stratum oriens (*OR*) and the upper blade of the dentate gyrus (*DG*) showed smaller responses. The response returned to baseline levels by 30 min at 22°C. **B)** A 10 min exposure to 10 μM DOM at 37°C evoked an irreversible change in LT. RAD and OR initially increased in response to to domoate but then decreased into an irreversible negative LT value, suggesting cell shrinkage. At the same time, the PYR (*arrows*) developed a large increase in LT which was also irreversible. Note similar response in the upper blade of the dentate gyrus. **C)** A similar response to (A) was seen with a 1 min exposure to 10 μM AMPA at 22°C.

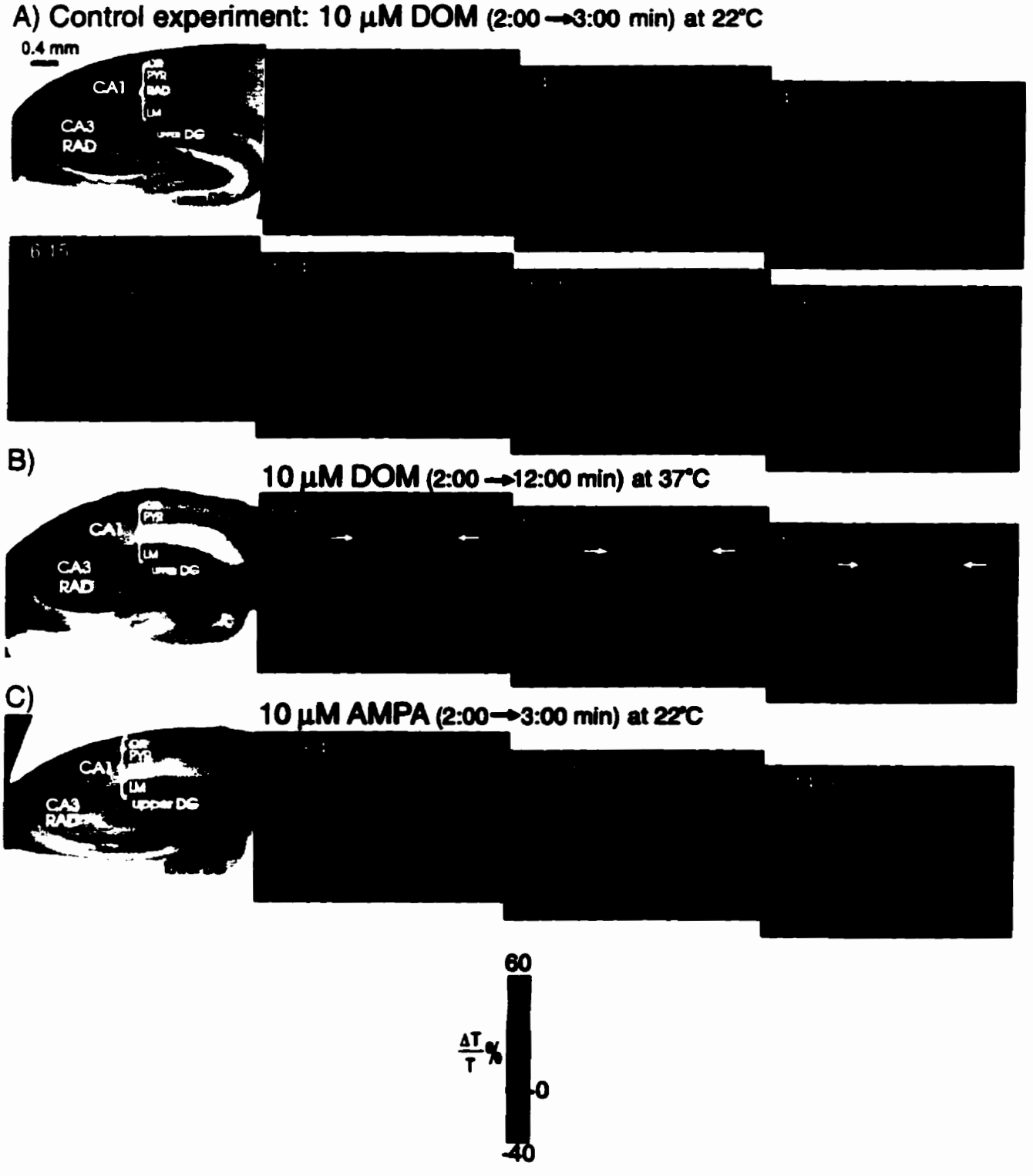
A) Control experiment: 10 µM DOM (2:00 → 3:00 min) at 22°C
0.4 mm
CA1
PYR
RAD
LM
CA3
RAD
upper DG
B)
10 µM DOM (2:00 → 12:00 min) at 37°C
CA1
PYR
LM
CA3
RAD
upper DG
C)
10 µM AMPA (2:00 → 3:00 min) at 22°C
CA1
PYR
LM
upper DG
CA3
RAD
60
ΔT/T %
0
-40

Figure 2.3: Digitized, pseudo-colored images demonstrating peak light transmittance changes (ΔT/T%). The first image in each sequence (left) is the digitized bright field image. The middle image is the peak response to a 1 min exposure of 10 μM DOM (*peak control*). **A)** Compared to a 1 min exposure to 10 μM DOM (*control*) at 22°C, the peak response to 40 mM KCl (3 min) evoked LT increases throughout the slice. **B)** TTX (1 μM) did not affect the DOM-evoked response.

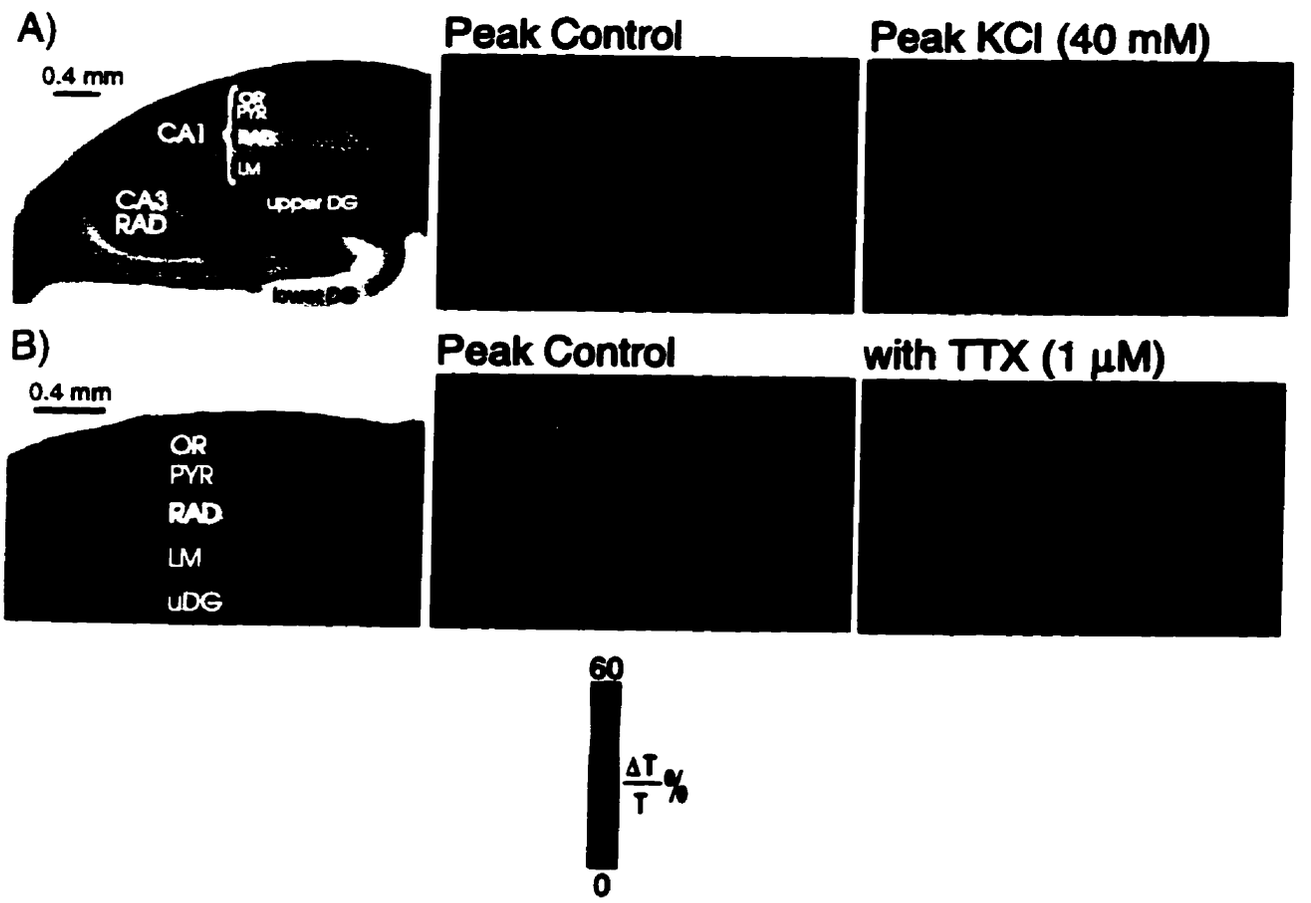
A)
0.4 mm
CA1
CA3
RAD
upper DG
Peak Control
Peak KCl (40 mM)
B)
0.4 mm
OR
PYR
RAD
LM
uDG
Peak Control
with TTX (1 μM)
60
ΔT/T %
0

Figure 2.4: A) Time course of regional light transmittance changes (ΔT/T%) following a 1 min exposure to domoate (DOM) at 22°C. Plotting averaged pixel intensities over time in CA1 RAD showed a rapid peak response and a slow return to baseline levels by 30 min. CA1 OR and CA1 PYR displayed smaller peaks. CA3 RAD showed little change. **B)** Dose response curve at 22°C showing the peak LT increases in CA1 RAD for a range of DOM concentrations (0.01-100 μM) following a 1 min exposure (n=5 slices at each dose). Each response is normalized as a percentage of the response to 10 μM DOM in CA1 RAD (% *Max. Response*).

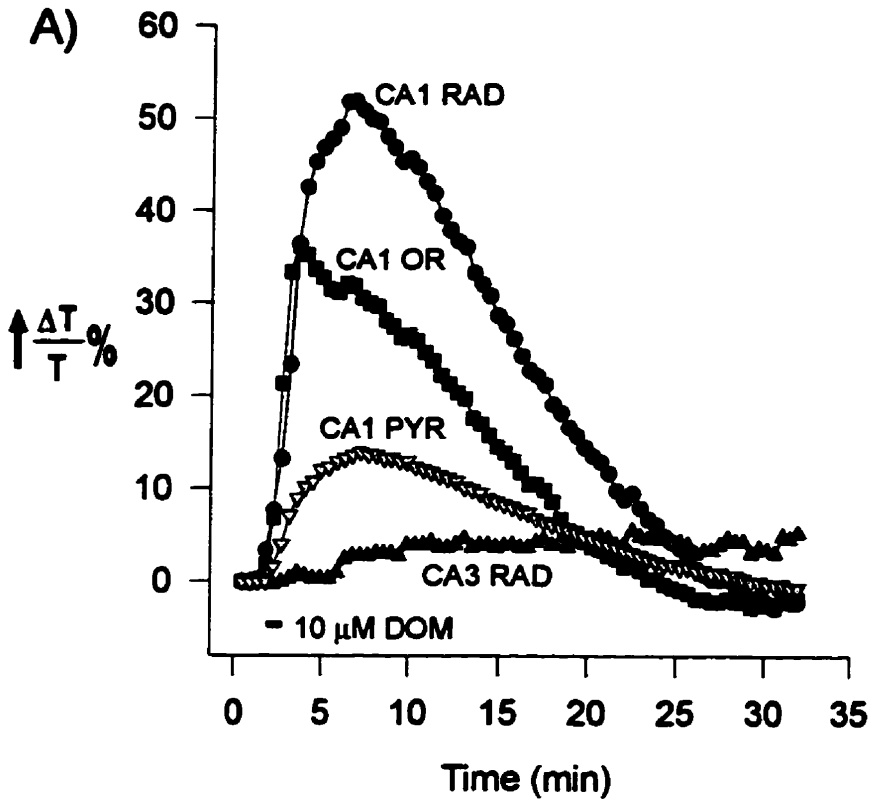
A)
60
50
40
30
20
10
0
CA1 RAD
CA1 OR
CA1 PYR
CA3 RAD
10 μM DOM
ΔT/T %
0
5
10
15
20
25
30
35
Time (min)

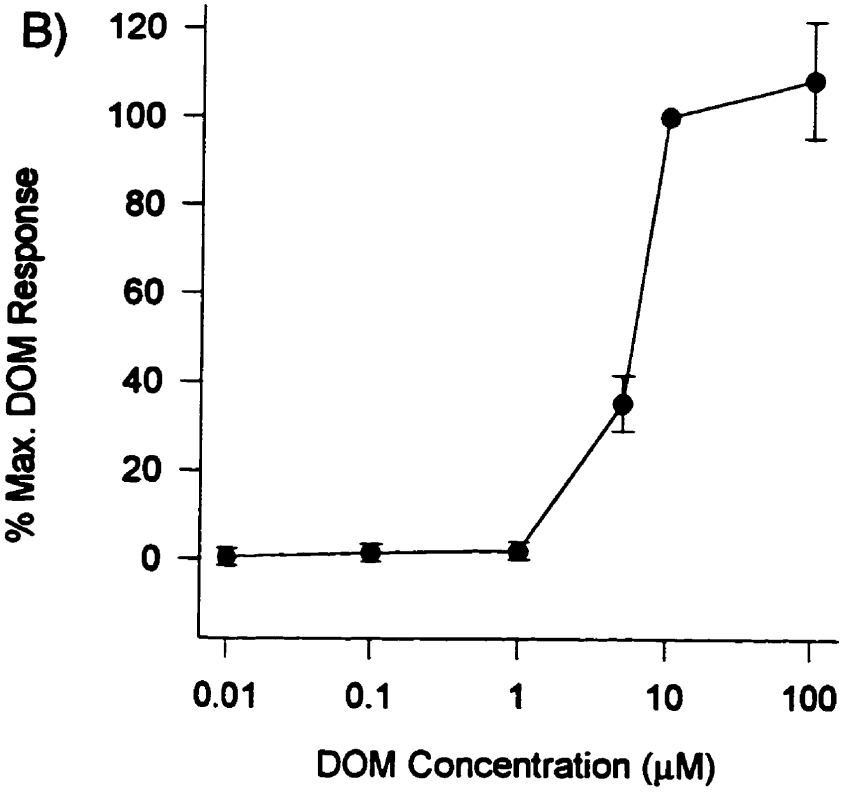
B)
120
100
80
60
40
20
0
% Max. DOM Response
0.01
0.1
1
10
100
DOM Concentration (μM)

Figure 2.5: Digitized, pseudo-colored images demonstrating peak light transmittance changes (ΔT/T%). The first image in each sequence (left) is the digitized bright field image. The middle image is the peak response to a 1 min exposure of 10 μM DOM in the absence (*peak control*) and presence (right) of a glutamate anatgonist at 22°C. 1 mM kynurenate **(A)**, 50 μM CNQX **(B)** or 50 μM DNQX **(C)** reversibly reduced the response induced by DOM. 100 μM GAMS **(D)** or 50 μM AP-5 **(E)** had no effect on the DOM-induced response.

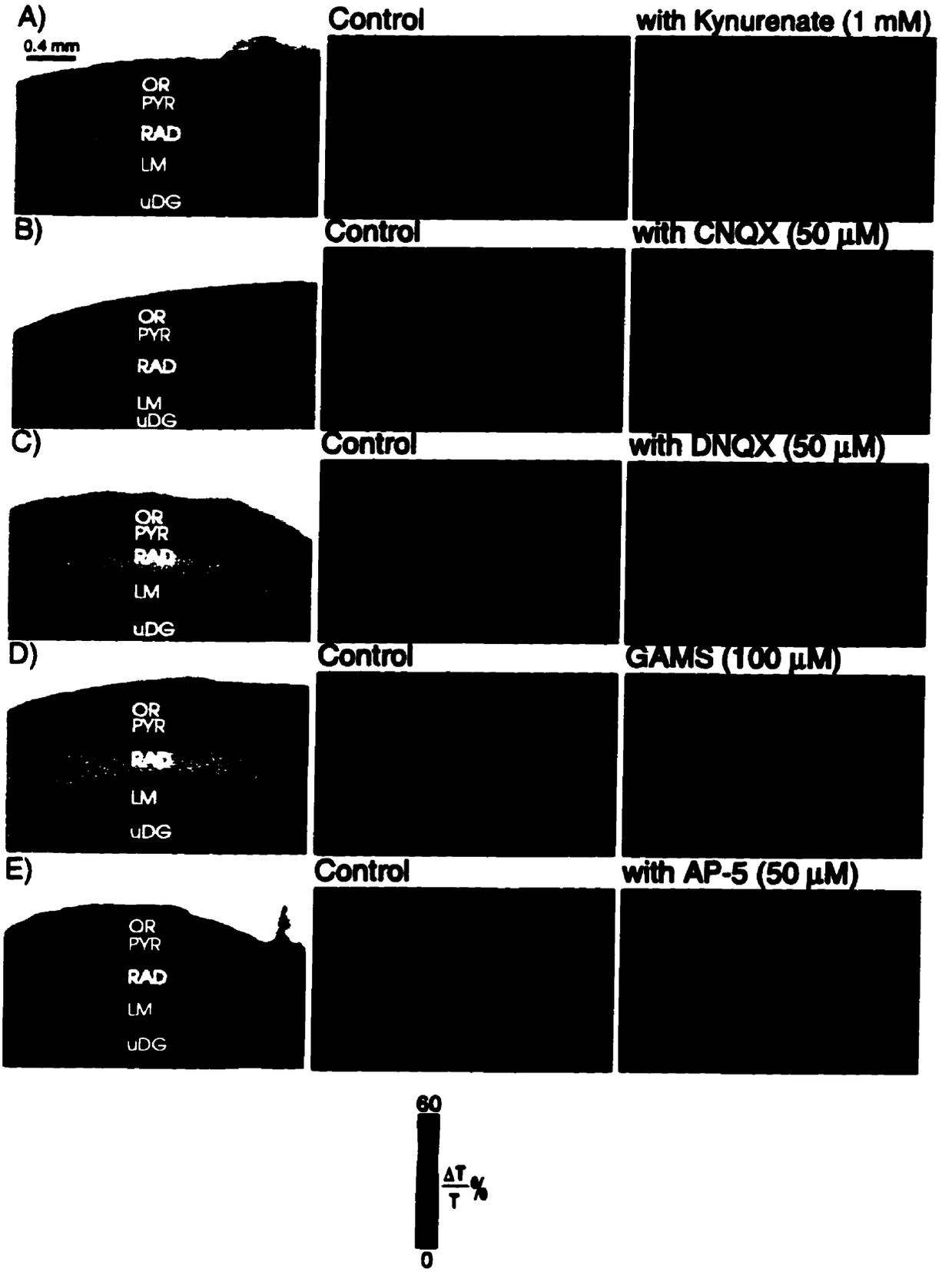
A)
Control
with Kynurenate (1 mM)
0.4 mm
OR
PYR
RAD
LM
uDG
B)
Control
with CNQX (50 µM)
OR
PYR
RAD
LM
uDG
C)
Control
with DNQX (50 µM)
OR
PYR
RAD
LM
uDG
D)
Control
GAMS (100 µM)
OR
PYR
RAD
LM
uDG
E)
Control
with AP-5 (50 µM)
OR
PYR
RAD
LM
uDG
60
ΔT/T %
0

Figure 2.6: Time course of the increased LT change measured in CA1 RAD following a 1 min exposure to 10 μM DOM in the presence of **A)** 50 μM CNQX or **B)** 50 μM AP-5 at 22°C. CNQX reduced the response to DOM but AP-5 did not. **C)** Summary of peak changes in T evoked by a 1 min exposure of 10 μM DOM measured in CA1 RAD with/without TTX or various glutamate antagonists.

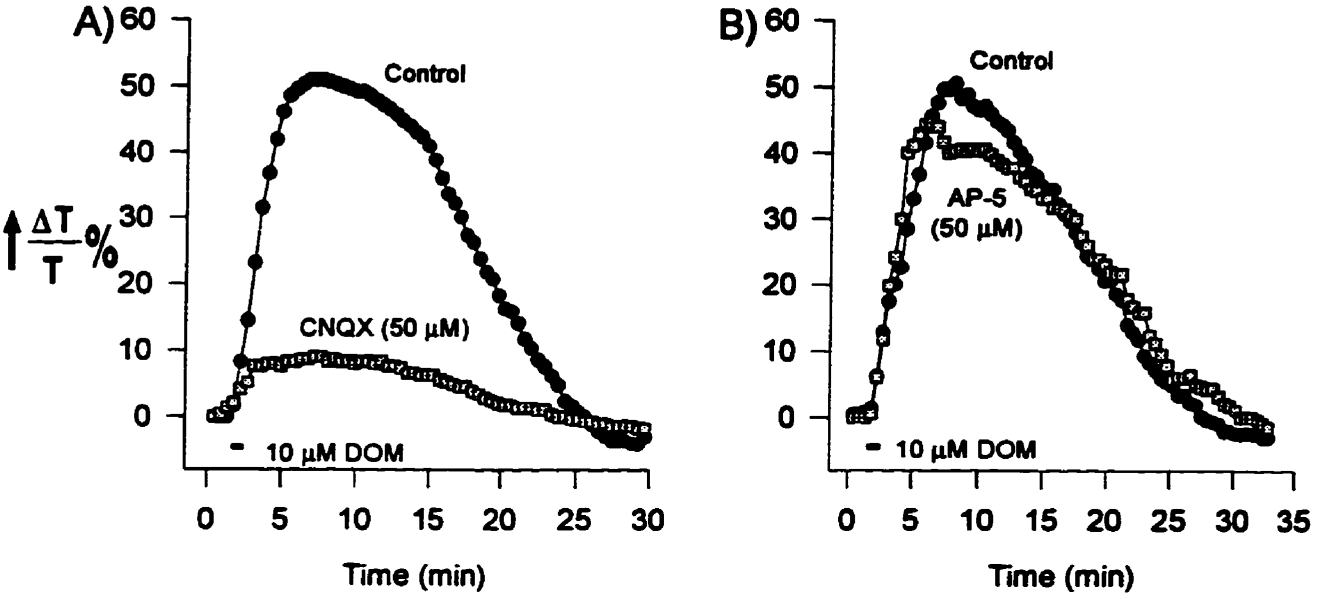
A)
B)
Control
CNQX (50 µM)
AP-5
(50 µM)
10 µM DOM
ΔT/T %
Time (min)

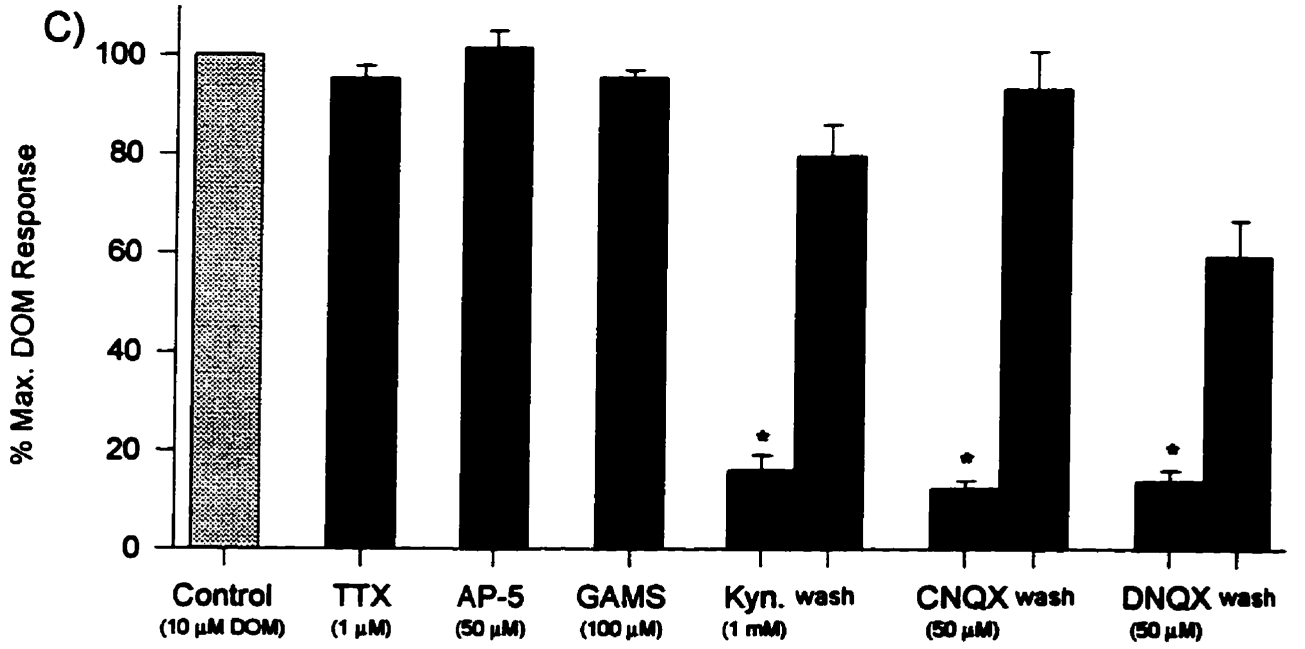
C)
% Max. DOM Response
Control
(10 µM DOM)
TTX
(1 µM)
AP-5
(50 µM)
GAMS
(100 µM)
Kyn. wash
(1 mM)
CNQX wash
(50 µM)
DNQX wash
(50 µM)

Figure 2.7: Time course of change in relative tissue resistance (R_{REL}) in response to: **A)** a 3 min exposure to hyperosmotic aCSF (mannitol, +60 mOsm) followed by 10 μM DOM. **B)** exposure to 10 μM DOM for 3 min (*control*) The slice was then incubated with kynurenate (1 mM, 15 min), followed by immediate re-exposure to 10 μM DOM (*Kyn.)*.

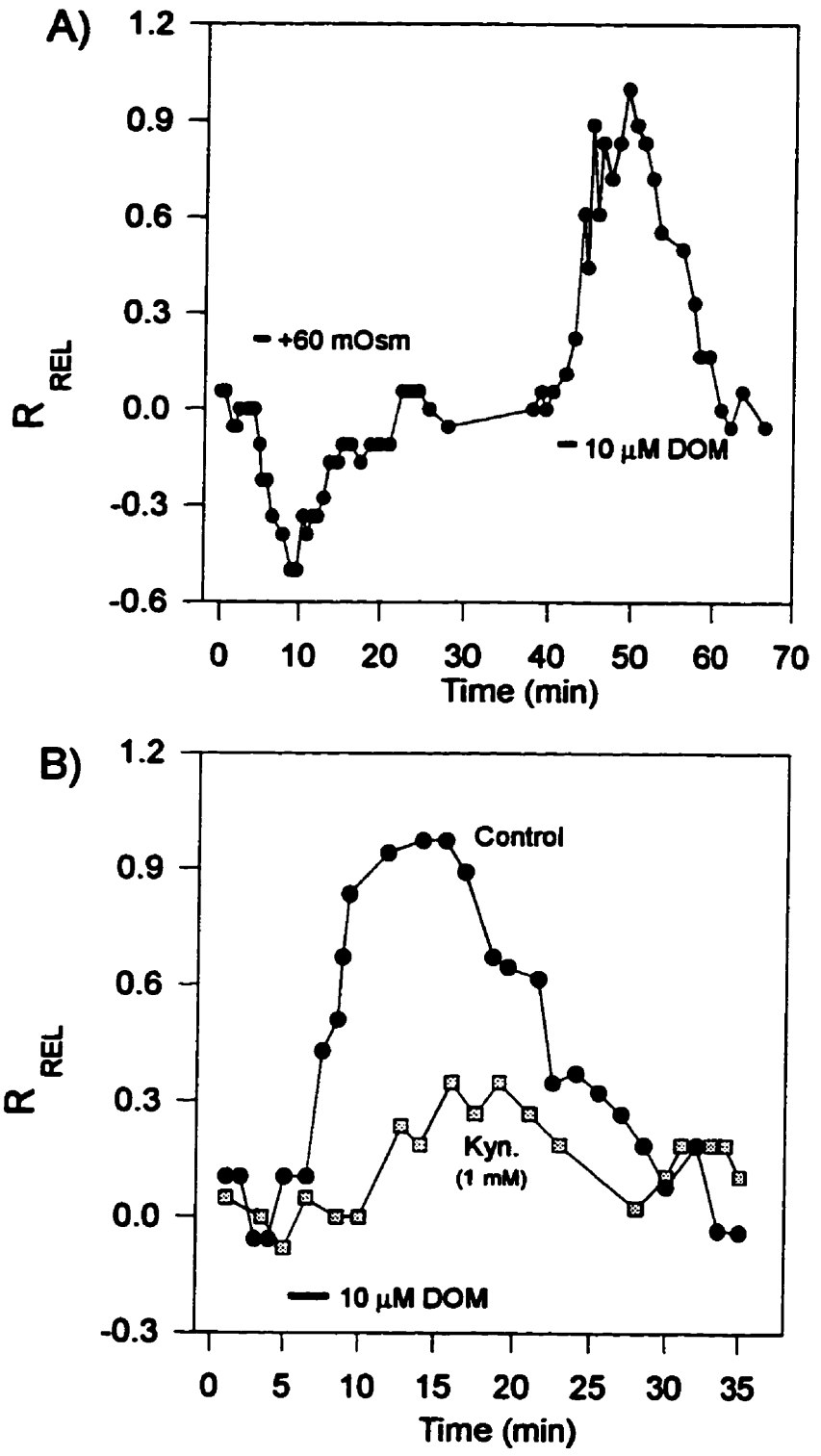
A)
1.2
0.9
0.6
0.3
0.0
-0.3
-0.6
R REL
+60 mOsm
10 µM DOM
0
10
20
30
40
50
60
70
Time (min)
B)
1.2
0.9
0.6
0.3
0.0
-0.3
R REL
Control
Kyn.
(1 mM)
10 µM DOM
0
5
10
15
20
25
30
35
Time (min)

CHAPTER 3

INTRINSIC OPTICAL SIGNALING DENOTING NEURONAL SWELLING AND DEATH IN RESPONSE TO ACUTE EXCITOTOXIC INSULT IN THE HIPPOCAMPAL SLICE

Ready for submission to *European Journal of Neuroscience*

ABSTRACT

Acute excitotoxicity involves swelling of the nerve cell body over a period of minutes, a process which may or may indicate a dead or dying neuron based on studies of cells in culture. However, one might expect swelling at the site of over-activated glutamate synapses along the dendritic arbor. In the hippocampal slice, we investigated the sequence of dendritic and somatic volume changes leading to neuronal death as defined by 1) loss of the evoked fixed potential, 2) irreversible changes in light transmittance and 3) histopathological evidence. Increased light transmittance (LT) through the submerged brain slice provides an indirect measure of cell swelling. We imaged changes in LT through hippocampal slices induced by the glutamate agonist domoic acid. At 37°C, a 1 min superfusion of 10 μM domoate induced a prolonged reversible increase in LT primarily in the dendritic regions of CA1 and dentate gyrus (DG). Spectral analysis revealed a wide-band transmittance increase across 400-800 nm indicating generalized swelling as a source of the intrinsic signal. The evoked field potential recorded in CA1 cell body region (PYR) completely recovered upon LT reversal. In contrast, increasing domoate exposure to 10 min elicited a distinct intrinsic optical sequence where the initial LT increase in dendritic regions evolved into an irreversible *decrease* in LT. At the same time, LT irreversibly *increased* in cell body regions (CA1 PYR and DG) and the evoked field potential was irretrievably lost. Spectral analysis of CA1 PYR revealed a wide-band transmittance

increase indicating cellular swelling as a source of the signal. Subsequent histological examination demonstrated severe CA1 and DG neuron damage in slices exposed to domoate for 10 min at 37°C. The optical changes generated by domoate required extracellular Cl^- but not Ca^{2+}. Lowering temperature protected the slice from the irreversible damage to the CA1 region. We conclude that domoate excitotoxicity involves dynamic and compartmentalized volume changes in cell body and dendritic regions leading to rapid neuronal death. The extent of the damage can be monitored in real time by imaging changes in light transmittance.

[Key Words: AMPA; calcium; cell swelling; chloride; domoic acid; excitotoxicity; intrinsic optical signals; kainic acid; temperature]

INTRODUCTION

Excitotoxicity involves excessive activation of glutamate receptors, leading to neuronal depolarization and death (for review see Olney 1990). Glutamatergic excitotoxic processes are involved in several neurodegenerative events including food poisoning, head trauma, and stroke. The possibility that excitatory amino acid receptor agonists of endogenous or environmental origin contribute to neuronal death and disease continues as a major focus of study (for reviews see Meldrum and Garthwaite 1990; Meldrum 1993; Olney 1994).

Cell swelling occurs early in an acute excitotoxic event but its involvement in neuronal death is poorly understood. In cultured neurons, excitotoxicity includes an acute phase of Na^+ and Cl^- influx followed by passive water movement causing neuronal swelling (Rothman 1985; Rothman and Olney 1986; Rothman 1992). However, the observation that delayed glutamate neurotoxicity in culture was calcium dependent (Choi 1987) shifted the focus from the role of cell swelling in excitotoxic cell death. Calcium-mediated excitotoxic cell death occurs over hours and days following glutamate exposure and is commonly referred to as "slow" or "delayed" toxicity (Rothman and Olney 1986; Beal 1992; Rothman 1992; Orrenius and Nicotera 1994). In contrast, cell swelling is associated with "rapid" or "acute" cell death which can occur within seconds and minutes (Rothman 1985; Rothman and Olney 1986; Rieppe and Carpenter 1995; Ikeda *et al.* 1996). How swelling is linked to

cell death is an important aspect of the neurodegenerative process.

Direct observation of cell swelling in the whole brain is not yet possible and studies beyond the culture dish are few (Rieppe and Carpenter 1995; Colwell and Levine 1996). Intrinsic optical signals (IOSs) from brain tissue involve change in the way light is transmitted, reflected, or absorbed. Whole brain studies have shown that IOSs can be used as an index of activation of the cortical surface (Grinvald *et al.* 1986; Federico *et al.* 1994; Poe *et al.* 1995). In brain slice preparations elevated light transmittance (LT) representing cell swelling accounts for essentially all of the change in IOSs (MacVicar and Hochman 1991; Andrew and MacVicar 1994; Kreisman *et al.* 1995; Holthoff and Witte 1996; Andrew *et al.* 1997).

Domoic acid (domoate, DOM) is a naturally occurring amino acid and seafood contaminant produced by marine algae and seaweed (Takemoto 1978; Meldrum 1993). Domoate is a non-NMDA receptor agonist (Bettler and Mulle 1995) which promotes temporal lobe epilepsy in humans (Cendes et al. 1995). Like kainate (Andrew, Adams, Polischuk 1996), domoate reversibly increases LT in CA1 dendritic areas at 22°C through activation of AMPA receptors (Polischuk and Andrew 1996). We have argued that dendritic swelling, initiated within seconds of glutamate agonist exposure, is a reversible event involving NMDA and non-NMDA receptor activation and actually precedes cell body swelling (Andrew, Adams, Polischuk 1996). Thus while most studies have focused on cell body swelling (Rieppe and Carpenter 1995; Colwell and Levine 1996), dendritic regions are where rapid and dynamic changes in volume first arise following brief exposure to

excitotoxins.

The goal of the present study was to map LT changes in dendritic and cell body regions leading to acute excitotoxic cell death in the hippocampal slice evoked by domoic acid. We present evidence that the LT changes denote compartmentalized alterations in cell volume which can lead to rapid neuronal death as defined by loss of the evoked field potential, irreversible LT changes and histopathology.

METHODS

Hippocampal Slice Preparation

Male Sprague-Dawley rats, 21-28 days old (Charles River, St. Constant, Quebec, Canada) were housed in a controlled environment (25°C, 12 hour light/dark cycle) with food and water available *ad libitum*. A rat was placed in a rodent restrainer and guillotined. The excised brain was hemisected and each hippocampus exposed under cold artificial cerbrospinal fluid (aCSF). Transverse slices were cut (400 μm) using a manual tissue slicer and stored at 22°C in aCSF oxygenated with 95% O_2 / 5% CO_2. Slices were incubated in aCSF for a minimum of 1 hour before being transferred to the recording chamber.

The aCSF contained (in mM): NaCl 120.0, KCl 3.3, $NaHCO_3$ 26.0, $MgSO_4$ 1.3, NaH_2PO_4 1.2, D-glucose 11.0, and $CaCl_2$ 1.8 dissolved in distilled water at pH 7.3-7.4. The aCSF was used for the dissection of the hippocampus, for the incubation and superfusion of slices, and as a vehicle for drug administration. The osmolality of the aCSF and its variants was 295 ± 2 mOsm as measured with a freezing point depression osmometer (Precision

Systems Inc.). For zero Ca^{2+} experiments, the aCSF contained 4 mM KCl, no $CaCl_2$ and 1 mM EGTA. Chemicals for the aCSF were obtained from the Sigma Chemical Co. (St. Louis, MO). Domoate (DOM) was obtained from Diagnostic Chemicals Ltd. (Charlettetown, PEI).

Imaging Intrinsic Optical Signals

Intrinsic optical signals were monitored using techniques previously described (Polischuk and Andrew 1996c). A slice was transferred to an imaging chamber where it was weighted at the edges with silver wire and submerged in flowing, oxygenated aCSF (2 mL/min) at 22°C or 37°C. The slice was viewed with an inverted microscope with only a coverslip between the slice and the 1.6x objective. Slices were transilluminated by a halogen lamp with a voltage regulated power supply (Leica). Video frames were obtained at 30 Hz using a charge-coupled device (CCD camera) which was set for maximum gain and a medium black level. With gamma set to 1.0, the output of the CCD is linear with respect to change in light intensity. Frames were averaged and digitized using an image processor board (DT2867, Data Translation) in a Pentium computer controlled by Axon Imaging Workbench software (Axon Instruments). Each averaged image was stored on a removable harddrive (Iomega).

Experiments entailed acquring an averaged image every 8 seconds (256 frames @ 30 Hz). The first averaged image in a series served as a control (T_{cont}) which was subtracted from each subsequent experimental image (T_{exp}) of that series. A series of subtracted images

revealed areas in the slice where light transmittance (LT) changed over time. LT was expressed as the digital intensity of the subtracted image (T_{exp}-T_{cont}) divided by the gain of the intrinsic signal which was set using the software program. This value was then expressed as a percentage of the digital intensity of the control image of that series. That is,

$$LT = \frac{(T_{exp} - T_{cont})/gain}{T_{cont}} \times 100\% = \frac{\Delta T}{T}\%$$

The control image was displayed using a gray intensity scale. Each subtracted image was displayed using a pseudo-colour intensity scale. To quantify and graphically display data, regions of interest (ROI) were boxed using the Axon Imaging Workbench software. The average digital intensity of each ROI was sampled, stored as text files, and graphed using SigmaPlot for Windows software (Jandel Scientific). A graphics program (CorelDRAW 3.0) was used to import and label images. Statistical analyses were performed using a one way ANOVA.

Measurement of Extracellular Field Potentials

Extracellular recording micropipettes (10-20 Mohms) were pulled from thin-walled capillary glass, filled with 2M NaCl and mounted on a three dimensional micromanipulator. A silver wire coated with AgCl connected the recording micropipette to an amplifier probe whose output was monitored with an on-line oscilloscope. Amplified signals were digitized (NeuroData Instruments) and stored on video cassette tape.

The recording micropipette was placed in the CA1 stratum pyramidale. A concentric bipolar electrode (Rhodes Electronics) was placed in the CA2 stratum radiatum to stimulate CA1 neurons orthodromically via Schaeffer collaterals. A current pulse (0.1-1.5 mA; 0.1 ms duration; 0.25 Hz) was applied to produce a near-maximal amplitude population spike. A calibrator connected between the chamber and ground generated a 10 mV, 5 ms pulse. Digitized data were signal averaged (6 sweeps/trace), displayed and plotted using pCLAMP software (Axon Instruments).

Spectrometry

Spectral analyses were performed on CA1 regions in the imaging chamber. A fiber optic cable replaced the CCD camera and was connected to a PC1000 spectrometer (Ocean Optics, Inc.). The light source output was increased to half its maximal intensity to accommodate the lower sensitivity of the spectrometer relative to the CCD. Relative transmittance levels in either CA1 stratum radiatum (RAD) or stratum pyramidale (PYR) were monitored over the 400-800 nm range and were displayed using SpectraScope software (Ocean Optics, Inc.). Each trace was an average of 10 measurements. Light transmittance levels were relative because of variations in slice thickness and regional translucence.

Histology

Hippocampal slices were fixed immediately after image analysis for 24 hrs. in 1.5% paraformaldehyde and 1% glutaraldehyde in 0.1 M cacodylate buffer (pH=7.2) with 4.35%

sucrose and 0.05% $CaCl_2$. Slices were processed for paraffin embedding, sectioned at 7 μm and stained with hematoxylin/eosin. Micrographs were taken with a color CCD (VK-C370, Hitachi) controlled by the Axon Imaging Workbench software and displayed using a graphics program (CorelDRAW 3.0).

RESULTS

Intrinsic Optical Signal Analysis

A series of pseudo-colored images showed a rapid and progressive increase in light transmittance (LT) in the CA1 dendritic regions of the hippocampal slice in response to a brief (1 min) exposure to 10 μM domoate (Fig. 3.1A2-4) at 37°C. The increase in LT, which represents cell swelling, was observed primarily in the CA1 stratum radiatum (RAD) and to a lesser extent in the stratum oriens and molecular layer (MOL) of the dentate gyrus (DG) (Fig. 3.1A4). The response peaked within 3 min of application (Fig. 3.2A, 3.3A) and consistently reversed (Fig. 3.1A5) within 15 min of application (Fig. 3.2A, 3.3A). Only a small response was measured in the cell body region of CA1, the stratum pyramidale (PYR; Fig. 3.1A4, 3.2A). There was no response in the granule cell layer (GC) of the DG (Fig. 3.1A4, 3.3A). Elevating the temperature to 37°C had no significant effect on the magnitude of the peak LT response measured in CA1 RAD (58 ± 2%, n=7, $p<0.001$) compared to our previous study at 22°C (58 ± 3%, n=10, Polischuk and Andrew 1996c). As well, the regional specificity of the LT response remained the same (i.e. CA1 and DG dendritic regions only). However the time course of the response was faster, lasting only ~15 min at 37°C compared

to ~30 min at 22°C.

When domoate exposure was increased from 1 min to 10 min at 37°C, an irreversible sequence resulted. As before, the LT increased in RAD and MOL (Fig. 3.1B2-4) but then rapidly *decreased* past baseline levels, resulting in negative LT changes (Fig. 3.1B5-7). At the same time an irreversible LT *increase* developed in the cell body regions of CA1 PYR and DG GC (Fig. 3.1B4-7). Both secondary changes (i.e. the LT reduction in dendritic regions and the LT increase in cell body regions) began *prior* to domoate removal and proved irreversible. LT levels remained at the 40-60% range at cell bodies (white arrows, Fig. 3.1B7) and below -30% in dendritic regions (asterisks, Fig. 3.1B7). The peak LT in CA1 RAD was not significantly different from the peek response to a 1 min exposure (57 ± 2%, n=10, $p<0.001$) and again only the CA1 and DG regions responded. When domoate was re-applied to slices that had progressed through this irreversible sequence, there were no subsequent LT changes (not shown). This suggested that this irreversible state represents CA1 pyramidal cell death as confirmed electrophysiological and histologically below.

Lowering temperature is known to help protect from excitotoxic damage (Busto et al. 1987). Accordingly the paradigm (10 μM domoate for 10 min) that lead to the irreversible LT changes in dendritic and cell body regions at 37°C (Fig. 3.1B) caused only swelling in dendritic regions at 22°C (Fig. 3.1C), a response which proved to be completely reversible (Fig. 3.1C5). When the temperature was lowered to 22°C during the 10 min exposure time, the RAD CA1 and DG displayed an LT increase (57 ± 2%, n=7, $p<0.001$) identical to the response when the temperature was maintained at 37°C.

Figure 3.4A summarizes the peak LT changes measured in CA1 RAD evoked by domoate for the three paradigms tested. Figures 3.4B and 3.4C summarize the peak LT changes measured in the dendritic (MOL) and cell body regions (GC) of the DG, respectively, evoked by domoate for the three paradigms tested. There were no large changes in LT measured in the CA3 region of the hippocampal slice in response to domoate (Figs. 3.1A-C) presumably because AMPA receptor concentrations are comparatively low (Andrew, Adams, Polischuk 1996; Polischuk and Andrew 1996c).

Spectral Analysis

The spectral content of transmitted light was measured in area CA1, the region displaying the largest intrinsic optical responses. Samples were taken at both peak and minimum time points as revealed by the imaging described above. A 1 min exposure to 10 μM domoate at 37°C (n=6) increased transmittance over the entire spectral range analyzed (400-800 nm) in the CA1 RAD (*peak*, Fig. 3.5A) with the largest increases at longer wavelengths. The peak response returned to baseline levels (*wash*, Fig.3.5A). In other words, LT increased over a broad spectrum and then reversed as did the intrinsic optical signal under this same 1 min domoate exposure (Fig. 3.1A).

When domoate exposure was increased to 10 min at 37°C (n=5), transmittance increased across the spectrum in CA1 RAD (*peak*, Fig. 3.5B) and then after several minutes fell irreversibly to below baseline levels (*wash*, Fig. 3.5B), suggestive of decreases in cell volume in this dendritic region as imaged in Figure 3.1B7. Meanwhile in CA1 PYR, the

signal irreversibly increased (*peak*, *wash*, Fig. 3.5C) as also seen with the imaging experiments (Fig. 3.1B5-7). All of these spectral changes are consistent with the IOS findings. Examination of the transmission spectra did not reveal any specific narrow band regions that could be attributed to cytochrome or hemoglobin activity probably because such changes involve very small changes in transmittance compared to signals associated with cell volume change.

Electrophysiological Analysis

To provide further evidence that we are imaging *neuronal* changes, we measured the evoked CA1 field potential while simultaneously imaging LT sequences. Slices were electrophysiologically monitored during the recording of intrinsic optical changes before, during, and after application of domoate. After 1 min of 10 μM domoate at 37°C in six slices, the evoked population spike recorded in CA1 PYR (Fig. 3.6A1) dropped in amplitude as changes in LT increased (Fig. 3.6A2) and was eventually lost before and during the peak change in LT (Fig. 3.6A3). The field potential began to recover just as LT levels returned to baseline and completely recovered within the ensuing 5 minutes (Fig. 3.6A4). In contrast, when domoate exposure time was increased to 10 min at 37°C in 6 other slices, the evoked field potential was irretrievably lost as LT peaked and then irreversibly decreased in CA1 RAD (Fig. 3.6B3). The field was not detectable even by the 50 min mark in all six slices (Fig. 3.6B4), confirming that this exposure paradigm resulted in permanent loss of the neuronal signal.

Histological Analysis

Slices were fixed and embedded for light microscopy immediately following image analysis of reversible or irreversible responses. Tissue was examined following domoate applications (10 μM at 37°C) of 0 min (control), 1 min or 10 min. There was no appreciable morphological damage in area CA1 between the control group (Fig. 3.7A) and 1 min group (Fig. 3.7B). In contrast, the 10 min group displayed a striking appearance response in the cell body region of CA1 (Fig. 3.7C). Swollen, vacuolated neurons were apparent along with shrunken, condensed cells surrounded by perineuronal spaces. The dark staining nuclei have been described previously as degenerating neurons evoked by domoate (Strain and Tasker 1991; Schmued *et al.* 1995). Also there was a granular appearance to the neighboring dendritic regions which is consistent with damage to the neuropil. Responses in the upper DG were identical to those seen in CA1: the cell bodies were vacuolated and the dendritic region granular. While control (Fig. 3.7D) and 1 min groups (Fig. 3.7E) showed no damage. The 10 min group showed swollen, vacuolated neurons and dark staining nuclei, again consistent with dead and degenerating neurons (Fig. 3.7F).

Zero Ca^{2+} and low Cl^- Experiments

To determine if calcium has a role in these acute responses to domoate, $CaCl_2$ was removed from the aCSF, osmolality adjusted and 1 mM EGTA was added to chelate trace amounts of Ca^{2+}. At 37°C, zero Ca^{2+} aCSF failed to reduce the reversible LT response

evoked by a 1 min application of 10 μM domoate (Fig. 3.8A; n=4). Similarly, the apparent neuronal death evoked by 10 min of 10 μM domoate developed in the absence of Ca^{2+} (Fig. 3.8B; n=6). We examined the importance of Cl^- in generating intrinsic optical changes in response to domoate in 6 additional slices. In contrast to lowered Ca^{2+}, when chloride was reduced from 120 mM to 1.8 mM, an application of 10 μM domoate (1 min, 37°C) failed to evoke an LT response (Fig. 3.8C). Returning the slice to normal aCSF restored domoate-induced LT changes (Fig. 3.8C).

DISCUSSION

Domoic Acid Evokes Specific Regional Transmittance Changes

The present study demonstrates a sequence of changes in light transmittance across the hippocampal slice generated in a region-specific pattern in response to domoic acid, a marine toxin and glutamate agonist. We propose that the characteristic optical end-point represents neuronal death which is supported by both electrophysiological and histological evidence. Reducing exposure time to domoate, lowering the temperature, or reducing extracellular [Cl^-] results in neuronal protection. Lowering extracellular Ca^{2+} had no effect on the optical sequence leading to neuronal death.

We recently showed that a 1 min application of 10 μM domoate at 22°C evokes a large, reversible LT increase in the CA1 dendritic regions (with no significant change in area CA3) primarily through AMPA receptor activation (Polischuk and Andrew 1996c). Similar effects were evoked by another non-NMDA agonist, kainic acid (Andrew, Adams, Polischuk

1996). Because the excitotoxic process is accelerated at higher temperature (Busto *et al.* 1987) and longer exposure (Dubinsky *et al.* 1995), the present study investigated the effects of increased temperature (37°C) and lengthened exposure (10 min) to domoic acid. We report here that the CA1 and DG regions, but not the CA3 region, display dramatic changes in LT which are irreversible at higher temperature and longer exposure.

A possible explanation for the distinct area-specific LT response is a regional difference in extracellular space in the hippocampal slice. Although there is a significantly smaller extracellular volume fraction in the CA1 cell body region compared to CA3 (McBain *et al.* 1990), no significant difference has been reported for the dendritic regions of these respective areas. Therefore it is unlikely that a constricted extracellular space is responsible for the large intrinsic optical signal in the CA1 dendritic region. Rather, we propose below that the regionality is due to glutamate receptor distribution.

Domoic Acid Stimulates AMPA Receptors in Dendritic Regions

Domoate demonstrates non-NMDA receptor specificity (Bettler and Mulle 1995) and is often described as a kainate-like agonist (Debonnel *et al.* 1989; Stewart *et al.* 1990; Chiamulera *et al.* 1992; Watson and Gridlestone 1995). Our recent antagonist studies show that LT changes evoked by domoate and kainate are mediated primarily by AMPA receptors (Andrew, Adams, Polischuk 1996; Polischuk and Andrew 1996c). Although labelling is found throughout the entire hippocampal formation, AMPA receptors are localized post-synaptically in the CA1 region (Rainbow *et al.* 1984; Keinanen *et al.* 1990; Schroeder 1993,

Wenthold *et al.* 1996). The highest AMPA receptor distribution is localized on CA1 dendrites (Blackstone *et al.* 1992) and minimally on pyramidal and granule cell bodies (Nielson *et al.* 1995). A recent study using (S)-[^{3}H]-5-fluorowillardine, a radioligand with extremely high affinity for the AMPA receptor, showed the highest AMPA receptor concentrations in rat brain in CA1 and DG (Hawkins *et al.* 1995), the regions that demonstrate large LT changes in response to domoate and kainate.

The highest kainate receptor concentration is in the CA3 region (Foster *et al.* 1981; Monaghan and Cotman 1982; Cotman *et al.* 1987; Ulas *et al.* 1990; Werner *et al.* 1991), an area that displays only a minor optical response to domoate (this study) or kainate (Andrew, Adams, Polischuk 1996). Kainate-preferring glutamate receptor channels do not contribute significantly to the glutamate evoked currents compared to NMDA and AMPA receptors (Spruston *et al.* 1995). Moreover one identified function of kainate receptors in the hippocampus id pre-synaptic inhibition (Chittajulla *et al.* 1996). We conclude that kainate receptors do not mediate sufficient ionic influx to cause measurable cell swelling when bound by domoate.

Domoate and AMPA potency at GluR1-4 binding sites are equivalent and display much greater potency than kainate (Bettler and Mulle 1995). Domoate (this study) and AMPA (Polischuk and Andrew 1996c) both elicit maximal LT responses in CA1 at a 10 μM concentration while a ten-fold increase is required to evoke the equivalent response by kainate (Andrew, Adams, Polischuk 1996). This order of agonist potency is consistent with AMPA, not kainate, receptor stimulation.

Domoic Acid Evokes Dendritic Swelling and Subsequent Cell Body Swelling

There is good evidence that the level of light transmittance can be used to monitor osmotically induced changes in cell volume in the brain slice (Andrew and MacVicar 1994; Kreisman *et al.* 1995; Andrew *et al.* 1997). LT also correlates with other measures of cell volume change including extracellular resistance (Henn and Turner 1993; Andrew, Adams, Polischuk 1996; Polischuk and Andrew 1996c) and extracellular marker concentration (Holthoff and Witte 1996).

Studies by Somjen and colleagues (1993) showed that CA1 somata resist osmotically induced swelling by shutting down channels that normally mediate the influx of ions and water. Accordingly, our sub-lethal exposure to domoate showed little indication of swelling in CA1 PYR or in DG GC. Most glutamate receptors are localized on the dendrites of hippocampal neurons (Blackstone *et al.* 1992; Spruston *et al.* 1995; Leranth *et al.* 1996) which presumably results in water entry there, rather than into the cell body. If this is the case, there is a remarkable compartmentalization of cytosol between the cell body and its dendrites of both CA1 neurons and granule cells.

As a result of refraction and reflection, the tissue scatters the light passing through it. In submerged brain slices, reduced light scattering means increased transmittance (particularly at the longer wavelengths) whereas absorbency appears to be a minor factor (MacVicar and Hochman 1991). Thus if altered cell volume is the major cause of the domoate-induced IOSs, the spectral content should change non-specifically and demonstrate greater change at longer wavelengths. This was in fact observed: transmittance increased

across the spectrum particularly in the 650-800 nm range during suspected cell swelling initially in CA1 RAD and subsequently in CA1 PYR. Conversely, transmittance decreased non-specifically in CA1 RAD during suspected cell shrinkage. These observations support the suggestion that excitotoxicity-related IOSs involve primarily cell volume change in the brain slices, similar to those responses observed following synaptic stimulation (MacVicar and Hochman 1991) and osmotic stress (Kreisman *et al.* 1995; Andrew *et al.* 1997).

We histologically examined morphological changes contributing to the irreversible LT responses. In slices where LT remained elevated after the 10 min application of domoate at 37°C there was vacuolization and swelling of neuronal cell bodies in both CA1 PYR and DG GC layers. In contrast, in slices where the signal returned to original levels (after domoate application for only 1 min), the cell body regions displayed the normal morphology of control slices not exposed to domoate. These observations confirm that irreversible changes in LT in the cell body regions correlate with histopathological damage.

Chloride plays an important role in neuronal swelling in response to excitatory amino acid exposure in culture (Rothman 1985). Prolonged depolarization induced glutamate receptor activation involves an influx of Na^+ followed by Cl^- and osmotically obligated water, presumably leading to cell lysis (Rothman and Olney 1986). Our study demonstrates that removal of Cl^- abolishes the cell swelling associated with domoate exposure which is in agreement with previous studies that attribute IOSs to cell swelling requiring extracellular chloride (MacVicar and Hochman 1991; Holthoff and Witte 1996; Trachsel *et al.* 1996).

The question remains as to whether the swelling induced by glutamate agonists is

neuronal, glial or both. The diverse evidence to date points to a large neuronal component. First, glutamate agonist-induced swelling is region-specific while glial swelling evoked by raising $[K^+]_o$ is diffuse (Andrew, Adams, Polischuk 1996; Polischuk and Andrew 1996c). Second, these studies also show that agonist-induced swelling is blocked by established glutamate receptor antagonists. Third, the evoked CA1 field potential is tightly correlated with LT changes. If the LT signal subsides, the evoked field potential fully recovers. With irreversible LT changes in CA1, the field potential never returns. Fourth, the irreversible intrinsic signal in CA1 RAD and PYR coincide with obvious histopathology in the CA1 stratum pyramidale. While the evidence points to neuronal damage as the *cause* of the intrinsic signal, a glial contribution cannot be ruled out because as neurons are damaged and release K^+, the adjacent glia will take up the K^+ accompanied by water. However this cannot explain the LT *reduction* in dendritic regions involving permanent cell damage.

Domoic Acid Can Evoke Rapid Neuronal Death

We used two experimental procedures independent of imaging to confirm that the irreversible LT signals were, in fact, an indicator of neuronal death. First, the extracellular field potential evoked in CA1 was permanently lost in all slices where irreversible LT changes were induced by domoate. This is consistent with the findings of others (Longo *et al.* 1995) showing loss of evoked fields in CA1 in response to either kainate or AMPA exposure. We have recently used this technique to correlate irreversible LT changes with NMDA-mediated toxicity (Andrew, Adams, Polischuk 1996). Second, histological analysis

of slices following a 10 min domoate exposure revealed swollen, vacuolated neurons, along with condensed cells surrounded by extracellular space which are presumably neurons that have undergone lysis. These pathological changes have been described previously and are consistent with descriptions of dead neurons (Meldrum and Garthwaite 1990; Stewart *et al.* 1990; Strain and Tasker 1991; Schmeud *et al.* 1995). Dendritic regions where LT was permanently decreased displayed a 'graininess' not observed in control tissue nor tissue where the dendritic signal recovered. The increased light scattering and granular appearance by these regions is likely due to dendritic dilations or beading (Stewart *et al.* 1990; Strain and Tasker 1991; Park *et al.* 1996) in addition to an overall shrinkage of the dendritic arbor. Dendritic retraction, which implies shrinkage and in theory could supply membrane to the expanding cell body, occurs in isolated neurons in response to strong osmotic stress (Wan *et al.* 1995) or anoxic insult (Friedman and Haddad 1994). The exact morphological changes that the dendritic regions undergo in the brain slice will require intracellular injection of tracer to delineate changes in single neuron arborization.

Time Course of Rapid Excitotoxicity

Neuronal cell body swelling in brain slices is observed 10-15 min following excitotoxin application (Reippe and Carpenter 1995; Colwell and Levine 1996; Ikeda 1996). These microscopical studies focused on cell body volume and would not have detected initial dendritic swelling. We propose that dendritic swelling is a necessary prerequisite for excitotoxic swelling of the cell body. In contrast to excitotoxic swelling, there is good

evidence that neuronal cell bodies in CA1 PYR can resist *osmotically* induced cell swelling by shutting down channels that normally would facilitiate influx of ions and water (Somjen *et al.* 1993). Even severe hypo-osmotic stress is not enough to induce cell body swelling and neuronal death (Andrew *et al.* 1997). Indeed it has been argued that excitotoxic cell swelling need not involve an osmotic gradient (Tomita and Gotoh, 1992). In contrast, the irreversible cell body swelling implicated in the present study is a specific excitotoxic response arising from initial receptor-mediated swelling in the dendritic regions.

In hippocampal cell culture, toxic responses produced by NMDA or kainate were blocked by removal of Cl^- (but not Ca^{2+}) from the incubating medium (Rothman 1985). In a more recent study, removal of Na^+ prevented anoxia-induced injury in dissociated CA1 hippocampal neurons which otherwise occurred over a period of minutes (Friedman and Haddad 1994). These findings are consistent with induced pattern of cell volume change leading to acute neuronal death that does not require extracellular Ca^{2+} (Michaels and Rothman 1990; Friedman and Haddad 1993).

FIGURES

Figure 3.1: Digitized, pseudo-colored images demonstrating light transmittance changes (ΔT/T%) in the rat hippocampal slice over time. Bright field images are at top. *A1, B1, C1* represent first subtracted image at time 0:00. **A)** One min exposure to 10 μM DOM at 37°C. The largest LT increase is in CA1 RAD (*A4*) while other dendritic regions (CA1 stratum oriens; *DG MOL*) display smaller responses. Cell body layers show little (*CA1 PYR*) or no response (*DG GC*). The response completely reverses, returning to baseline within 15 min of initial application (*A5*). **B)** Ten min exposure to 10 μM DOM at 37°C evokes similar increases in LT in CA1 and DG dendritic regions (*B4*) but then in B5-B7, the responses *decreased* to an irreversible negative LT value (*asterisks, B7*). The time course of this signal reversal is plotted in Figs. 2B and 3B. At the same time, CA1 PYR (upper arrow) and DG GC (lower arrow) develop a large *increase* in LT which is also irreversible (*arrows, B5-B7*). **C)** Ten min exposure to 10 μM DOM at 22°C. Lowering the temperature did not reduce peak LT changes measured in CA1 RAD or DG MOL (*C4*) but it appears to protect against the onset of irreversible changes (*C5*).

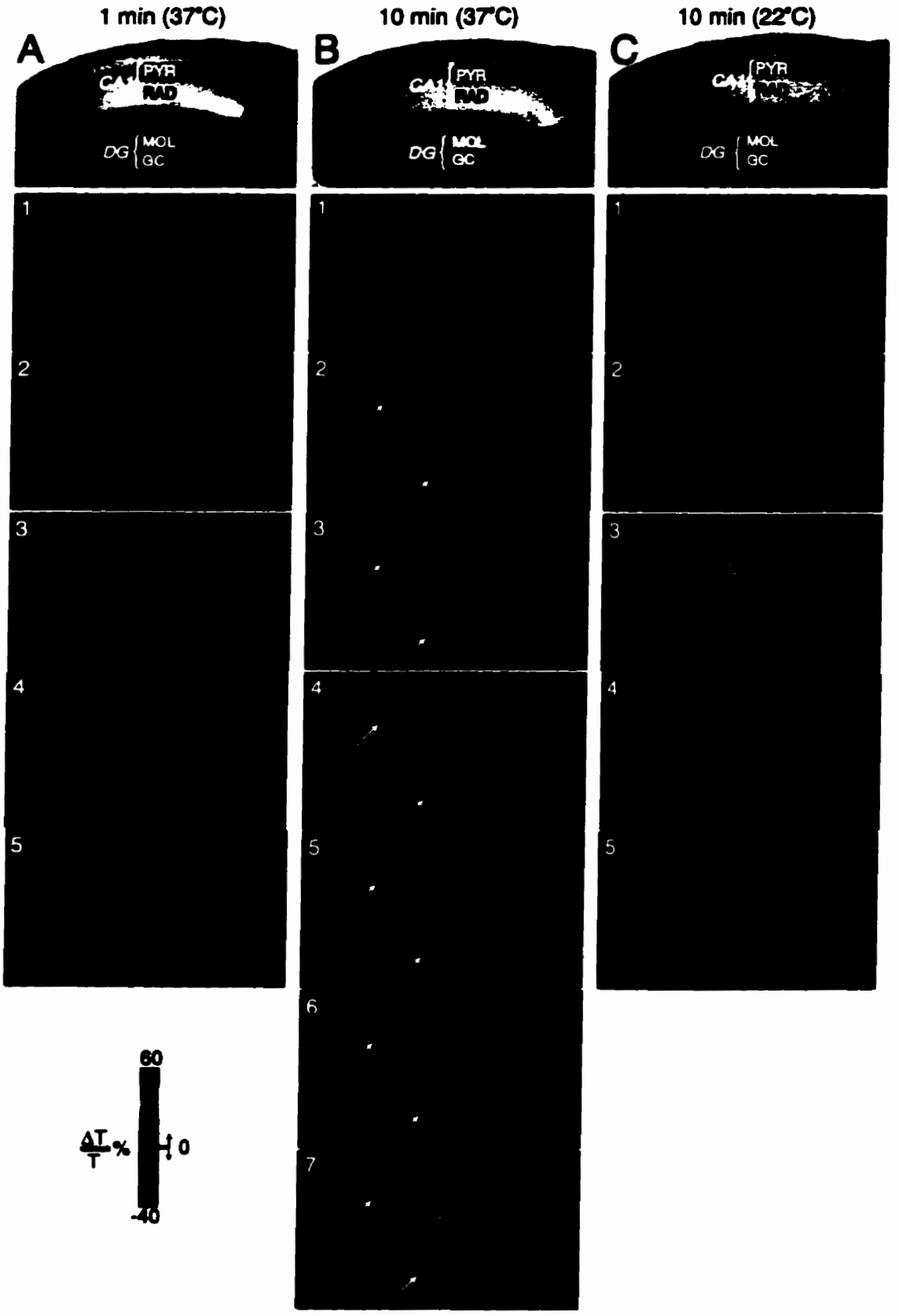
1 min (37°C)
10 min (37°C)
10 min (22°C)
A
B
C
CA1
PYR
RAD
DG
MOL
GC
1
2
3
4
5
6
7
60
ΔT/T %
0
-40

Figure 3.2: Time course of regional LT change (ΔT/T%) in CA1 RAD and PYR following exposure to domoate (*DOM*). Numbers along plot refer to corresponding image in Figure 1. **A)** LT response to 10 μM DOM at 37°C for 1 min (*bar*). CA1 RAD displays a rapid rise (*A2-A4*) and return to baseline levels (*A5*) within 15 min of exposure. CA1 PYR displays a smaller peak and reverses within 5-7 min of exposure. **B)** LT response to 10 μM DOM at 37°C for 10 min (*bar*). Again, CA1 RAD showed a rapid LT increase (*B2-B4*) but the return to baseline is faster and undershoots baseline, leading to an irreversible negative value (*B7*). Simultaneously, LT in CA1 PYR slowly increases and does not reverse. **C)** Ten μM DOM at 22°C for 10 min (*bar*). Lowering temperature prolongs recovery from dendritic swelling in CA1 RAD (*C2-C4*) and protects the region (C5).

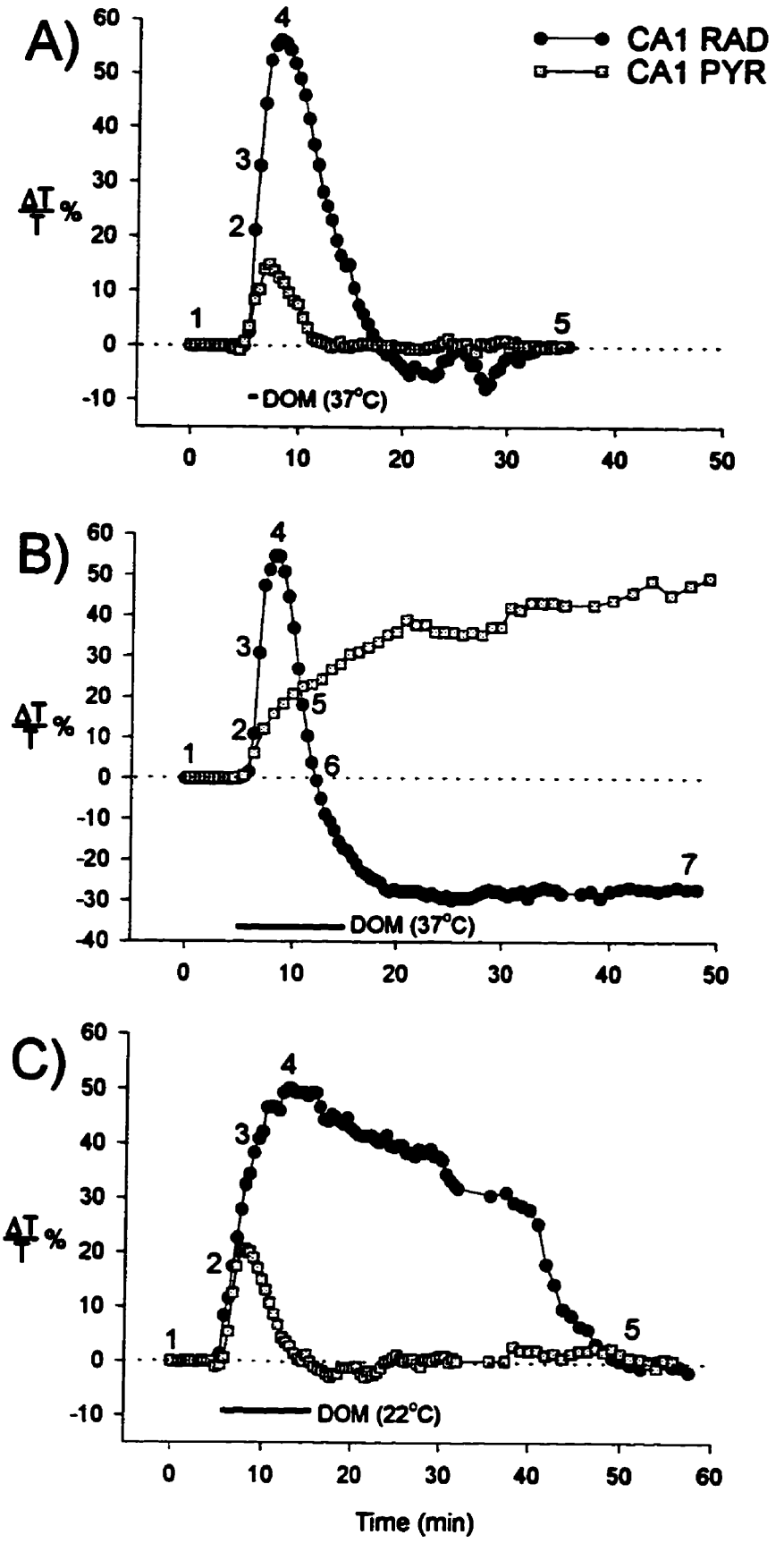
A)
CA1 RAD
CA1 PYR
ΔT/T %
DOM (37°C)
B)
DOM (37°C)
C)
DOM (22°C)
Time (min)

Figure 3.3: Time course of regional LT change (ΔT/T%) in the molecular layer (*DG MOL*) and granule cell layer (*DG GC*) of the upper dentate gyrus following exposure to 10 μM domoate (*DOM*). Numbers along plot refer to corresponding image in Figure 1. Responses to domoate are similar to the CA1 region (Figure 2). Either brief exposure **(A)** or a long exposure at low temperature **(C)** evoke LT responses that recover. However, combining long duration exposure and high temperature cause irreversible LT responses **(B)**. Specifically the dendritic region (*DG MOL*) remains well below baseline while the cell body region (*DG DC*) remains high.

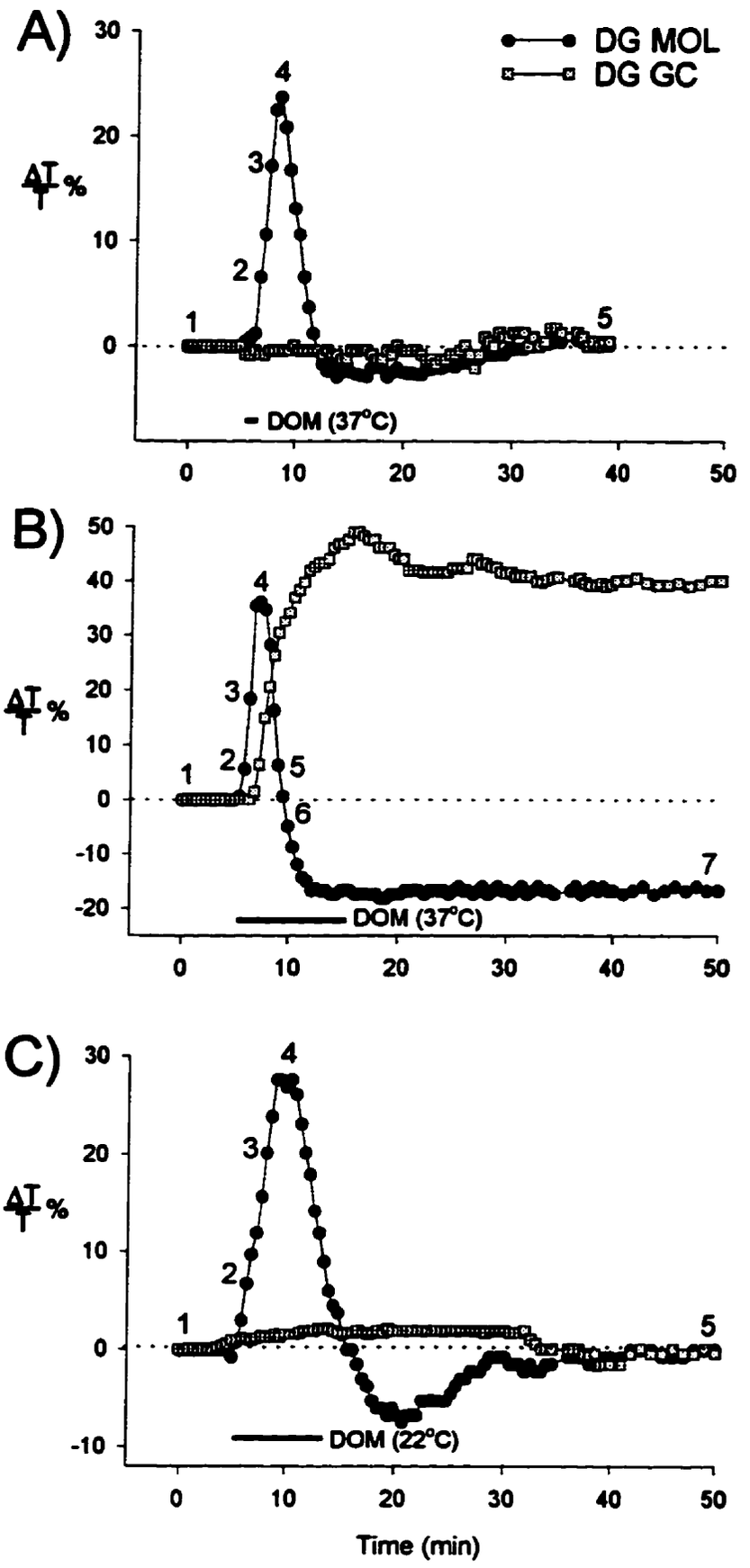
A)
DG MOL
DG GC
ΔI %
30
20
10
0
1
2
3
4
5
DOM (37°C)
0
10
20
30
40
50
B)
ΔI %
50
40
30
20
10
0
-10
-20
1
2
3
4
5
6
7
DOM (37°C)
C)
ΔI %
30
20
10
0
-10
1
2
3
4
5
DOM (22°C)
Time (min)

Figure 3.4: Summary of LT change (ΔT/T%) in response to 10 μM DOM for 1 min at 37°C (n=7), 10 min at 37°C (n=10), or 10 min at 22°C (n=7). **A)** There is no significant difference between peak responses measured in the dendritic region of CA1 (*CA1 RAD*) for each exposure paradigm. Peak LT responses range between 50-63% and average between 57-58%. Minimum values (***Wash***) are defined as the lowest LT value reached following the peak response during the wash. Only when the temperature and exposure time of the DOM are increased *together* is a significant difference found (*, $p<0.001$). **B)** There is no significant difference in the peak responses in the molecular layer of the dentate gyrus (*DG MOL*) for each exposure paradigm where peak LT ranged between 21-33% and averaged between 26-27%. Only when the temperature and exposure time were increased together is a significant difference detected (*, $p<0.001$). **C)** In the cell body region of the dentate gyrus (*DG GC*), only increasing exposure and temperature together evokes significant (*, $p<0.001$) and irreversible swelling.

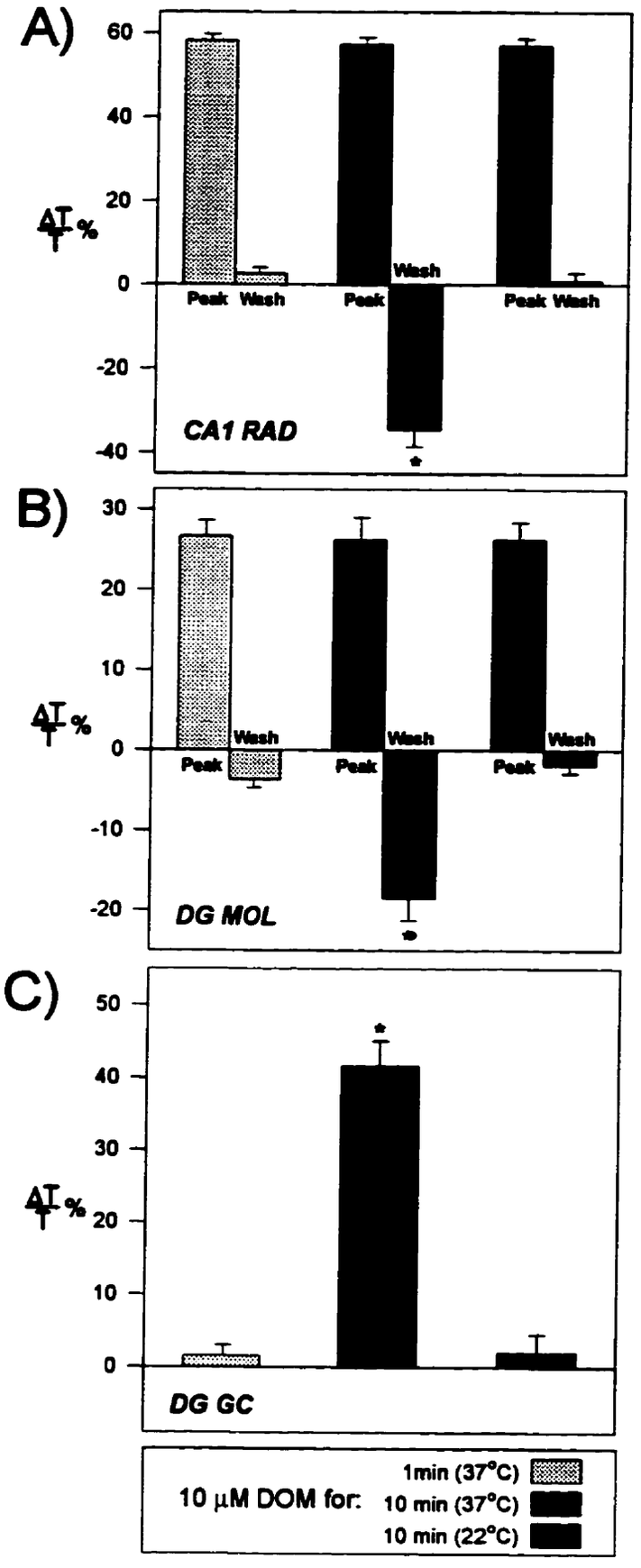
A)
60
40
20
0
-20
-40
ΔT %
Peak
Wash
Peak
Wash
Peak
Wash
CA1 RAD
B)
30
20
10
0
-10
-20
ΔT %
Peak
Wash
Peak
Wash
Peak
Wash
DG MOL
C)
50
40
30
20
10
0
ΔT %
DG GC
10 μM DOM for:
1min (37°C)
10 min (37°C)
10 min (22°C)

Figure 3.5: Spectral analysis of light transmitted by a hippocampal slice before (*Pre-DOM*), during (*Peak*), and after (*Wash*) an application of 10 μM DOM at 37°C. Light transmittance measured in relative units (ordinate) across the 400-800 nm spectrum (abscissa). **A)** One min exposure to DOM at 37°C elevated transmittance from pre-DOM levels across the entire spectrum in the CA1 RAD (*Peak*). The signal returns to baseline level following wash-out (*Wash*). **B)** Ten min exposure at 37°C again elevates transmittance in CA1 RAD (*Peak*) but relative transmittance then irreversibly decreases below baseline (*Wash*). **C)** Conversely in CA1 PYR, the transmittance slowly elevates (*Peak*) irreversibly (*Wash*).

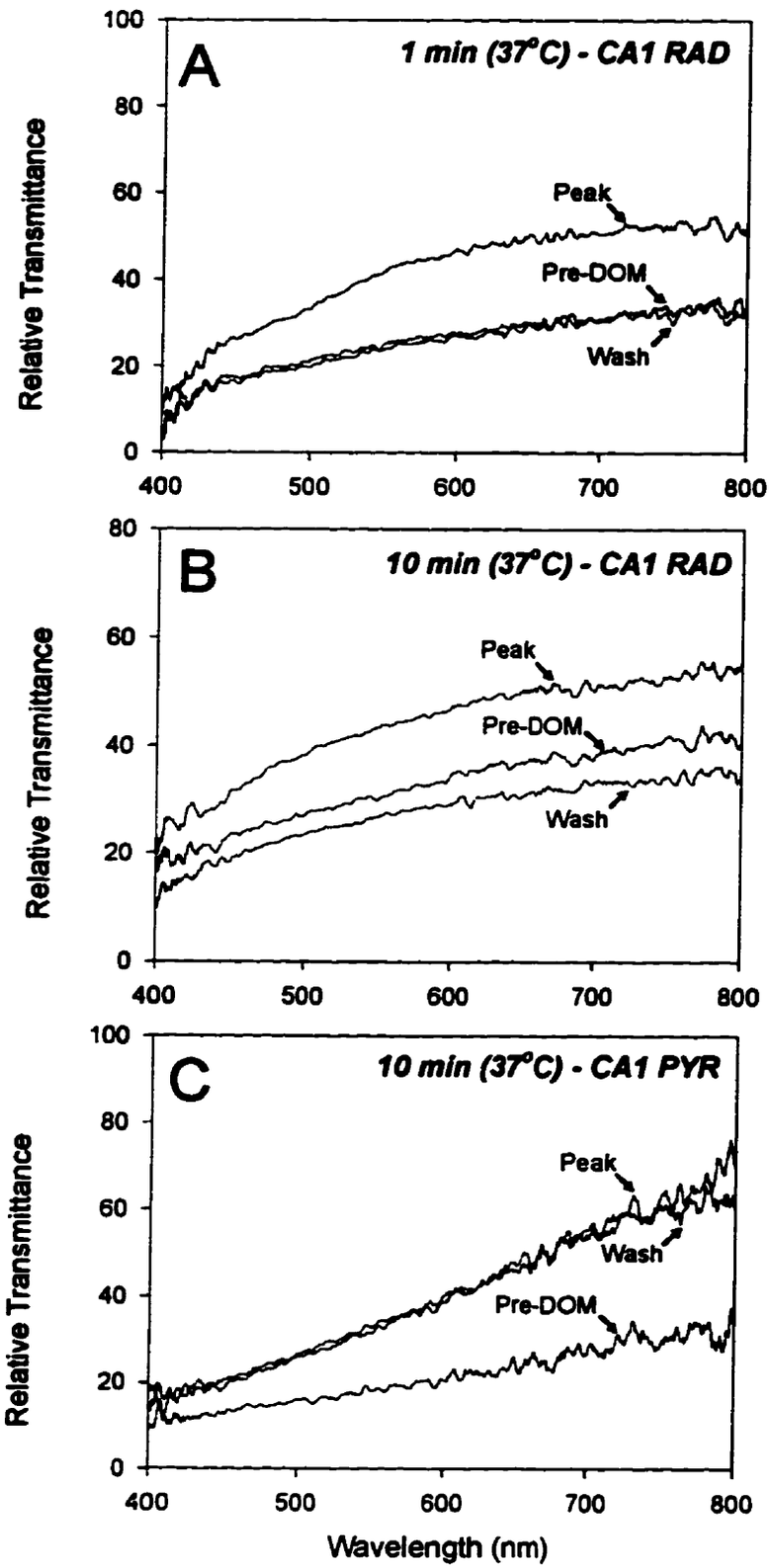
A
1 min (37°C) - CA1 RAD
Peak
Pre-DOM
Wash
B
10 min (37°C) - CA1 RAD
Peak
Pre-DOM
Wash
C
10 min (37°C) - CA1 PYR
Peak
Wash
Pre-DOM
Relative Transmittance
Wavelength (nm)
0
20
40
60
80
100
400
500
600
700
800

Figure 3.6: Simultaneous intrinsic optical signals (left) and electrophysiological recordings (right) from CA1 region during bath application of DOM. Numbers along plot refer to the point where averaged traces (right) are sampled. **A)** Ten μM DOM for 1 min at 37°C (*bar)* evokes a large but reversible increase in LT in CA1 RAD. Signal onset coincides with a loss of the evoked CA1 field potential (traces *A2, A3*). LT return to baseline marks the start of a gradual recovery (*A4*). **B)** Ten μM DOM for 10 min at 37°C (*bar*) initially evokes a large increase in LT in CA1 RAD, the onset coinciding with a loss of the evoked CA1 field potential (*B2*). The evoked field does not return once LT goes negative traced (*B3,B4*).

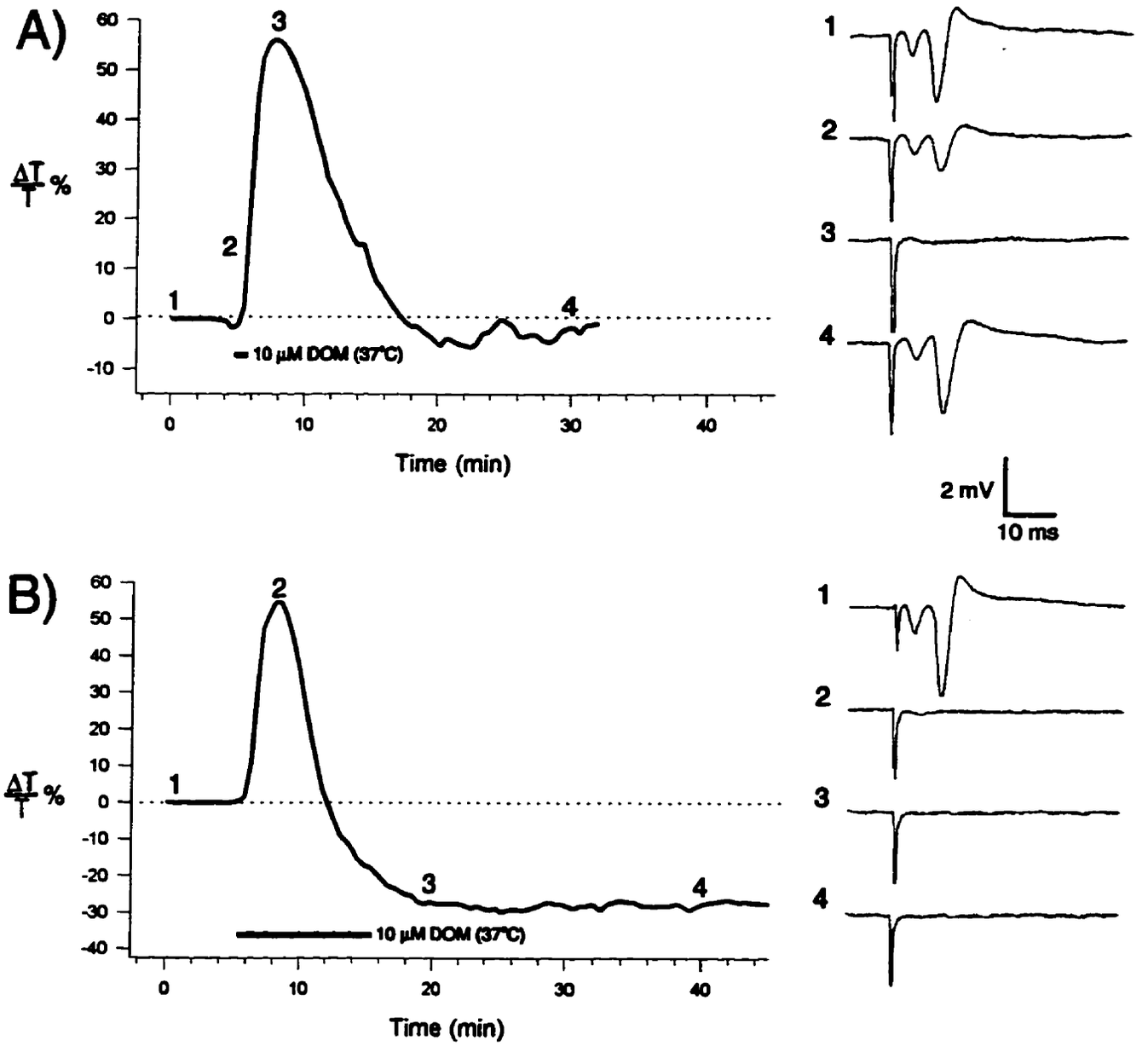
A)
60
50
40
30
20
10
0
-10
ΔT/T %
1
2
3
4
10 µM DOM (37°C)
0
10
20
30
40
Time (min)
1
2
3
4
2 mV
10 ms
B)
60
50
40
30
20
10
0
-10
-20
-30
-40
ΔT/T %
1
2
3
4
10 µM DOM (37°C)
0
10
20
30
40
Time (min)
1
2
3
4

Figure 3.7: Paraffin sections of hippocampal slices stained with hematoxylin and eosin showing the CA1 region (A-C; 4x and 25x) and the dentate gyrus (D-F; 4x and 25x). Histology confirms suspected neuronal damage implicated by irreversible transmittance changes. An untreated slice (Control) showed no neuronal damage in CA1 region **(A)** and dentate gyrus **(D)**. Similarly, a slice treated with 10 μM DOM for 1 min at 37°C (that lead to reversible LT changes) also shows no damage **(B and E)**. Only the DOM exposure for 10 min at 37°C (that lead to *ir*reversible LT changes) causes cellular damage to dendritic and particularly to cell body layers in both the CA1 region **(C)** and the dentate gyrus **(F)**.

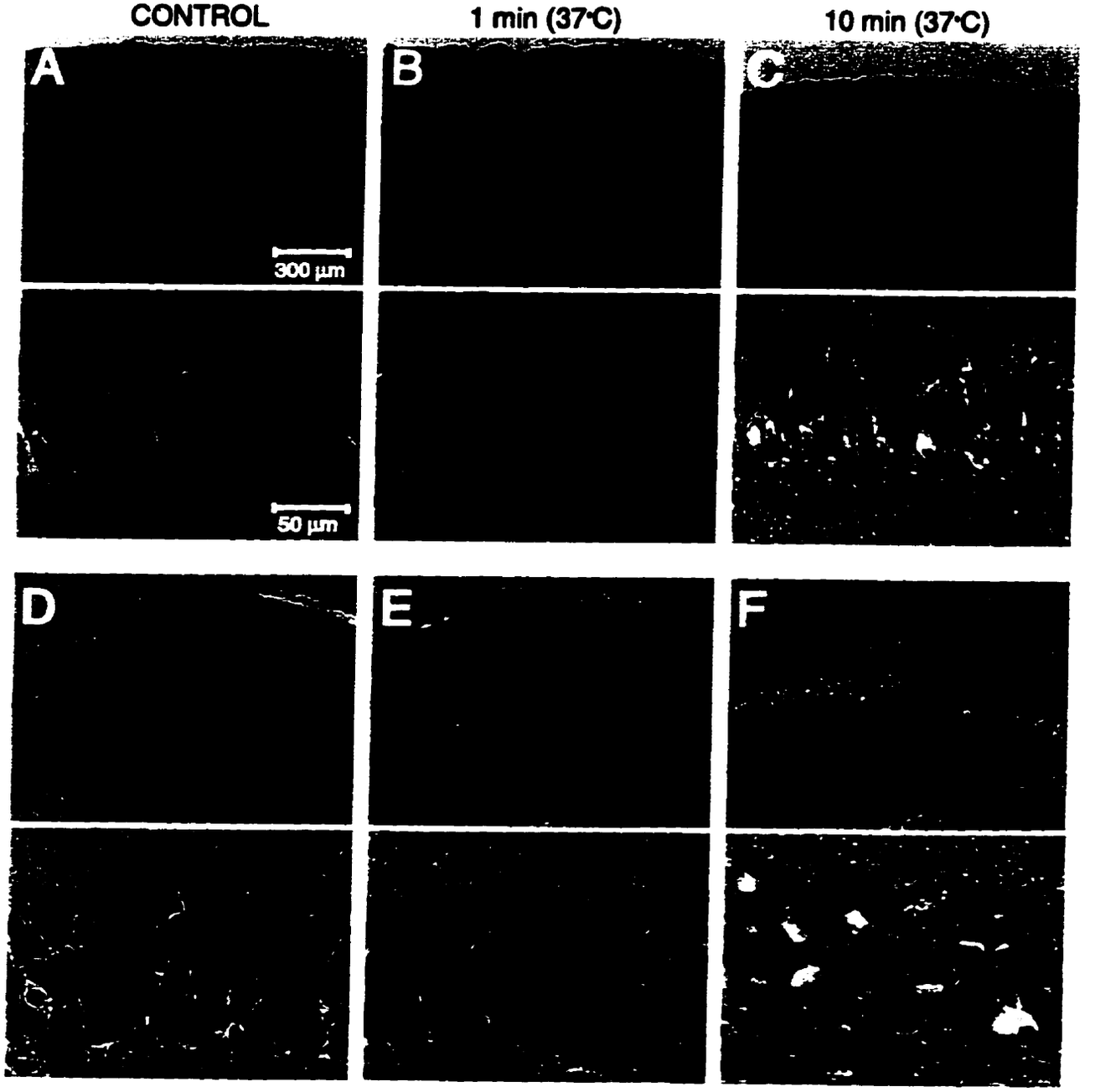
CONTROL
1 min (37°C)
10 min (37°C)
A
B
C
300 µm
50 µm
D
E
F

Figure 3.8: Low Cl^- saline but not zero Ca^{2+} saline affords protection from damage by domoate. Time course of LT changes ($\Delta T/T\%$) in CA1 RAD following domoate exposure. **A)** A 1 min exposure in normal aCSF (*black circles*) or in zero Ca^{2+} aCSF (*grey squares*) in the same hippocampal slice evokes a similar LT increase (n=5 slices). **B)** A 10 min exposure to DOM in zero Ca^{2+} aCSF (*grey squares*) elicites the irreversible dendritic shrinkage (and cell body swelling), suggesting permanent neuronal damage. **C)** A 1 min exposure to DOM in low Cl^- aCSF (*grey squares*) evokes no measurable LT response whereas DOM in normal aCSF (*black circles*) evokes a large, reversible response in the same slice (n=6 slices).

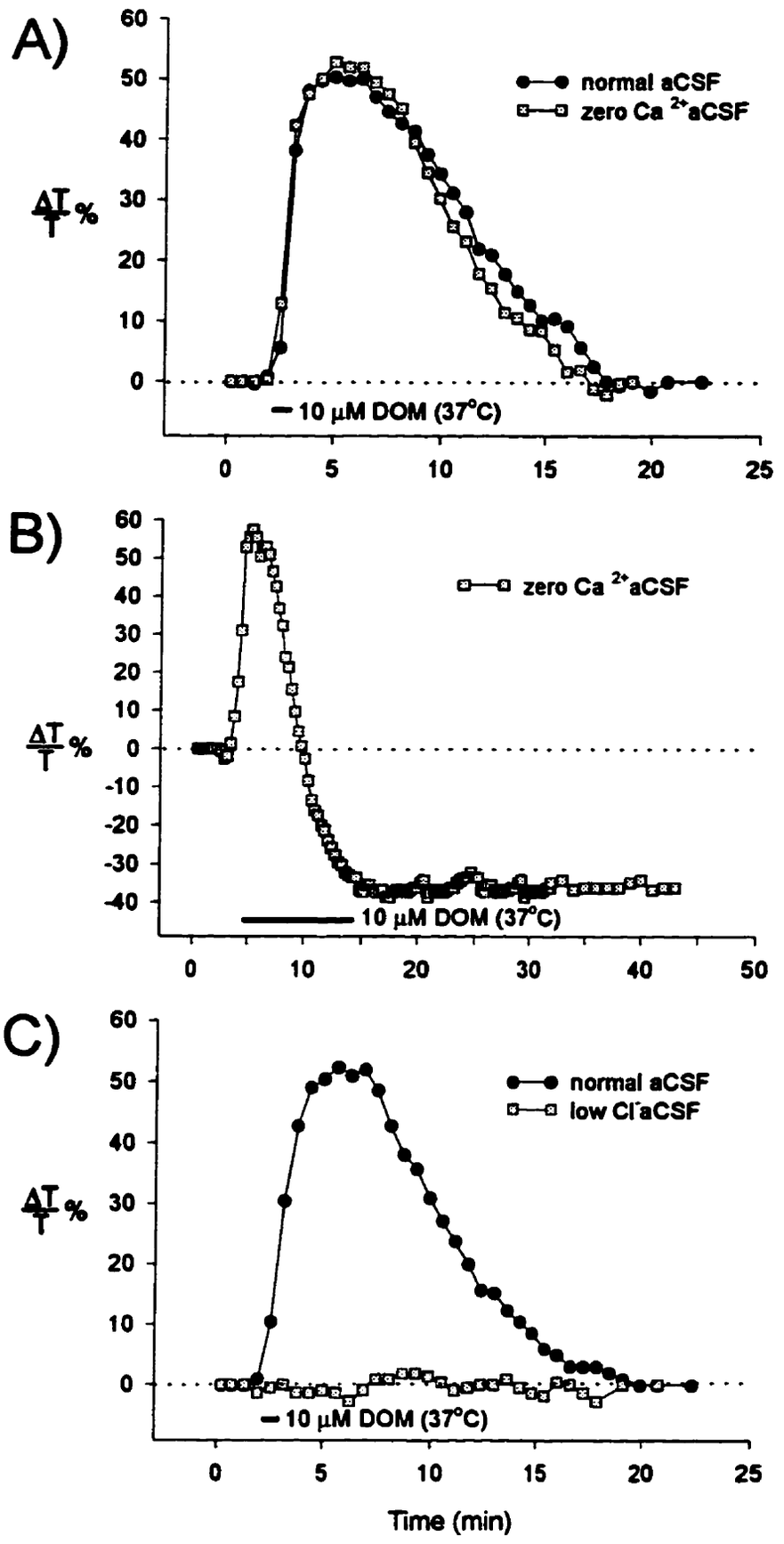
A)
normal aCSF
zero Ca 2+aCSF
ΔT/T %
10 µM DOM (37°C)
B)
zero Ca 2+aCSF
ΔT/T %
10 µM DOM (37°C)
C)
normal aCSF
low Cl-aCSF
ΔT/T %
10 µM DOM (37°C)
Time (min)

CHAPTER 4

ANTAGONISM OF ACUTE NEUROTOXICITY OF CA1 NEURONS EVOKED BY DOMOIC ACID BY AMPA BUT NOT KAINATE RECEPTOR BLOCKADE

Ready for submission to *NeuroReport*

ABSTRACT

We investigated the ability of two glutamate receptor antagonists to reduce domoic acid stimulation and toxicity *in vitro*. Non-NMDA receptor activation leads to neuronal swelling and death in the hippocampal slice preparation, but whether the receptors are of the AMPA or kainate subtype is unclear. We measured cell volume change in response to domoate, a seafood toxin and non-NMDA glutamate agonist, by imaging changes in light transmittance (LT) producing an index of excitotoxicity across several hippocampal regions. A 1 min exposure to 10 μM domoate at 22°C evoked large, reversible changes in LT primarily in CA1 dendritic regions. Little change was observed in the CA3 region. The CA1 response was significantly blocked by GYKI 52466 [1-(4-aminophenyl)-4-methyl-7,8-methylenedioxy-5H-2,3-benzodiazepine HCl], a non-competitive antagonist of GluR1-4 (AMPA) receptors. However, NS-102 [5-nitro-6,7,8,9-tetrahydrobenzol[*g*]indol-2,3-dione-3-oxime], a new antagonist of low affinity kainate receptors (GluR5-7), failed to antagonize domoate stimulation. A 10 min exposure to 10 μM domoate at 37°C evoked irreversible changes in LT (toxicity) primarily in the CA1 region. GYKI 52466 significantly protected against domoate-induced toxicity produced by prolonged agonist exposure while NS-102 did not. Exposure to 10 μM AMPA (α-amino-3-hydroxy-5-mehtyl-isoxazole-4-propionate) evoked responses similar to that of DOM at both 22°C and 37°C. Like domoate, both AMPA-evoked responses (i.e. dendritic swelling at 22°C

and CA1 toxicity at 37°C) were antagonized by GYKI 52466. We conclude that rapidly triggered volume changes leading to neuronal toxicity in the CA1 region evoked by domoate are mediated by AMPA, not kainate, receptors.

[Key Words: AMPA, CA1, cell swelling, domoic acid, excitotoxicity, glutamate receptors, hippocampus, imaging, kainic acid, non-NMDA receptors]

INTRODUCTION

The excitatory amino acid L-glutamate is the most common neurotransmitter in the brain. Excessive glutamate release and accumulation in the brain has been implicated in rapidly triggered neuronal death which can result from head trauma, stroke, and food poisoning (Choi 1990). This phenomenon, termed excitotoxicity, refers to the overstimulation of glutamate receptors and subsequent neuronal degeneration in response to immediate increases in intracellular concentrations of Na^+, Cl^-, and Ca^{2+} (Rothman 1985; Choi 1990). Specific glutamate agonists and antagonists provides a useful tool for investigating the processes that underlie excitotoxicity.

Domoic acid (DOM), a naturally occurring amino acid produced by marine algae and seaweed, is a potent glutamate receptor agonist. A severe outbreak of food poisoning from domoate-contaminated mussels in Canada during the late 1980's intensified the study into the actions of domoate. Domoate was initially described as a highly specific kainate-receptor agonist (Debonnel *et al.* 1989a, 1989b; Stewart *et al.*1990; Chiamulera *et al.* 1992). But with the discovery of multiple receptor subunits, classification has become more complex (Tasker *et al.* 1996). AMPA preferring receptors are assembled from subunits GluR1-4 whereas kainate receptors are assembled from subunits GluR5-7 (low affinity) and KA1-2 (high affinity) (Bettler and Mulle 1995). Domoate is now considered to be a mixed agonist acting on both AMPA and kainate (KA) receptors with different affinities (Hampson *et al* 1992;

Zhou *et al.* 1993; Bettler and Mulle 1995). However, the physiological significance of domoate interaction with AMPA-preferring and kainate-preferring receptors is still unknown. Both domoate and kainate produce toxicity by similar mechanisms (Debonnel *et al.* 1989a; 1989b; Stewart *et al.* 1990) but differences in behavioral properties induced by the two excitotoxins provide indirect evidence that their mechanisms are not identical (Tasker *et al.* 1991). Variability in hippocampal damage (Strain and Tasker 1991), in specific binding (Kunig *et al.* 1995), and in their pharmacological profiles (Tasker *et al.* 1996) indicate that slightly different pools of receptors mediate domoate and kainate effects. The lack of specific non-NMDA antagonists that differentiate between AMPA and kainate receptor-mediated responses has made the classification process difficult. Recently however, two novel compounds have been shown to specifically block these receptors.

GYKI 52466 [1-(4-aminophenyl)-4-methyl-7,8-methylenedioxy-5H-2,3-benzodiazepine HCl] non-competitively blocks AMPA-receptor mediated responses (Ouardouz *et al.* 1991; Donevan and Rogawski 1993; Renard *et al.* 1995; Rammes *et al.* 1996). In whole-cell voltage clamp recordings from cultured hippocampal neurons, 100 μM GYKI 52466 completely antagonizes AMPA-activated currents but is inactive against NMDA or GABA responses (Donevan and Rogawski 1993). Moreover, GYKI 52466 (100 μM) distinguishes between AMPA receptor- and kainate receptor-mediated responses in rat cerebellar slice cultures (Renard *al.* 1995). It also decreases the peak amplitude of hippocampal area CA1 AMPA receptor-mediated excitatory post-synaptic currents in rat hippocampal slices (Rammes *et al.* 1996).

NS-102 [5-nitro-6,7,8,9-tetrhydrobenzol[g]indol-2,3-dione-3-oxime] is a highly specific antagonist for low-affinity kainate receptors (Johansen *et al.* 1993; Verdoon *et al.*1994). In transfected fibroblasts, NS-102 reduces currents mediated by GluR6 receptors (IC_{50}=3 μM) with little effect on currents mediated by GluR2/4 receptors (Verdoon *et al.*1994). As well, 10 μM NS-102 (IC_{50}=1 μM) almost completely inhibits [^{3}H]kainate binding to GluR6 receptors (Verdoon *et al.*1994), shows a high selectivity for low affinity versus high affinity [^{3}H]kainate binding sites and only weakly inhibits AMPA binding (Johansen *et al.* 1993). Changes in light transmittance (LT) are correlated with cell volume changes in the CA1 region of the hippocampal slice (Andrew and MacVicar 1994; Kriesman *et al.* 1995).

Activation of either NMDA or non-NMDA receptors leads to immediate swelling in dendritic regions of CA1 and dentate gyrus that can progress to cell body swelling and permanent loss of the evoked field potential, indicating acute excitotoxic cell death (Andrew, Adams, Polischuk 1996; Polischuk and Andrew 1996b). We showed in previous studies (Polischuk and Andrew 1995, 1996a, 1996c) that domoate-induced LT changes were probably mediated by AMPA receptor stimulation but, lacking a specific kainate receptor antagonist, GluR5-7 or KA1-2 mediation could not be ruled out.

The present study investigated the effects of highly specific non-NMDA glutamate receptor antagonists on both domoate- and AMPA-induced IOSs in the rat hippocampal slice. Our objective was to further characterize the pharmacology of domoic acid-induced cell swelling *in vitro* by: (1) comparing the IOS produced by AMPA to that of domoate, (2)

studying the effects of GYKI 52466 and NS-102 on domoate- and AMPA- induced cell swelling, and (3) determining the protective ability of these antagonists against irreversible damage induced by domoate.

METHODS

Hippocampal Slice Preparation

Male Sprague-Dawley rats, 21-28 days old (Charles River, St. Constant, Quebec, Canada) were housed in a controlled environment (25°C, 12 hour light/dark cycle) with food and water available *ad libitum*. A rat was placed in a rodent restrainer and guillotined. The excised brain was hemisected and each hippocampus exposed under cold artificial cerebrospinal fluid (aCSF). Transverse slices were cut (400 μm) using a manual tissue slicer and stored at 22°C in aCSF oxygenated with 95% O_2 / 5% CO_2 for a minimum of 1 hour before being transferred to the recording chamber.

Drugs and Reagents

The aCSF contained (in mM): NaCl 120, KCl 3.3, $NaHCO_3$ 26, $MgSO_4$ 1.3, NaH_2PO_4 1.2, D-glucose 11.0, and $CaCl_2$ 1.8 dissolved in distilled water at pH 7.3-7.4. The aCSF was used for the dissection of the hippocampus, for the incubation and superfusion of slices, and as a vehicle for drug administration in the imaging chamber. The osmolality of the aCSF and its variants was 295 ± 2 mOsm as measured with a freezing point depression osmometer (Precision Systems Inc.). Chemicals for the aCSF were from the Sigma Chemical Co. (St.

Louis, MO), domoic acid from Diagnostic Chemicals Ltd. (Charlettetown, PEI), GYKI 52466 from Research Biochemicals International (RBI; Natick, MA), and NS-102 from NeuroSearch A/S (Glostrup, Denmark).

Intrinsic Optical Signal Imaging

Intrinsic optical signals (IOSs) representing primarily changes in light transmittance (MacVicar and Hochman 1991; Kreisman *et al.* 1995; Andrew *et al.* 1997) were monitored using techniques previously described (Polischuk and Andrew 1996c). A slice was transferred to an imaging chamber where it was weighted at the edges with silver wire and submerged in flowing, oxygenated aCSF (2 mL/min) at 22°C or 37°C. The slice was viewed with an inverted microscope with only a coverslip between the slice and the 1.6x objective. The slice was transilluminated by a halogen lamp with a voltage regulated power supply (Leica). Video frames were obtained at 30 Hz using a charge-coupled device (CCD camera) which was set for maximum gain and a low black level. With gamma set to 1.0, the output of the CCD is linear with respect to change in light intensity. Frames were averaged and digitized using an image processor board (DT2867, Data Translation) in a Pentium PC controlled by Axon Imaging Workbench software (Axon Instruments). A series of averaged images were stored on a removable hard drive (Iomega).

Experiments entailed acquiring an averaged image every 8 seconds (256 frames @ 30 Hz). The first averaged image in a series served as a control (T_{cont}) which was subtracted from each subsequent experimental image (T_{exp}) of that series. A series of subtracted images

revealed areas in the slice where light transmittance (LT) changed over time. LT was expressed as the digital intensity of the subtracted image (T_{exp}-T_{cont}) divided by the gain of the intrinsic signal which was set using the software program. This value was then expressed as a percentage of the digital intensity of the control image of that series. That is,

$$LT = \frac{(T_{exp}-T_{cont})/gain}{T_{cont}} \times 100\% = \frac{\Delta T}{T}\%$$

The control image was displayed using a gray intensity scale (bright field image). Each subtracted image was displayed using a pseudo-colour intensity scale. To quantify and graphically display data, zones of interest were boxed using the Axon Imaging Workbench software. The average digital intensity of each zone was sampled, stored as text files, and graphed using SigmaPlot for Windows software (Jandel Scientific). Statistical analysis included a comparison of means using Student t-tests. A graphics program (CorelDRAW 3.0) was used to import and label images.

Agonist/Antagonist Exposure Paradigms

Two paradigms of agonist exposure were used. A *1 min* exposure to 10 μM domoate (or AMPA) at 22°C produces a *reversible* IOS which we have shown previously to represent reversible cell swelling (Andrew, Adams, Polischuk 1996; Polischuk and Andrew 1996c). This paradigm has been used previously to characterize the effects of other antagonists on domoate-induced IOSs (Polischuk and Andrew 1996c). A *10 min* exposure to 10 μM domoate at 37°C produces *irreversible* changes in LT, representing cell death (Andrew,

Adams, and Polischuk 1996; Polischuk and Andrew 1996b). NS-102 is approximately ten times more potent than GYKI 52466 at antagonizing their respective receptor-mediated responses. *In vitro,* GYKI 52466 has a IC_{50} of ~10 μM for antagonizing AMPA-induced currents while 100 μM completely blocks responses (Donevan and Rogawski 1993; May and Robison 1993; Rammes *et al.* 1996). Whereas NS-102 has an IC_{50} of ~1 μM for displacing [^{3}H]kainate in rat cortical membranes, while 10 μM was near maximal (Johnasen *et al.* 1993). Furthermore, doses of >10 μM NS-102 are not testable because of its limited solubility in saline solution. Thus maximal antagonist concentrations of 100 μM and 10 μM for GYKI 52466 and NS-102, respectively, were chosen. All hippocampal slices were superfused for >15 min with the antagonist before and during agonist exposure.

RESULTS

Effects of non-NMDA antagonists on reversible domoic acid-induced IOSs.

Brief (1 min) exposure to 10 μM domoate resulted in dramatic but reversible increases in LT in certain dendritic regions of the hippocampal slice. LT increased by over 50% in CA1 stratum radiatum (RAD) and responses were also significant in CA1 stratum oriens (OR) and the molecular layer of the dentate gyrus (DG MOL) (Table 4.1; Fig. 4.1B,E). All responses reversed to baseline within 30 min (Fig. 4.3A,B). However, the CA3 dendritic region (CA3 RAD) was not significantly affected (Table 4.1; Fig. 4.1B,E). The cell body region in CA1 (stratum pyramidale, PYR) was minimally affected and no significant change was measured in the cell body regions of either CA3 or DG (Table 4.1; Fig. 4.1B,E).

GYKI 52466 at 100 μM significantly reduced domoate-induced LT changes at 22°C (Table 4.1). Peak responses in the dendritic regions of CA1 RAD, CA1 OR, and DG MOL were reduced to near control levels (i.e. aCSF alone) (Table 4.1; Fig. 4.1C). Figure 4.3A plots the time course of increased LT in CA1 RAD, the area of greatest response, to domoate in the absence and presence of 100 μM GYKI 52466.

In contrast, 10 μM NS-102 did not significantly reduce domoate-induced changes in LT (Table 4.1; Fig. 4.1F) which were identical to those induced by domoate alone in dendritic regions of CA1 and DG (Fig. 4.1E). Figure 4.3B plots the typical time course of increased LT in CA1 RAD, the area of greatest response, to 1 min exposure to 10 μM domoate in the absence and presence of 10 μM NS-102.

We next compared domoate-induced changes in LT to those induced by AMPA. A 1 min application of 10 μM AMPA resulted in a profile of LT change similar to 10 μM domoate (Table 4.1; Fig. 4.1H). Again, large increases in LT occurred primarily in CA1 dendritic regions (RAD and OR) with no significant change in area CA3. Responses completely reversed to baseline within 15 min of exposure. Additionally, like domoate, this equipotent dose of AMPA was completely blocked by pre-exposure to 100 μM GYKI 52466 (Table 4.1; Fig. 4.1J). Figure 4.3C plots the typical increase in LT in CA1 RAD following a 1 min exposure to 10 μM AMPA, both in the absence and presence of 100 μM GYKI 52466. The only obvious difference between the AMPA and DOM responses was the absence of a response in the dendritic region in the DG.

Effects of non-NMDA antagonists on irreversible domoic acid-induced IOSs.

We also examined if either antagonist could protect against a toxic exposure to domoate. Our previous studies determined that a 10 min exposure to 10 μM domoate at 37°C killed neurons in area CA1 as determined by electrophysiological and histological evidence (Polischuk and Andrew 1996b). An initial LT increase in CA1 dendritic regions (RAD and OR; Fig. 4.2B) was followed by a large, irreversible negative LT shift. A concomitant irreversible increase in LT in CA1 cell bodies occurred (Fig. 4.2C). A similar sequence also developed in the molecular and cell body layer of the DG (Fig. 4.2B,C). Table 4.2 summarizes initial peak LT changes in CA1 RAD and subsequent irreversible changes in CA1 RAD and PYR.

GYKI 52466 reduced initial LT increase in CA1 dendritic regions (Table 4.2; Fig. 4.2E), abolished the generation of the negative LT dendritic response, and prevented cell body swelling in CA1 and DG (Table 4.2; Fig. 4.2F). Figure 4.4A demonstrates the time course of LT change as measured in CA1 RAD, first in the presence and then absence of the antagonist.

In contrast, pre-treatment with 10 μM NS-102 failed to reduce LT changes induced by prolonged exposure to domoate at 37°C. Initial peak regional responses to domoate in the presence of NS-102 were not significantly different than domoate alone (Table 4.2; Fig. 4.2H) nor did NS-102 prevent an irreversible change in LT in CA1 (Fig. 4.2J). Both the increased transmittance in CA1 PYR and the decreased transmittance in CA1 RAD were maintained during the wash (Table 4.2). Figure 4.4B plots the LT change over time in CA1

RAD in response to 10 μM domoate at 37°C.

The effect of a similar 10 min exposure to AMPA was also examined. Like domoate, 10 μM AMPA at 37°C resulted in pronounced, irreversible changes in LT primarily in area CA1 (Fig. 4.2M). Initial peak LT increases in CA1 RAD (Fig. 4.2L) were similar to 10 μM domoate (*CA1 RAD peak*, Table 4.2) and were followed by a similar increase in LT in CA1 PYR coupled to a dramatic negative shift in CA1 RAD and OR (Fig. 4.2M). Decreased LT changes in CA1 dendrites (*CA1 RAD wash*, Table 4.2) and increased LT changes in cell bodies (*CA1 PYR wash*, Table 4.2) were statistically similar than those induced by domoate. Figure 4.4C illustrates the regional LT changes over time in response to 10 μM AMPA at 37°C.

Like domoate, irreversible AMPA-induced changes in LT were blocked by 100 μM GYKI 52466. The antagonist reduced initial increases in LT in CA1 dendritic regions (Table 4.2; Fig. 4.2P) and abolished the irreversible LT signal induced by 10 min of AMPA at 37°C and restored reversibility of the response (Table 4.2; Fig. 4.2Q). Figure 4.4C demonstrates a typical time course of LT change as measured in CA1 RAD induced by AMPA, in the presence of GYKI 52466.

DISCUSSION

GYKI 52466 is a non-competitive and selective blocker of AMPA receptors (Ouardouz *et al.* 1991; Donevan and Rogawski 1993; May and Robison 1993; Renard *et al.* 1995; Rammes *et al.* 1996). Renard and colleagues (1995) used GYKI 52466 to distinguish

domoate responses at AMPA and kainate receptors in Purkinje cell slice cultures. GYKI 52466 reduced whole-cell currents induced by both AMPA and domoate and was a more efficient antagonist of the responses mediated through the activation of AMPA receptors than those mediated via kainate receptors. A large disparity between IC_{50} of GYKI 52466 for currents evoked by AMPA (~10 μM) or domoate (~105 μM) was attributed to domoate activating both AMPA and kainate receptors on Purkinje cells. This indicated that GYKI 52466 can discriminate between domoate-induced activity on AMPA and kainate receptors.

The newly developed antagonist, NS-102, exhibits affinity and selective antagonism for the low affinity [^{3}H]kainate binding site but it failed to completely antagonize domoate-induced depolarizations in the rat cortical wedge preparation even at a maximal concentration (10 μM) suggesting mediation by AMPA receptors (Johansen *et al.* 1993). In our study, NS-102 did not significantly reduce domoate-induced cell swelling nor toxicity in our slice preparation. However it produced a 50% reduction in domoate toxicity in mouse hippocampus (Tasker *et al.* 1996) suggesting that toxicity also occurs via non-AMPA (i.e. kainate) receptors. Certainly the CA3 region is a major site of domoate toxicity (Debonnel *et al.* 1989a, 1989b; Stewart *et al.*1990; Tasker and Strain 1991; Gross *et al.* 1995; Tasker *et al.* 1996). If kainate receptors alone do mediate neuronal toxicity, our study indicates that rapidly triggered changes in cell volume are not involved. Otherwise NS-102 blocks only some of the receptors sensitive to domoate and remaining toxicity is dependent on non-kainate receptor-mediated activity. Differentially sensitive populations of hippocampal pyramidal neurons to domoate-induced elevations of calcium provides evidence for two

domoic acid-sensitive non-NMDA receptor subtypes (Xi and Ramsdell 1996).

Post-synaptic kainate receptors have not been identified in adult hippocampal neurons (reviewed by Malva *et al.* 1996). Rather, kainate receptors are localized presynaptically in the CA3 subregion and domoate (or kainate) induced toxicity in the CA3 is dependent pre-synaptic excitation via the presence of an intact mossy fibre projection on CA3 neurons (Debonnel 1989b; Terrain *et al.* 1991; Malva *et al.* 1996). As such, in our preparation, domoate-evoked swelling may be only acting at AMPA receptors in CA1. Domoate is likely acting at kainate receptors as well, but they do not appear involved with neuronal volume changes which are mediated post-synaptically. Since kainate receptors on mossy fibers may be inhibitory (Chittajulla *et al.* 1996) it is difficult to understand how their activation would be excitotoxic. Excitotoxic activation of CA3 neurons *in vivo* may result from extra-hippocampal stimulation. For example the septal nuclei, which contain AMPA receptors (Cotman *et al.* 1987) and are stimulated by domoate (Gross *et al.* 1995). These then indirectly project to the hippocampus and subsequently CA3 (Swanson *et al.* 1987).

Although many reports indicate CA3 as a major target for domoate-induced neurotoxicity, most also report activity in the CA1 region, regardless of the route of exposure (Debonnel *et al* .1989a; Stewart *et al.* 1990; Tasker and Strain 1991; Gross *et al.* 1995; Tasker *et al.* 1996). Additionally, post-mortem assessment of patients who died after ingesting contaminated mussels demonstrated that hippocampal necrosis occurred maximally in H1 and H3 (homologues of areas in CA1 and CA3, respectively, in rats) (Teitelbaum *et al.* 1990).

The spatial response induced by domoate in our preparation also suggests involvement of AMPA and not KA receptors. That is, domoate-induced cell swelling was primarily localized to an area where AMPA receptors predominate, namely area CA1 (Cotman *et al.* 1987; Schroeder 1993: Seeburg 1993). KA receptors, are mainly localized to CA3, specifically in the terminal field of mossy fibers (Monaghan and Cotman 1982; Cotman *et al.* 1987), an area surprisingly unresponsive to domoate-induced swelling. AMPA receptors are relatively sparse in the CA3 region (Cotman *et al.* 1987).

Compared to kainate, domoate has an approximately ten-fold potency (10 μM vs 100 μM) for inducing maximal LT changes in area CA1 of the hippocampal slice (Andrew, Adams, Polischuk 1996) and the present study shows that AMPA and domoate are roughly equipotent (10 μM). Thus, the observed order of agonist potency, domoate≈AMPA>kainate , is consistent with the activity for an active AMPA receptor. The agonist potency order is not compatible with the activity expected for a functionally active kainate receptor (i.e. domoate>kainate>>AMPA) (Bettler and Mulle 1995).

In conclusion, our results indicate that the neuronal volume changes evoked by domoic acid *in vitro* are mediated through AMPA receptor stimulation. Domoic acid toxicity is localized to area CA1 and the DG. AMPA itself presents a similar pattern of toxicity with a similar potency to domoate but without a response in DG. The AMPA-receptor antagonist, GYKI 52466, completely blocks AMPA-evoked toxicity in the hippocampal slice. Because GYKI 52466 also completely antagonizes all domoic acid-

evoked toxicity measured by LT changes, the action appears to be through AMPA receptors alone. Conversely, the specific kainate receptor antagonist, NS-102, does not inhibit domoic acid volume change or toxicity. This study furthers the notion that more than one receptor exists which are sensitive to domoic acid, a kainate-like agonist. This study demonstrates that rapidly triggered neuronal death is mediated through AMPA receptors whereas excitotoxicity arisung from kainate receptor activation must be a more subtle, longer term event.

TABLES

Table 4.1: Mean peak changes in light transmittance (ΔT/T%) of hippocampal regions in response to 1 in exposure to glutamate agonists at 22°C.

Hippocampal Region	aCSF (n=5)	10 μM DOM (n=8)	10 μM DOM + 100 μM GYKI (n=5)	10 μM DOM + 10 μM NS 102 (n=3)	10 μM AMPA (n=5)	10 μM AMPA + 100 μM GYKI (n=5)
CA1 RAD	2.2±1.0	52.6±2.6*	4.6±1.5†	51.8±3.1*	55.0±1.7*	2.4±1.0‡
CA1 OR	2.1±0.8	31.1±2.7*	4.9±0.6†	28.1±6.6*	38.0±2.3*	2.4±2.2‡
CA1 PYR	1.1±1.4	8.8±2.2*	0.8±1.2†	9.5±2.0*	9.3±3.7*	0.4±0.8‡
DG MOL	1.6±0.8	18.2±2.7*	2.9±1.9†	27.0±5.1*	4.6±1.8	0.2±0.3
DG GC	1.8±1.1	2.1±1.4	1.1±0.3	4.7±0.6	1.6±1.2	0.0±0.4
CA3 RAD	0.1±1.2	1.1±0.5	-0.2±0.5	-0.1±1.6	-0.2±2.2	0.7±0.5
CA3 PYR	0.1±1.0	0.9±0.7	0.6±0.4	-0.7±1.2	0.5±0.8	0.5±0.2

Data reported are means ± SE.

*significantly different than aCSF alone (p<0.01).

†significantly different than 10 μM DOM alone (p<0.01).

‡significantly different than 10 μM AMPA alone (p<0.01).

Table 4.2: Mean changes in light transmittance (ΔT/T%) of CA1 hippocampal regions in response to 10 min exposure to glutamate agonists at 37°C.

Hippocampal Region	10 μM DOM (n=7)	10 μM DOM + 100 μM GYKI (n=5)	10 μM DOM + 10 μM NS 102 (n=5)	10 μM AMPA (n=7)	10 μM AMPA + 100 μM GYKI (n=5)
CA1 RAD (Peak)	57.3±3.2	20.6±3.2*	55.3±3.5	53.9±3.2	16.3±3.8†
CA1 RAD (Wash)	-34.4±4.1	-4.3±2.7*	-39.2±2.8	-40.1±2.7	0.5±4.3†
CA1 PYR (Wash)	50.5±3.2	2.5±0.7*	52.8±2.3	49.9±3.1	2.3±1.1†

Data reported are means ± SE.
*significantly different than 10 μM DOM alone (p<0.01).
†significantly different than 10 μM AMPA alone (p<0.01).

FIGURES

Figure 4.1: Digitized, pseudo-colored images demonstrating light transmittance changes in the rat hippocampal slice in responses to 1 min exposures to glutamate agonists at 22°C. Bright field images are shown at left (**A,D,G**). A 1 min exposure to 10 μM domoate [DOM] (**B,E**) or 10 μM AMPA (**H**) evoked the largest increases in LT in the dendritic regions of area CA1 [stratum radiatum (RAD) and stratum oriens (OR)] and to a lesser extent in the dentate gyrus (DG). Little or no change was observed in area CA3. 100 μM GYKI almost completely reduced DOM-induced LT change (**C**) while 10 μM NS-102 had no effect (**F**). 100 μM GYKI completely blocked AMPA-induced transmittance changes (**J**).

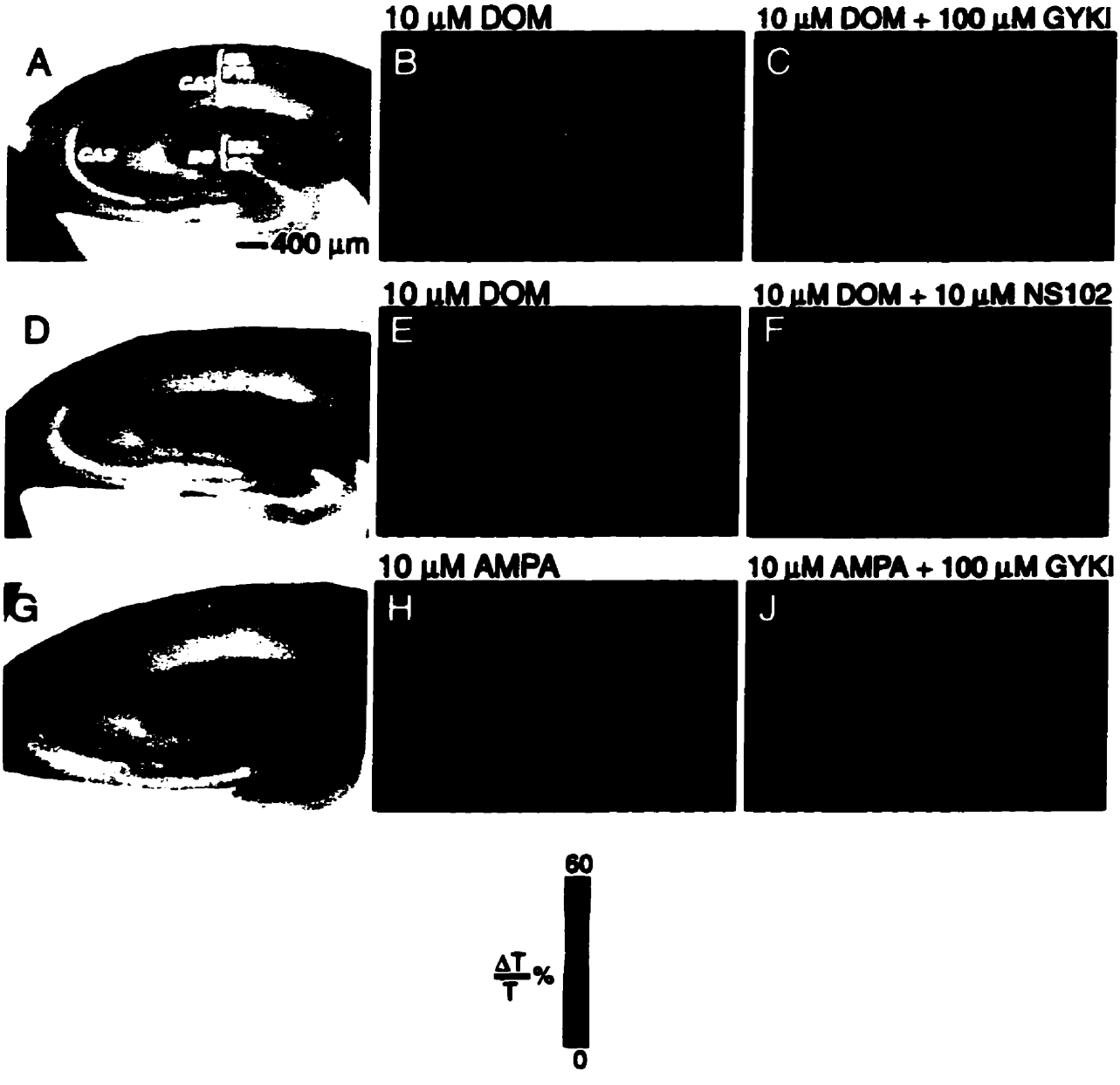
10 μM DOM
10 μM DOM + 100 μM GYKI
A
B
C
400 μm
10 μM DOM
10 μM DOM + 10 μM NS102
D
E
F
10 μM AMPA
10 μM AMPA + 100 μM GYKI
G
H
J
60
ΔT/T %
0

Figure 4.2: Digitized, pseudo-colored images demonstrating light transmittance changes in the rat hippocampal slice in responses to 10 min exposures to glutamate agonists at 37°C. Bright field images are shown at left (**A,D,G,K,N**). A 10 min exposure to 10 μM DOM initially evoked increased LT primarily in CA1 RAD and OR and to a lesser extent in the DG molecular layer [MOL] (**B**). A dramatic increase in LT in CA1 stratum pyramidale (PYR) follows concomitantly with a large negative decrease in CA1 RAD and OR, resulting in an irreversible sequence of LT changes (**C**). The DG is affected similarly. 100 μM GYKI reduced initial peak increases in LT induced by DOM (**E**), and blocked the expected progression of irreversible LT change, restoring complete reversibility of the response back to baseline levels (**F**). 10 μM NS-102 failed both to reduce peak LT changes induced by DOM (**H**) or block the irreversibility of the response (**J**). A prolonged exposure to 10 μM AMPA at 37°C for 10 min also initially increased LT primarily in CA1 RAD and OR (**L**) which then progressed into large, irreversible LT changes in CA1 RAD, OR, and PYR (**M**). The DG was spared. 100 μM GYKI reduced initial peak increases in LT induced by AMPA (**P**), and blocked the expected progression of irreversible LT change, restoring complete reversibility of the response back to baseline levels (**Q**).

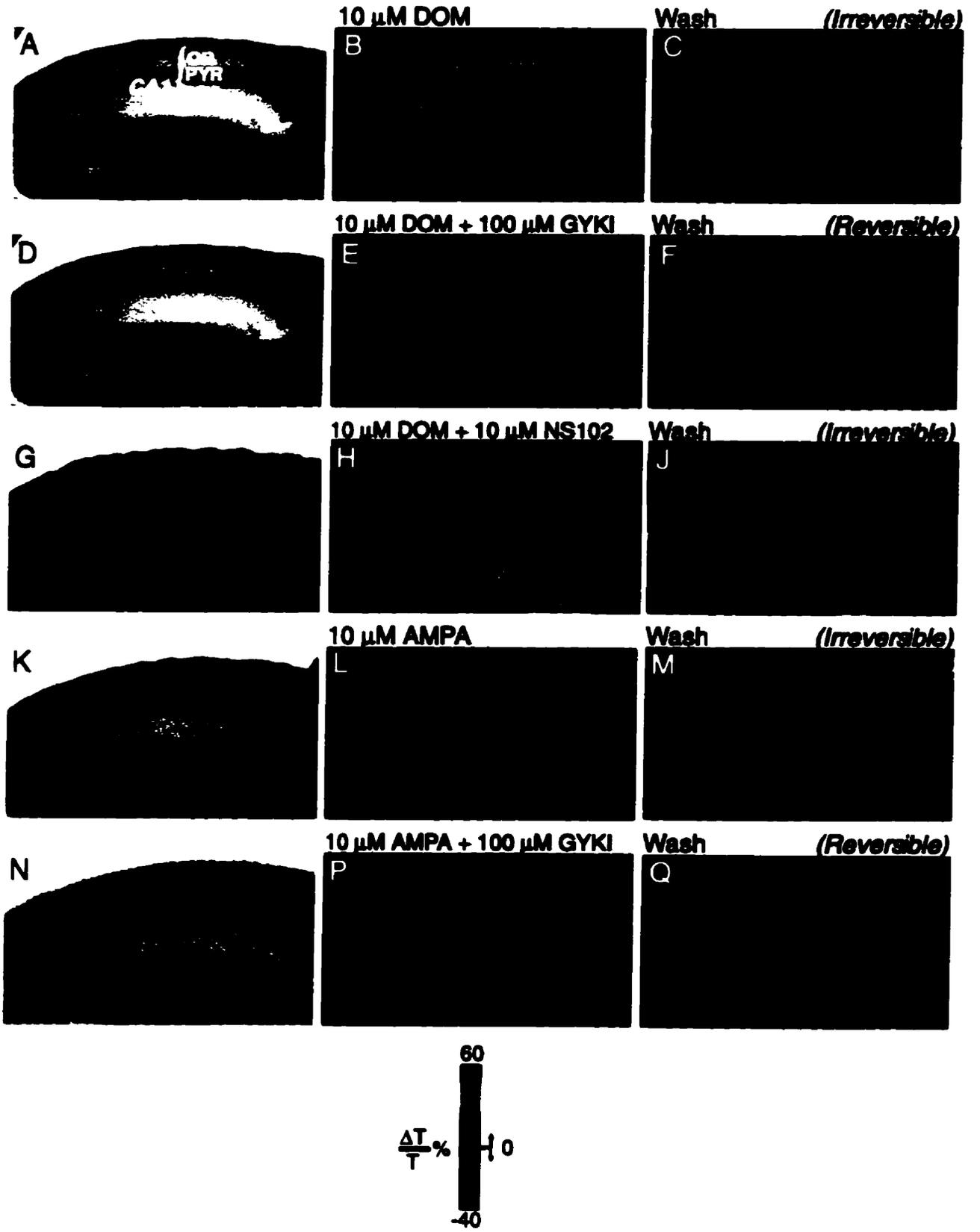
A
10 µM DOM
B
Wash
(Irreversible)
C
SO
PYR
D
10 µM DOM + 100 µM GYKI
E
Wash
(Reversible)
F
G
10 µM DOM + 10 µM NS102
H
Wash
(Irreversible)
J
K
10 µM AMPA
L
Wash
(Irreversible)
M
N
10 µM AMPA + 100 µM GYKI
P
Wash
(Reversible)
Q
60
ΔT/T %
0
-40

Figure 4.3: Time course of light transmittance changes (ΔT/T%) measured in CA1 stratum radiatum (CA1 RAD) over time. Responses are from representative slices in response to brief (1 min) exposure to glutamate agonists at 22°C. Reversible changes in transmittance are evoked by 10 μM domoate (DOM) and are blocked by 10 μM AMPA (**A**) but not by 10 μM NS-102 (**B**). 10 μM AMPA also elicits a large increase in LT that is blocked by 100 μM GYKI (**C**).

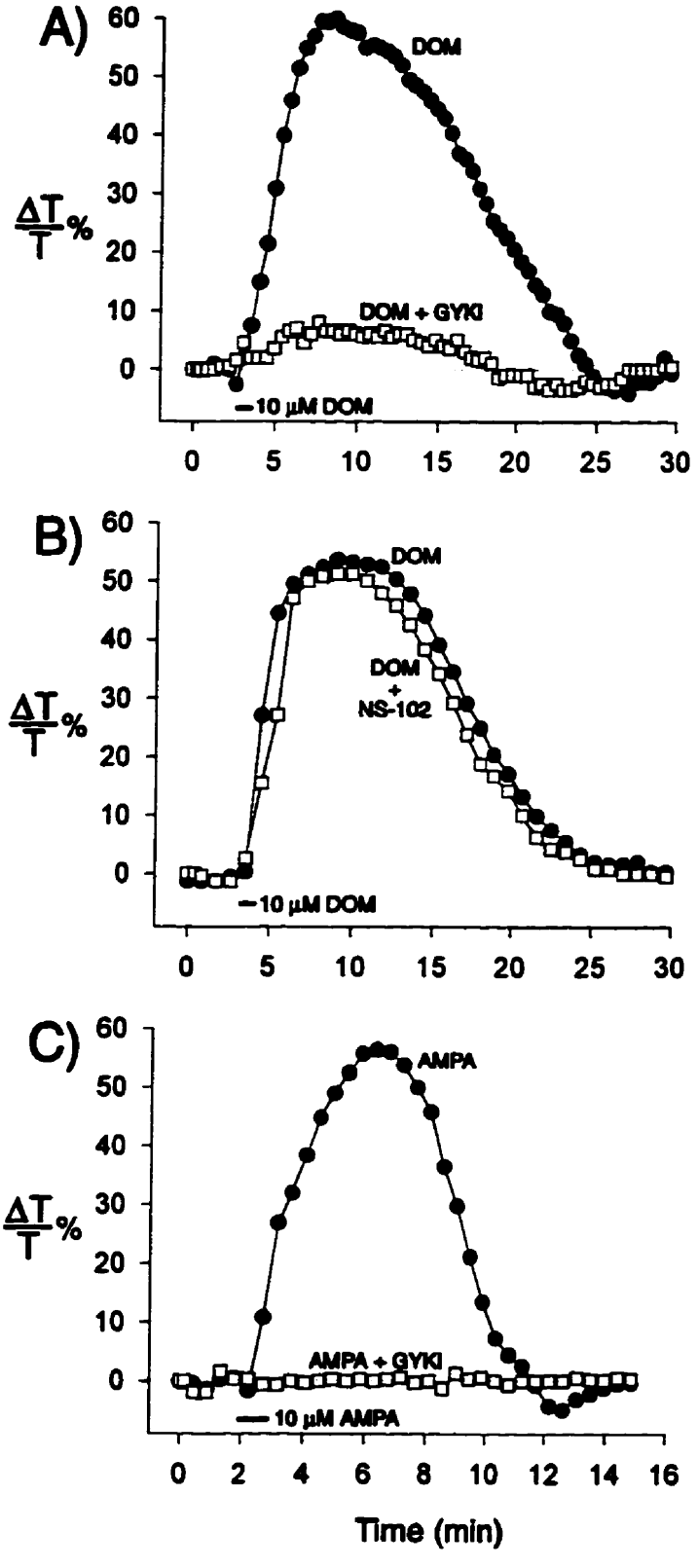
A)
B)
C)
ΔT/T %
DOM
DOM + GYKI
10 µM DOM
DOM
+
NS-102
10 µM DOM
AMPA
AMPA + GYKI
10 µM AMPA
Time (min)

Figure 4.4: Time course of light transmittance changes (ΔT/T%) measured in CA1 stratum radiatum (CA1 RAD) over time. Responses are from representative slices in response to prolonged (10 min) exposure to glutamate agonists at 37°C. A large initial increase in transmittance is evoked by 10 μM domoate (DOM) which progresses into an irreversible negative shift; both these processes are blocked by 100 μM GYKI, restoring transmittance to baseline levels upon wash (**A**). This same response is not blocked by 10 μM NS-102 (**B**). 10 μM AMPA evokes a similar irreversible change in LT that is blocked by 100 μM GYKI (**C**).

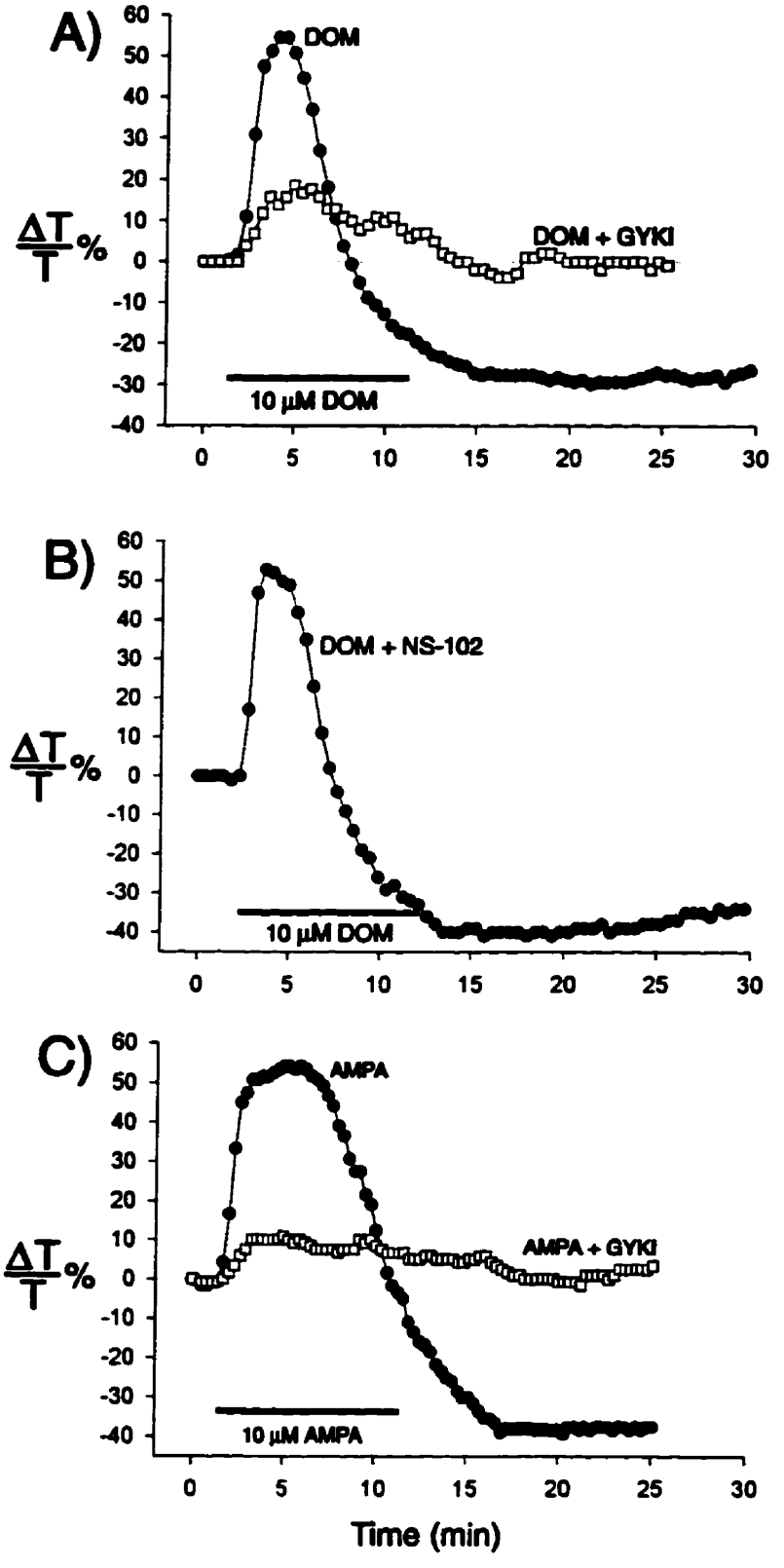
A)
DOM
DOM + GYKI
10 µM DOM
ΔT/T %
B)
DOM + NS-102
10 µM DOM
C)
AMPA
AMPA + GYKI
10 µM AMPA
Time (min)

CHAPTER 5

GENERAL DISCUSSION

CHAPTER 5: GENERAL DISCUSSION

In broad terms, this thesis explores excitotoxic processes in the mammalian brain evoked by the marine toxin and glutamate agonist, domoic acid. Specifically we examined domoate-induced changes in neuronal volume associated with acute, rapidly triggered excitotoxicity by monitoring changes in the intrinsic optical properties of *in vitro* hippocampal slices exposed to this naturally produced toxin. Current excitotoxic theory is derived primarily from cell culture experiments and behavioral/postmortem observations of *in vivo* studies. As a result there is little direct experimental data regarding early excitotoxic processes derived from intact brain tissue. However, a novel imaging technology developed by Dr. Brian A. MacVicar and associates of the University of Calgary has enabled us to image, in real time, changes in intrinsic optical signals associated with cell swelling over unparalleled spatial and temporal axes. The present study examined the effects of domoate on LT changes in the rat hippocampal slice preparation in order to characterize (1) which hippocampal regions were affected, (2) which subtype of receptors were involved, (3) if cell swelling played a role in the response, and (4) the ability of novel antagonists to block DOM-evoked toxicity

The second chapter outlines the first of its kind to utilize intrinsic optical signals to monitor changes in light transmittance in response to applications of an exogenous glutamate agonist on brain slices (Polischuk and Andrew 1996c). This work quantified and characterized both regional and temporal changes in LT induced by domoate in transverse hippocampal slices at 22°C. A portion of the hippocampal formation, area CA1, is a locale known to be particularly vulnerable to excitotoxic damage both in experimental and clinical

neurodegenerative states. Area CA1 was the primary target of domoate in this study. Specifically, the largest changes in LT, and thus presumably the largest changes in cell volume, occurred in the dendritic regions of CA1. This result was somewhat puzzling first because most studies have identified cell body swelling (Riepe and Carpenter 1995; Ikeda *et al.* 1996) as the area most responsive to excitotoxic change. Second, domoate has been considered a classical kainate agonist (Debonnel *et al.* 1989a, 1989b; Stewart *et al.* 1990), and so was expected to primarily target area CA3, the brain region most abundant in kainate receptors (Foster *et al.* 1981; Monaghan and Cotman 1982; Monaghan *et al.* 1983.; Unnerstall and Wamsley 1983; Werner *et al.* 1991; Benke *et al.* 1993). We argue that a significant portion of these kainate receptors are located pre-synaptically (Cotman et al. 1987; Henley 1995) and that intrinsic optical signals that we observe originate post-synaptically (MacVicar and Hochman 1991; Andrew and MacVicar 1994; Holthoff and Witte 1996) and are mediated by AMPA receptors.

We addressed how LT changes were induced by domoate in the slice through the use of available glutamate antagonists. Initial results showed that non-NMDA glutamate receptors were involved. Although specific antagonists for AMPA receptors had not been developed at the time our initial studies, the observations pointed towards an almost exclusive AMPA receptor involvement. Positive confirmation that AMPA receptors were involved required antagonists with higher levels of specificity.

We provided an independent line of evidence that the observed initial LT increases in CA1 RAD were, in fact, representative of cell swelling by utilizing an electrophysiological technique that records voltage changes across brain tissue (Traynelis and Dingledine 1989).

Using constant current pulses and Ohm's Law (V=IR) relative tissue resistance (R_{REL}) is calculated from the voltage change during domoate exposure and recovery. Increased changes in tissue resistance across CA1 RAD (indicative of cell swelling) paralleled the time course of the LT increase and subsequent reversal in response to domoate. The ability of a glutamate receptor antagonist to block domoate-induced increases in both LT and R_{REL} provides strong evidence that domoate evokes cell swelling mediated by glutamate receptors.

A major goal of the study was to image excitotoxic cell death. The second chapter illustrated reversible responses in LT (reversible swelling) evoked by various concentrations of domoate at 22°C that appeared to have no permanent, deleterious effects on the slice. A logical scenario was to examine the same paradigm but at higher temperature (37°C) to evoke a lethal response to domoate. The third chapter examined not only the effects of this increased temperature but also studied the effect of prolonged exposure times (10 min) to domoate. When compared to the lower temperature study, identical responses were obtained when either the temperature increased although the reversal time was shortened. When the temperature *and* exposure time were increased together, the initial LT increase in dendritic regions evolved into an irreversible *decrease* in LT over a period of just minutes. At the same time, LT irreversibly *increased* in cell body regions (CA1 and DG). The irreversibility of this phenomenon alone was insufficient to claim cell death as the cause so we search for additional evidence. A histopathological analysis and loss of evoked field potentials in hippocampal slices treated with domoate for 10 min at 37°C yielded evidence of damaged neurons consistent with previous excitotoxic profiles of neuronal death (Meldrum and Garthwaite 1990; Stewart *et al.* 1990; Strian and Tasker 1991; Schmeud *et al.*1995; Longo

et al. 1995). As well, an almost identical intrinsic sequence was generated with prolonged exposure to NMDA at high temperature (Andrew, Adams, and Polischuk 1996). Thus, we concluded that it was possible to image acute excitotoxic cell death in real time.

Spectral analysis of the transmitted light correlated well with the intrinsic signal, confirming a generalized swelling as a source of the signal (MacVicar and Hochman 1991; Kriesman *et al.* 1995). Furthermore, histopathological evidence confirmed obvious vacuolization and swelling in cell body regions, again correlating with the intrinsic signal measured in that area. Histology also suggested that the negative shift observed in the CA1 dendritic region was due dendritic beading (Park *et al.* 1996) or possibly dendritic retraction (Wan *et al.* 1995; Friedman and Haddad 1994).

At this point, the sum of our observations suggests that we are imaging primarily neuronal, not glial, changes in volume. Specifically, the observations that in the hippocampal slice (1) high K^+ aCSF results in a generalized swelling; (2) glutamate agonists give very specific laminar responses in regions high in NMDA and non-NMDA receptors; and (3) large signals in cell body layers (CA1 PYR and DG GC) that develop when neurons are electrophysiologically dead contain a very small glial component; together suggest that the source of the LT signal is due to alterations in neuronal volume. However we still do not have direct evidence that the LT response is purely neuronal. Preliminary experiments in our laboratory using flourescent microscopy to observe single neuron injections of lucifer yellow in domoate treated slices strongly supports this notion.

The third chapter also explored the ionic basis of the domoate-induced intrinsic signals. Removal of chloride afforded protection from damage by domoate, consistent with

original culture studies (Rothman 1985). Removal of extracellular calcium had no effect on cell survival, contrary to some culture studies that showed Ca^{2+} was responsible for acute neuronal death (Choi 1987). The study of calcium and its relationship to excitotoxic events and neurodegenerative disorders, especially in terms of NMDA receptor activity, dominates the literature today (Choi 1995). This study, in conjunction with the first study (Polischuk and Andrew 1996c), emphasizes the relationship between non-NMDA receptor activation and acute cell swelling. The sequence of cell volume change presented here is a totally new idea and Ca^{2+} may not play a role in any of these acute volume changes. Perhaps calcium-dependent theories of excitotoxicity need to be rethought with a more comprehensive and inclusive approach to acute excitotoxic neuronal death.

To this end, we are now preparing to simultaneously measure both cell swelling and intracellular calcium fluxes in hippocampal slices. This approach will allow us to image both IOSs and Ca^{2+} fluxes to determine the roles of both cell swelling and calcium in glutamate-agonist induced toxicity in the same preparation. An intriguing possibility is that the reversible IOS induced by domoate, although Ca^{2+}-independent, may initiate significant Ca^{2+} influx at the same time or activate Ca^{2+} stores. Elevated $[Ca^{2+}]_i$ in turn mediates a series of calcium-dependent events that result in death hours later, consistent with the notion of delayed rapidly triggered cell death (Choi 1990, 1993). A marriage of these imaging technologies with very thin slices, which might survive for days and would permit imaging at the single cell level, would create a novel *in vitro* model in which delayed cell death could be observed.

With a model of acute excitotoxicity established in the first two papers, the intrinsic

optical imaging technology was used in the fourth chapter to explore the effects of two novel glutamate antagonists on glutamate toxicity. AMPA, a non-NMDA glutamate agonist, was shown to have a similar spatial and temporal pattern of toxicity compared to domoate. Domoate- or AMPA-induced stimulation was significantly blocked by GYKI 52466, a non-competitive antagonist of AMPA receptors (Ouardouz and Durand 1991; Donevan and Rogawski 1993; Renard *et al.* 1995; Rammes *et al.* 1996). However, NS-102, a novel antagonist of low affinity kainate receptors (Verdoon *et al.* 1994; Johansen *et al.* 1993), failed to antagonize domoate stimulation. GYKI 52466 was able to significantly protect against both domoate- or AMPA-induced damage (irreversible IOS) produced by 10 min agonist exposure while NS-102 failed to afford any protection against domoate-evoked toxicity. This paper indicates that any therapeutic approach to reducing acute neuronal death must include blockade of AMPA receptors

Finally, the study outlined in Chapter 4 confirmed the suggestion put forward in Chapter 2: that swelling induced by domoate, a compound previously described as a classical kainate agonist (Debonnel *et al.* 1989a, 1989b; Stewart *et al.* 1990), is mediated by AMPA receptors.

REFERENCES

Adams ME, Swanson G. (1994) Neurotoxins. Trends Neurosci. Supplement April 1994.

Andrew RD, MacVicar BA. (1994) Imaging cell volume changes and neuronal excitation in the hippocampal slice. Neuroscience. 62:371-382.

Andrew RD, Adams JR, Polischuk TM. (1996) Imaging NMDA- and kainate-induced intrinsic optical signals from the rat hippocampal slice. J. Neurophys. 76:2707-2717.

Andrew RD, Lobinowich ME, Osehobo EP. (1997) Evidence against volume regulation by cortical brain cells during acute osmotic stress. Exptl. Neurol. 143:300-312.

Basavappa S, Ellory JC. (1996) The role of swelling-induced anion channels during neuronal volume regulation. Mol. Neurobiol. 13:137-153.

Beal MF. (1992) Mechanisms of excitotoxicity in neurologic diseases. Fed. Amer. Soc. Exp. Biol. J. 6:3338-3344.

Beal MF. (1995) Aging, energy, and oxidative stress in neurodegenerative diseases. Ann. Neurol. 38:357-366.

Benke TA, Jones OT, Collingridge GL, Angelides KJ. (1983) *N*-methyl-D-aspartate receptors are clustered and immobilized on dendrites in living cortical neurons. Proc. Nat. Acad. Sci. 90:7819-7823.

Bettler B, Mulle C. (1995) Review: Neurotransmitter receptors II AMPA and kainate receptors. Neuropharm.34:123-139.

Biscoe TJ, Evans RH, Headley PM, Martin M, Watkins JC. (1975) Domoic and quisqualic acids as potent amino acid excitants of frog and rat spinal neurones. Nature 255:166-167.

Blackstone CD, Moss SJ, Martin LJ, Levey AI, Price DL, Huganir RL. (1992) Biochemical characterization and localization of a non-*N*-Methyl-D-Aspartate glutamate receptor in rat brain. J. Neurochem. 58:1118-1126.

Blandini F, Porter RHP, Greenamyre JT. (1996) Glutamate and Parkinson's disease. Mol. Neurobiol. 12:73-94.

Bonhoeffer T. (1995) Optical imaging of intrinsic signals as a tool to visualize the functional architecture of adult and developing visual cortex. Drug Res. 45:351-356.

Brusa R, Zimmermann F, Koh DS, Feldmeyer D, Gass P, Seeburg PH, Sprengel R. (1995) Early-onset epilepsy and postnatal lethality associted with an editing-deficient GluRB allele in mice. Science. 270:1677-1680.

Buchan AM, Lesiuk H, Barnes KA, Hui L, Huang Z, Smith KE, Xue D. (1993) AMPA antagonists: Do they hold more promise for clinical stroke trials than NMDA antagonists? Stroke. 24:I148 - I152.

Burt AM (1993) *Chemical Transmission* In: Textbook of Neuroanatomy. WB Saunders Co. pp. 92-114.

Busto R, Dietrich WD, Globus MYT, Valdes I, Scheinberg P, Ginsberg MD. (1987) Small differences in intraischemic brain temperature critically determine the extent of ischemic neuronal injury. J. Cerb. Blood Flow Metab. 7:729-738.

Cendes F, Andermann F, Carpenter S, Zatorre RJ, Cashman NR. (1995) Temporal lobe epilepsy caused by domoic acid intoxication: Evidence for glutamate receptor-mediated excitotoxicity in humans. Ann. Neurol. 37:123-126.

Chan PH, Fishman RA, Longar S, Chen S and Yu A (1985) Cellular and molecular effects of polyunsaturated fatty acids in brain ischemia and injury. Prog. Brain Res. 63:227-235.

Chen Q, Harris C, Brown CS, Howe A, Surmeier DJ, Reiner A. (1995) Glutamate-mediated excitotoxic death of cultured striatal neurons is mediated by non-NMDA receptors. Exp. Neurol. 136:212-224.

Chiamulera C, Costa S, Valerio E, Reggiani A. (1992) Domoic acid toxicity in rats and mice after intracerebroventricular administration: Comparison with excitatory amino acid agonists. Pharmacol. Toxicol. 70:115-120.

Chittajulla R, Vignes M, Dev KK, Barnes JM, Collingridge, GL, Henley JM. (1996) Regulation of glutamate release by presynaptic kainate receptors in the hippocampus. Nature. 379:78-81.

Choi DW. (1987) Ionic dependence of glutamate neurotoxicity in cortical cell culture. J. Neurosci. 7:380-390.

Choi DW. (1990) Methods for antaognizing glutamate neurotoxicity. Cerebrovasc. & Brain Metab. Rev. 2:105-147.

Choi DW. (1992) Excitotoxic cell death. J. Neurobiol 23:1261-1276.

Choi DW. (1994) Glutamate receptors and the induction of excitotoxic neuronal death. Prog. Brain Res. 100:47-51.

Choi DW. (1995) Calcium: still center-stage in hypoxic-ischemic neuronal death. Trends Neurosci. 18:58-60.

Cohen LB. (1973) Changes in neuron structure during action potential propogation and synaptic transmission. Physiol. Rev. 53:373-418.

Cohen LB, Keynes RD. (1971) Changes in light scattering associated with the action potential in crab nerves. J. Physiol. 212:259-275.

Colwell CS, Levine MS. (1996) Glutamate-induced toxicity in neostriatal cells. Brain Res. 724:205-212.

Corsi M, Marcon C, Censabella C, Trist C, Reggiani A. (1993) Further evidence that the effects of kanic acid, domoic acid and AMPA are mediated via two distinct receptors. Brit. J. Pharmacol. 108:269.

Cotman CW, Monoghan DT, Ottersen OP, Storm-Mathisen J. (1987) Anatomical organization of excitatory amino acid receptors and their pathways. Trends Neurosci. 10:273-280.

Coyle JT, Puttfarcken P. (1993) Oxidative stress, glutamate, and neurodegenerative disorders. Science. 262:689-695.

Craig AM, Blackstone CD, Huganir RL, Banker G. (1993) The distribution of glutamate receptors in cultured rat hippocampal neurons - postsynaptic clustering of AMPA-selective subunits. Neuron. 10:1055-1068.

Curtis DR, Watkins LC. (1960) The excitation and depression of spinal neurones by structurally related amino-acids. J. Neurochem. 6:117-141.

Dakshinamurti K, Sharma SK, Sundaram M. (1991) Domoic acid induced seizure activity in rats. Neurosci. Lett. 127:193-197.

Davies J, Watkins JC. (1985) Depressant actions of γ-D-glutamylaminomethyl sulfonate (GAMS) on amino acid-induced and synaptic excitation in the cat spinal cord. Brain Res. 113-120.

Davies JD, Evans RH, Francis AA, Watkins JC. (1979) Excitatory amino acids and synaptic excitation in the mammalian central nervous system. J. Physiol. 75:641-654.

Dawson VL, Dawson TM, London ED, Bredt DS and Snyder SH (1991) Nitric oxide mediates glutamate neurotoxicity in primary cortical cultures. Proc. Natl. Acad. Sci. USA 88:6368-6371.

Debonnel G, Beauchesne L, de Montigny C. (1989a) Domoic acid, the alleged "mussel toxin", might produce its neurotoxic effect through kainate receptor activation: an electrophysiological study in the rat dorsal hippocamous. Can. J. Physiol. Pharmacol. 67:29-33.

Debonnel G, Weiss M, de Montigny C. (1989b) Reduced neuroexcitatory effect of domoic acid following mossy fiber denervation of the rat dorsal hippocampus: further evidence that toxicity of domoic acid involoves kainate receptor activation. Can. J. Physiol. Pharmacol. 67:904-908.

Dingledine R, Hume RI and Heinemann SF. (1992) Structural determinants of barium permeation and rectification in non-NMDA glutamate receptor channels. J. Neurosci. 12:4080-4087.

Dodt HU, Hager G, Zieglgansberger W. (1993) Direct observation of neurotoxicity in brain slices with infrared videomicroscopy. J. Neurosci. Meth. 50:165-171.

Donevan SD, Rogawski MA. (1993) GYKI 52466, a 2,3-benzodiazepine, is a highly selective, non-competitive antagonist of AMPA/ kainate receptor responses. Neuron. 10:51-59 (1993).

Dubinsky JM, Kristal BS, Elizondo-Fournier M. (1995) On the probabilistic nature of excitotoxic neuronal death in the hippocampus. Neuropharmacol. 34:707-711.

Dykens JA, Stern A, Trenkner E. (1987) Mechanism of kainate toxicity to cerebellar neurons *in vitro* is analogous to reperfusion injury. J. Neurochem. 49:1222-1228.

Ebner TJ, Chen G. (1995) Use of voltage-sensitive dyes and optical recordings in the central nervous system. Prog. Neurobiol. 46:463-506.

Egebjerg J, Heinemann S. (1993) Ca^{2+} permeability of an unedited and editred version of the kainate selective glutamate receptor GluR6. Proc. Natl. Acad. Sci. 90:755-759.

Federico P, Borg SG, MacVicar BA. (1994) Mapping patterns of neuronal activity and seizure propogation by imaging intrinsic optical signals in the isolated whole brain of the guinea-pig. Neurosci. 58:461-480.

Fleck MW, Henze DA, Barrionuevo G, Palmer AM. (1993) Aspartate and glutamate mediate excitatory synaptic transmission in area CA1 of the hippocampus. J. Neurosci. 13(9):3944-3955.

Foster AC, Mena EE, Monaghan DT, Cotman CW. (1981) Synaptic localization of kainic acid binding sites. Nature 289:73-75.

Friedman JE, Haddad GG. (1994) Removal of extracellular sodium prevents anoxia-induced injury in freshly dissociated rat CA1 hippocampal neurons. Brain Res. 641:57-64.

Garthwaite J, Garthwaite G. (1990) Mechanisims of excitatory amino acid neurotoxicity in rat brain slices. In *Excitatory Amino Acids and Neuronal Plasticity.* Y. Ben-Ari, ed. pp. 505-518.

Garthwaite J, Charles SL, Chess-Williams R (1988) Endothelium derived relaxing factor release on activation of NMDA receptors suggests role as intercellular messenger in the brain. Nature. 336:385-388.

Giberti A, Ratti E, Gaviraghi G, van Amsterdam FTM. (1991) Binding of DL-[^{3}H]AMPA to rat cortex membranes reveals two sites of affinity states. J. Receptor Res. 11:727-741.

Gramsbergen JBP, Smulders P. (1992) Effect of kynurenate and diethyldithiocarbamate on kainic acid neurotoxicity as determined by $^{45}CaCl_2$-autoradiography and a nonperfusion Timm method. Ann. New York Acad. Sci. 648:279-282.

Grinvald A, Liecke E, Frostig RD, Gilbert CD, Wiesel TN. (1986) Functional architecture of cortex revealed by optical imaging of intrinsic signals. Nature. 324:361-364.

Gross PM, Polischuk TM, Wainman DS, Weaver DF. (1995) Hippocampal excitation and toxicity produced *in vivo* by domoic acid. Soc. Neurosci. Abstr. 25:2045.

Gwag BJ, Lobner D, Koh J, Wie MB, Choi DW. (1994) Blockade of glutamate receptors during oxygen or glucose deprivation unmasks apoptosis in cultured cortical neurons. Soc Neurosci Abstr. 20:248.

Hampson DR, Huang X, Wells JW, Walter JA, Wright JLC. (1992) Interaction of domoic acid and several derivatives with kainic acid and AMPA binding sites in rat brain. Europ. J. Pharmacol. 218:1-8.

Hawkins LM, Beaver KM, Jane DE, Taylor PM, Sunter DC, Roberts PJ. (1995) Characterization of the pharmacology and regional distribution of (S)-[^{3}H]-5-fluorowillardiine binding in rat brain. Brit. J. Pharmacol. 116:2033-2039.

Henley JM. (1995) Subcellular localization and molecular pharmacology of distinct populations of [^{3}H]-AMPA binding sites in rat hippocapus. Brit. J. Pharmacol. 115:295-301.

Henn JS, Turner DA. (1993) Optical imaging of intrinsic signals and extracellular resistance in hippocampal slices: correlative measures of cell swelling. Soc. Neurosci. Abstr. 19:1322.

Hill DK, Keynes RD. (1949) Opacity changes in stimulated nerve. J. Physiol. Lond. 108:278-281.

Hill DK. (1950) The volume change resulting from stimulation of a giant nerve fibre. J. Physiol. Lond. 111:304-327.

Hollmann M, Heinemann S. (1994) Cloned glutamate receptors. Ann. Rev. Neurosci. 17:31-38.

Holtoff K, Witte OW. (1996) Intrinsic optical signals in rat neocortical slices measured with near-infared dark-field microscopy reveal changes in extracellular space. J. Neurosci. 16:2740-2749.

Honoré T, Davies SN, Drejer J, Fletcher EJ, Jacobsen P, Lodge D, Nielsen SE. (1988) Quinoxalinediones: potent competitive non-NMDA glutamate receptor antagonists. Science. 241:701-703 (1988).

Horner RA, Kusske MB, Moynihan BP, Skinner RN, Wekell JC. (1993) Retention of domoic acid by Pacific razor clams, *Siliqua patula* (Dixon 1789): preliminary study. J. Shellfish Res. 12:451-456.

Hume RI, Dingledine R, Heinemann S. (1991) Identification of a site in glutamate receptor subunits that controls calcium permeability. Science. 253:1028-1031.

Ikeda J, Terakawa S, Murota S, Morita I, Hirakawa. (1996) Nuclear disintegration as a leading step of glutamate excitotoxicity in brain neurons. J. Neurosci. Res. 43:613-622.

Insel TR, Miller LP, Gelhard RE. (1990) The ontogeny of excitatory amino acid receptors in rat forebrain - I. N-methyl-D-aspartate and quisqualate receptors. Neuroscience. 35:31-43.

Ishida M, Shinozaki H. (1991) Novel kainate derivatives: potent depolarizing actions on spinal motoneurones and dorsal root fibers in newborn rats. Br. J. Pharmacol. 104:873-878.

Iverson F, Trulove J. (1994) Toxicology and seafood toxins: domoic acid. Natural Toxins. 2:334-339.

Jhamandas KH, Boegman RJ, Beninger RJ. (1994) Quinolinic acid induced brain neurotransmitter deficits: modulation by endogenous excitotoxn antagonists. Can J Physiol Pharmacol 72:1473-1482.

Johansen TH, Drejer J, Wätjen F, Nielsen EØ. (1993) A novel non-NMDA receptor antagonist shows selective displacement of low-affinity [^{3}H]kainate binding. Eur J Pharmacol. 246:195-204.

Jonas P, Sakmann B (1992) Glutamate receptor channels in isolated patches from CA1 and CA3 pyramidal cells of rat hippocampal slices. J. Physiol. 455:143-171.

Kaku DA, Goldberg MP, Choi DW. (1991) Antagonism of non-NMDA receptors augment the neuroprotective effect of NMDA receptor blockade in cortical cultures subjected to prolonged deprivation of oxygen and glucose. Brain Res. 554:344-347.

Katsuwanda T *et al.* (1992) Nature. 358:36-40.

Keinanen K, Wisden W, Sommer B, Werner P, Herb A, Verdoorn TA, Sakmann B, Seeburg PH. (1990) A family of AMPA selective glutamate receptors. Science 249:556-560.

Kimelberg HK. (1995) Current concepts in brain edema. J. Neurosurg. 83:1051-1059.

King LS, Agre P. (1996) Pathophysiology of the aquaporin water channels. Ann. Rev. Physiol. 58:619-48.

REFERENCES

Köhler M, Burnashev N, Sakmann B, Seeburg PH. (1993) Determination of Ca^{2+} permeability in both TM1 and TM2 of high-affinity kainate receptor channels, diversity by RNA editing. Neuron. 10:491-500.

Kreisman NR, LaManna JC, Liao SC, Yeh ER, Alcala JR. (1995) Light transmittance as an index of cell volume in hippocampal slices: optical differences of interfaced and submerged positions. Brain Res. 693:179-186.

Krogsgaard-Larsen P, Hansen JJ. (1992) Naturally-occuring excitotory amino acids as neurotoxins and leads in drug design. Toxicol. Lett. 65:409-416.

Kunig G, Hartmann J, Krause F, Deckert J, Heinsen H, Ransmayr G, Beckmann, H, Riederer. (1995). Regional differences in the interaction of the excitotoxicns domoate and 1-β-oxalyl-amino-alanine with [^{3}H]kainate binding in human hippocampus. Neurosci. Lett. 187:107-110.

Lanius RA, Shaw C. (1993) High-affinity kainate binding sites in living slices of rat neocortex: characterization and regulation. Neurosci. 55:139-145.

Lees GJ. (1996) Theraputic potential of AMPA receptor ligands in neurological disorders. CNS Drugs 5:51-74.

Leranth C, Szeidemann Z, Hsu M, Buzsaki G. (1996) AMPA receptors in the rat and primate hippocampus: a possible absence of GluR2/3 subunits in most interneurons. Neuroscience. 70:631-652.

Li H, Buchan AM. (1993) Treatment with an AMPA antagonist 12 hours following severe normothermic forebrain ischemia prevents CA1 neuronal injury. J. Cereb. Blood Flow Metab. 13:933-939.

Lieke EE, Frostig RD, Arieli A, Ts'o DY, Hildesheim R, Grinvald A. (1989) Optical imaging of cortical acitivity: real-time imaging using extrinsic dye-signals and high resolution imaging based on slow intrinsic signals. Annu. Rev. Physiol. 51:543-559.

Lipton P. (1973) Effects of membrane depolarization on light scattering by cerebral cortical slices. J. Physiol. 231:365-383

Lomeli H, Wisden W, Kohler M, Keinanen K, Sommer B, Seeburg PH. (1992) High-affinity kainate and domoate receptors in rat brain. Fed. Eur. Biochem. Soc. 307:139-143.

Long DM. (1982) Traumatic brain edema. Clin. Neurosurg. 29:174-202.

Longo R, Domenici MR, Scotti de Carolis A, Sagratella, S. (1995) Felbamate selectively blocks in vitro hippocampal kainate-induced irreversible electrical changes. Life Sci. 56:PL409-414.

Lopes da Silva FH, Witter MP, Boeijinga PH, Lohmann AHM. (1990) Anatomic organization and physiology of the limbic cortex. Physiol. Rev. 70:453-511.

Lucas DR, Newhouse JP (1957) The toxic effetcs of sodium-L-glutamate on the inner layers of the retina. Arch. Opthamol. 58:193-201.

MacVicar BA, Hochman D. (1991) Imaging of synaptically evoked intrinsic optical signals in hippocampal slices. J. Neurosci. 11:1458-1469.

Maguro H *et al.* (1992) Nature. 358:70-75.

Malva JO, Carvalho AP and Carvalho CM. (1996) domoic acid induces the release of glutamate in the rat hippocampal CA3 subregion. Neuroreport 7:1330-1334.

Martin JH. (1989) The Limbic System. In *Neuroanatomy Text and Atlas.* pp.375-396. Elsevier, New York.

Mattson MP, Wang H, Michaelis EK. (1991) Developmental expression, compartmentalization, and possible role in excitotoxicity of a putative NMDA receptor protein in cultured hippocampal neurons. Brain Res. 565:94-108.

May PC, Robison PM. (1993) GYKI 52466 protects against non-NMDA receptor-mediated excitotoxicity in primary rat hippocampal cultures. Neurosci. Lett. 152:169-172.

McBain CJ, Traynelis SF, Dingledine R. (1990) Regional variation of extracellular space in the hippocampus. Science 249:674-676.

Meldrum B, Garthwaite J. (1990) Excitatory amino acids and neurodegenerative disease. Trends Pharmacol. Sci. 11:379-387.

Meldrum B. (1993) Amino acids as dietary excitotoxins: a contribution to understanding neurodegenerative disorders. Brain Res. Rev. 18:293-314.

Michaelis EK (1996) Glutamate neurotransmission: characteristics of NMDA receptors in the mammalian brain. Neural Notes. 11:3-7.

Miller LP, Johnson AE, Gelhard RE, Insel TR. (1990) The ontogeny of excitatory amino acid receptors in the rat forebrain - II. Kainic acid receptors. Neuroscience. 35:45-51.

Monaghan DT, Cotman CW. (1982) The distribution of [^{3}H]kainic acid binding sites in rat CNS as determined by autoradiography. Brain Res. 252:91-100.

Monaghan DT, Holets VF, Toy DW, Cotman CW. (1983) Anatomical distribution of four pharmacologically distinct [3H]-L-glutamate binding sites. Nature (Lond) 306:176-179.

Monyer H, Sprengel R, Schoepfer R, Herb A, Higuchi M, Lomeli H, Burnashev N, Sakmann B, Seeburg PH. (1992) Heteromeric NMDA receptors: molecular and functional distinction of subtypes. Science. 258:1217-1221.

Moriyoshi K, Masu M, Ishii T, Shigemoto R, Mizuno R, Nakanishi S. (1991) Molecular cloning and characterization of the rat NMDA receptor. Nature. 354:31-36.

Mosinger JL, Price MT, Bai HY, Xiao H, Wozniak DF, Olney JW. (1991) Blockade of both NMDA and non-NMDA receptors is required for optimal protection against ischemic neuronal degeneration in the adult mammalian retina. Exp. Neurol. 113:10-17.

Nicotera P, Orrenius S. (1992) Ca^{2+} and cell death. Ann. New York Acad. Sci. 163:17-27.

Nielson EO, Johansen TH, Watjen F, Dreger J. (1995) Characterization of the binding of [^{3}H]NS 257, a novel competitive AMPA receptor antagonist, to rat brain membranes and brain sections. J. Neurochem. 65:1264-1273.

Obeidat AS, Adams JR, Andrew RD (1994) Imaging intrinsic optical signals associated with brief hypoxia/hypoglycemia in rat hippocampal slice. Soc. Neurosci. Abst. 20:180.

Olney JW. (1969a) Glutamate-induced retinal degeneration in neonatal mice. Electron microscopy of the acutely evolving lesion. J. Neuropathol. Exp. Neurol. 28:455-474.

Olney JW. (1969b) Brain lesions, obesity and other disturbances in mice treated with monosodium glutamate. Science 164:719-721.

Olney JW. (1990) Excitotoxicity: an overview. Can. Dis. Weekly Rep. 16:47-58

Olney JW. (1994) Excitotoxins in foods. NeuroTox. 15:535-544.

Olney JW, Ho O. (1970) Brain damage in infant mice following oral intake of glutamate, aspartate or cysteine. Nature 227:609-611.

Olney JW, Sharpe LG, Feigin RD. (1972) Glutamate-induced brain damage in infant primates. J Neuyropathol Exp Neurol 31:464-488.

Olney JW, Rhee V, Ho OL. (1974) Kainic acid: a powerful neurotoxic analogue of glutamate. Brain Res. 77:507-512.

Orrenius S, Nicotera P. (1994) The calcium ion and cell death. J. Neural Trans. 43:1-11.

Ouardouz M, Durand J. (1991) GYKI 52466 antagonizes glutamate responses but not NMDA and kainate responses in rat abducens motoneurones. Neurosci Lett 125:5-8.

Park JS, Bateman MC, Goldberg MP. (1996) Rapid alterations in dendrite morphology during sublethal hypoxia or glutamate receptor activation. Neurobiol. Dis. 3:215-227.

Peillet EL, Arvin B, Moncada C, Meldrum BS. (1992) The non-NMDA antagonists, NBQX and GYKI 52466, protect against cortical and striatal loss following transient global ischaemia in the rat. Brain Res. 571:115-120.

Perl TM, Bedard L, Kosatsky T, Hockin JC, Todd ECD, Remis RS. (1990) An outbreak of toxic encephalopathly caused by eating mussels contaminated with domoic acid. N. Engl. J. Med. 322:1775-1780.

Petralia RS, Wenthold RJ. (1992) Light and electron immunocytochemical localization of AMPA-selective glutamate receptors in the rat brain. J. Comp. Neurol. 318:329-354.

Petrie BF, Pinsky C, Standish NM, Bose R, Glavin GB. (1991) Parental domoic acid impairs spatial learning in mice. Pharmacol. Biochem. Behav. 41:211-214.

Pinsky C, Glavin GB, Bose R. (1989) Kynurenic acid protects against neurotoxicity and lethality of toxic extracts from contaminated Atlantic coast mussels. Prog. Neuro-Psychopharm. Biol. Psychiat. 13:595.

Pinsky C, Bose R, delCampo M, Sutherland GR, Glavin GB, Bruni JE. (1990) Kynurenate antagonism of domoic acid-provoked EEG seizure activity in the mouse. Europ. J. Pharm. 183:514-515.

Poe GR, Nitz DA, Rector DM, Kristensen MP, Harper RM. (1996) Concurrent reflectance imaging and microdialysis in the freely behaving cat. J. Neurosci. Meth. 65:143-149.

Polischuk TM, Andrew RD (1995) Imaging cell swelling and toxicity in the hippocampal slice produced by domoic acid and antagonized by GYKI 52466. Soc. Neuroci. Abstr. 21:1586.

Polischuk TM, Andrew RD. (1996a) Effect of temperature on domoic acid induced intrinsic optical signals in the hippocampal slice. Can. J. Physiol. Pharmacol. 74:Axxviii.

Polischuk TM, Andrew RD (1996b) Imaging excitotoxic cell swelling and neuronal death in the hippocampal slice: confirmation with spectrometry and electrophysiology. Soc. Neurosci. Abstr. 22:804.

Polischuk TM, Andrew RD. (1996c) Real time imaging if intrinsic optical signals during early excitotoxicity evoked by domoic acid in the rat hippocampal slice. Can. J. Physiol. Pharmacol 74:712-722.

Rainbow TC, Wieczorek CM, Halpain S (1984) Quantitative autoradiography of binding sites for [^{3}H]AMPA, a structural analogue of glutamic acid. Brain Res. 309:173-177.

Rammes G, Swandulla D, Collingridge GL, Hartmann S, Parsons CG. (1996) Interactions of 2,3-benzodiazepines and cyclothiazide at AMPA receptors: patch clamp recordings in cultured neuons and area CA1 in hippocampal slices. Brit J Pharmacol 117:1209-1221.

Renard A, Crépel F, Audinat E. (1995) Evidence for two types of non-NMDA receptors in rat cerebellar Purkinge cells maintained in slice cultures. Neuropharmacol. 34:335-346.

Repressa A, Tremblay E, Ben-Ari Y. (1987) Kainate binding sites in the hippocmapl mossy fibres: localisation and plasticity. Neuroscience. 20:739-748.

Rieppe M, Carpenter DO. (1995) Delayed increase of cell volume of single pyramidal cells in live rat hippocampal slices upon kainate application. Neurosci. Lett. 191:35-38.

Robinson JH, Deadwyler SA (1981) Kainic acid produces depolarization of CA3 pyramidal cells in the in vitro hippocampal slice. Brain Res. 221:117-127.

Rolfe NG, Andrew RD. (1996) Imaging swelling in the neocortex during acute excitotoxicity. Soc. Neurosci. Abst. 22:798.

Rothman SM. (1985) The neurotoxicity of ecitatory amino acids is produced by passive chloride influx. J. Neurosci. 5:1483-1489.

Rothman SM. (1992) Excitotoxins: possible mechanisms of action. Ann. New York Acad. Sci. 648:133-139.

Rothman SM, Olney JW. (1986) Glutamate and the pathophysiology of hypoxic-ischemic brain damage. Ann. Neurol. 19:105-111.

Schmeud LC, Scallet AC, Slikker W. (1995) Domoic acid-induced neuronal degeneration in the primate forebrain revealed by degeneration specific histochemistry. Brain Res. 695:64-70.

Schroeder H. (1993) Cellular and subcellular distribution of receptors in the entorhinal-hippocampal system: morphogenic and biochemical aspects. Hippocampus 3:139-148.

Schwarzc R, Du F, Schmidt W, Turski WA, Gramsbergen JBP, Okuno E, Roberts RC. (1992) Kynurenic Acid: a potential pathogen in brain disorders. Ann. New York Acad. Sci. 648:140-153.

Seeburg PH. (1993) The molecular biology of mammalian glutamate receptor channels. Trends Neurosci. 16:359-365.

Shaw PJ. (1992) Excitatory amino acid transmission, excitotoxicity and excitotoxins. Curr. Opinion Neurol. Neurosurg. 5:3830-390.

Sheardown MJ, Neilson EO, Hansen AJ, Jacobsen P, Honore T. (1990) 2,3-Dihydroxy-6-nitro-7-sulfamoyl-benzo (F) qiunoxaline: a nueroprotectant for cerebral ischemia. Science 247:571-574.

Siman R, Noszek JC, Kegerise C. (1989) Calpain I activation is specifically related to excitatory amino acid induction of hippocampal damage. J. Neurosci. 9:1579-1590.

Smith SE, Meldrum BS. (1992) Cerebroprotective effect of a non-N-methyl-D-aspartate antagonist, GYKI 52466, after focal ischemia in the rat. Stroke 23:861-864.

Somjen GG, Faas GC, Vreugdenhil M, Wadman WJ. (1993) Channel shutdown: a response of hippocampal neurons to adverse environments. Brain Res. 632:180-194.

Sommer B, Köhler M, Sprengel R and Seeburg PH (1991) RNA editing in the brin controls a determinat ion flow in glutamate-gated channels. Cell 67:11-19.

Spencer PS, Ludolph AC, Kisby GE. (1992) Are human neurodegenerative disorders linked to environmental chamicals with excitotoxic properties? Ann. New York Acad. Sci. 648:154-160.

Spruston N, Jonas P, Sakmann B. (1995) Dendritic glutamate receptor channels in rat hippocampal CA3 and CA1 pyramidal neurons. J. Physiol. 482:325-352.

Staub F, Peters J, Kempski O, Schneider GH, Schürer L, Baethemen A. (1993) Swelling of glial cells in lactacidosis and by glutamate: significance of Cl^- transport. Brain Res. 610:69-74.

Stewart GR, Zorumski CF, Price MT, Olney JW. (1990) Domoic acid: a dementia-inducing excitotoxic food poison with kainic acid receptor specificity. Exp. Neurol. 110:127-138.

Stone R. (1993) Hot Feild: Neurotoxicity. Science 259:1397.

Strain SM, Tasker RAR. (1991) Hippocampal damage produced by systemic injections of domoic acid in mice. Neurosci. 44:343-352.

Sutherland RJ, Hoesing JM, Whishaw IQ. (1990) Domoic acid, an environmental toxin, produces hippocampal damage and severe memory damage. Neurosci. Lett. 120:221-223.

Swanson LW, Koehler C, Bjorklund A. (1987) The septohippocampal system. In *Handbook of Chemical Neuroanatomy Vol. 5.* (A. Bjorklund, T Hoekfelt and LW Swanson eds.) pp.125-277. Elsevier Scientific Publishers, Amsterdam.

Takemoto T. (1978) Isolation and structural identification of naturally occurring excitatory amino acids. In *Kainic Acid as a Tool in Neurobiology* (EG McGeer, JW Olney, and PL McGeer, Eds.), pp. 1-15. Raven Press, New York.

Tasker RAR, Connell BJ, Strain SM. (1991) Pharmacology of systemically administered domoic acid in mice. Can. J. Physiol. Pharmacol. 69:378-382.

Tasker RA, Strain SM, Drejer J. (1996) Selective reduction in domoic acid toxicity *in vivo* by a novel non-NMDA receptor antagonist. Can. J. Physiol. Pharmacol. 74:1047-1054.

Teitelbaum JS, Zatorre RJ, Carpenter S, Gendron D, Evans AC, Gjedde A, Cashman NR. (1990) Neurologic sequelae of domoic acid intoxication due to the ingestion of contaminated mussels. N. Engl. J. Med. 332:1781-1787.

Terrian DM, Conner-Kerr TA, Privette TH, Gannon RL. (1991) Domoic acid enhances the K^+-evoked release of endogenous glutamate from guinea pig hippocampal mossy fiber synaptosomes. Brain Res. 551:303-307.

Todd ECD. (1990) Chronology of the toxic mussels outbreak. Can. Dis. Weekly Rep 16(1E):47-58.

Tomita M, Gotoh F. (1992) Cascade of cell swelling: thermodynamic potential discharge of brain cells after membrane injury. Amer. J. Physiol 262:H603-H610.

Trachsel L, Dodt HU, Zieglgansberger W. (1996) The intrinsic optical signal evoked by chiasm stmulation in the rat superchiasmatic nuclei exhibits GABAergic day-night variation. Eur. J. Neurosci.8:319-328.

Traynelis SF, Dingledine R. (1989) Role of extracellular space in hyperosmotic suppression of potassium-induced electrographic seizures. J. Neurophys. 67:927-938.

Tryphonas L, Truelove J, Nera E, Iverson F. (1990) Acute neurotoxicity of domoic acid in the rat. Toxicol. Pathol. 18:1-9.

Ts'o DY, Frostig RD, Liecke EE, Grinvald A. (1990) Functional organization of primate visual cortex revealed by high resolution optical imaging. Science 249:417-420.

Turner DA, Aitken PG, Somjen GG. (1995) Optical mapping of translucence changes in rat hippocampal slices during hypoxia. Neurosci. Lett. 195:209-213.

Turski L, Meldrum BS, Jones AW, Watkins JC. (1985) Anticonvulsant action of stereoisomers of γ-glutamylaminomethylsulphonic acid in mice. Europ. J. Pharmacol. 111:279-283.

Ulas J, Monaghan DT, Cotman CW. (1990) Kainate receptors in the rat hippocampus: A distribution and time course of changes in response to unilateral lesions of the entorhinal cortex. J. Neurosci. 10:2352-2362.

Unnerstall JR, Wamsley JK. (1983) Autoradiographic localization of high-affinity [^{3}H]kainic acid binding sites in the rat forebrain. Eur. J. Pharmac. 86:361-371.

Verdoon TA, Johansen TH, Drejer J, Nielsen EØ. (1994) Selective block of recombinant glur6 receptors by NS-102, a novel non-NMDA receptor antagonist. Eur. J. Pharmacol. 269:43-49.

Viviani R, Boni L, Cattani O, Milandri A, Poletti R, Pompei M, Sansoni G. (1995) ASP, DSP, NSP and PSP monitoring in "mucilaginous aggregates and in mussels in a coastal area of the Northern Adriatic Sea in 1988, 1989 and 1991. Sci. Total Environ. 165:203-211.

Walz W, Hinks EC. (1985) Carrier-mediated KCl accumulation accompanied by water movements is involved in the control of physiological K^+ levels by astrocytes. Brain Res. 343:44-51.

Walz W, Hinks EC. (1986) A transmembrane sodium cycle in astrocytes. Brain Res. 368:226-232.

Walz PM, Garrison DL, Graham WM, Cattey MA, Tjeerdema RS, Silver MW. (1994) Domoic acid-producing diatom blooms in Monterey Bay, Califorina: 1991-1993. Natural Toxins. 2:271-279.

Wan X, Harris JA, Morris CE. (1995) Responses of neurons to extreme osmomechanical stress. J. Membrane Biol. 145:21-31.

Watkins JC, Pook PCK, Sunter DC, Davies J, Honore T. (1990) Experiments with kainate and quisqualate agonists and antagonists in relation to the sub-classification of "non-NMDA" receptors. Adv. Exp. Med. Biol. 268:49-55.

Watson S, Girdlestone D. (1995) Receptor and ion channel nomenclature supplement. Trends Pharmacol. Sci. 6:30.

Wekell JC, Gauglitz EJ, Barnett HJ, Hatfield CL, Simons D, Ayres D. (1994) Occurence of domoic acid in Washington State razor clams (*Siliqua patula*) during 1991-1993. Natural Toxins. 2:197-205.

Wenthold RJ, Petralia RS, Blahos II J, Niedzielski AS. (1996) Evidence for multiple AMPA receptor complexes in hippocampal CA1/CA2 neurons. J. Neurosci. 16:1982-1989.

Werner, P., Voigt, M., Keinanen, K., Wisden, W. and Seeburg, P.H. (1991) Cloning of a putative high- affinity kainate receptor expressed predominately in hippocampal CA3 cells. Nature 351:742-748.

Wright JLC, Boyd RK, de Feitas ASW, Falk M, Foxall RA, Jamieson WD, Laycock MV, McCulloch AW, McInnes AG, Odense P, Pathak MA, Quilliam MA, Ragan MA, Sim PG, Thibault P, Walter JA, Gilgan M, Richard DJA, Dewar D. (1989) Identification of domoic acid, a neuroexcitatory amino acid, in toxic mussels from eastern Prince Edward Island. Can. J. Chem. 67:481-490.

Wright JLC, Falk M, McInnes AG, Walter JA. (1990) Identification of isodomoic acid D and two new geometrical isomers of domoic acid in toxic mussels. Can. J. Chem. 68:22.

Xi D and Ramsdell JS. (1996) Glutamate receptors and calcium entry mechanisms for domoic acid in hippocampal neurons. Neuroreport. 7:1115-1120.

Zhou N, Hammerland LG, Parks TN. (1993) γ-D-glutamylaminomethyl sulfonic acid (GAMS) distinguishes kainic acid- from AMPA-induced responses in *Xenopus* oocytes expressing chick brain glutamate receptors. Neuropharm 32:767-775.